Title
Utilizing the zebrafish model to investigate the endocannabinoid system, neural signaling, and behavior

Author
Melgoza, Adam David

Publication Date
2021

Peer reviewed|Thesis/dissertation

Utilizing the zebrafish model to investigate the endocannabinoid system, neural signaling, and behavior

by
Adam Melgoza

DISSERTATION
Submitted in partial satisfaction of the requirements for degree of
DOCTOR OF PHILOSOPHY

in

Pharmaceutical Sciences and Pharmacogenomics

in the

GRADUATE DIVISION
of the
UNIVERSITY OF CALIFORNIA, SAN FRANCISCO

Approved:

DocuSigned by:
Jeanne Paz
129DDCD87B64445...

Jeanne Paz
Chair

DocuSigned by:
Su Guo

Su Guo

DocuSigned by:
Ashish Raj
13BDA73A066E4E0...

Ashish Raj

Committee Members

Dedicated to my family – Margie Melgoza, Manuel Melgoza, and Adrian Melgoza –

who never for a second stopped believing in me

Acknowledgements

On the path to completing my PhD, I was fortunate enough to have a support system filled with incredible individuals who supported, encouraged, and guided me. None of this would be possible without the following people:

First, I would like to express my deepest gratitude to my dissertation advisor Dr. Su Guo. Su was instrumental in sharpening my lens as a scientist and teaching me to think critically about the scientific questions I pursued. She made it a point to be accessible for me if I ever needed input on my project, which I appreciated immensely, especially in the early stages of my PhD. I vividly remember one time being disillusioned when the results of a major experiment didn't go as planned. Su noticed this and asked "Are you disappointed?", to which I responded "Yes". She then explained to me how rather than being disappointing, the results of any (well performed) experiment, even negative results, are an exciting opportunity to learn something new; where is the fun if everything is already figured out? Su's genuine passion for scientific investigation shined through alongside her outstanding mentoring, encouraging me to keep moving forward.

I would like to thank my thesis committee: Dr. Jeanne Paz, Dr. Roland Wu, and Dr. Ashish Raj for their immense support regarding research direction, navigating PhD, and career development. I would also like to thank the leadership of the Pharmaceutical Sciences and Pharmacogenomics (PSPG) graduate program, Dr. Deanna Kroetz, Dr. Nadav Ahituv, and Rebecca Dawson, for their arduous and never-ending work in trying to make graduate school safe and supportive for PSPG grad students.

Though lab members have come and gone during my time in the Guo lab, the factor that has always remained constant is the collaborative and encouraging attitude from everybody. I'm sincerely grateful to everyone in the Guo lab, and cannot have imagined pursuing my PhD in any other lab. I would like to especially thank Dr. Francesca Oltrabella, one of my first mentors in the Guo lab. She opened the world of zebrafish biology and the endocannabinoid system to me, and her upbeat attitude and excitement for science was infectious. I also thank Dr. Oltrabella for her permission to include our hybrid paper as a chapter in this thesis. Additionally, Dr. Mahendra Wagle, essentially the 'father' of the lab, has been one of the most patient, kind, and helpful mentors I have ever had the pleasure of working with. I would like to thank Lana Harshman, Fatima Murad, Sacha Salphati, and Patrick Honma for being motivated and hard-working mentees. I would also like to thank Zixuan Yuan, Dr. Maria Burdyniuk, and Kássia Pereira for their wonderful company both inside and outside of lab.

I was fortunate enough to have classmates who took the time to listen to my practice talks, bounce back ideas regarding navigating my project, notify me when they saw career opportunities that fit my interests, and overall were a fun bunch of talented individuals. A huge thank you to my PSPG classmates!

My support system was instrumental in providing me the motivation to move forward even during the most challenging of obstacles. An enormous thank you to Amanda Carbajal, Dr. Stella Belonwu, Dina Buitrago Silva, Gibu George, Natalie Lopez, Amina Beltran, Vanessa Castro, Sara Sumrak, Jon Caña, Paayal Singh, Carmen Sandoval Espinosa, Megan Koleske, Marcus Chin, Bianca Vora, Nilsa La Cunza, and Hongtai Huang for being there with me during the ups and downs.

Lastly, I would never have even made it to grad school without the love and support from my beautiful family. Thank you Mom, Dad, and Adrian for always encouraging me, lifting me up, and reminding me that I can do this. I love you so much.

Contributions

Some chapters contain previously published material. In some cases this material has been altered and does not necessarily reflect its published form.

Basis for Chapter 1:

Melgoza A, and Guo S. “Systematic Screens in Zebrafish Shed Light on Cellular and Molecular Mechanisms of Complex Brain Phenotypes.” Molecular-Genetic and Statistical Techniques for Behavioral and Neural Research, 2018, pp. 385–400., doi:10.1016/b978-0-12-804078-2.00016-7.

Basis for Chapter 2:

Oltrabella F, Melgoza A, Nguyen B, Guo S. Role of the endocannabinoid system in vertebrates: Emphasis on the zebrafish model. Dev Growth Differ. 2017 May;59(4):194-210. doi: 10.1111/dgd.12351. Epub 2017 May 17. PMID: 28516445; PMCID: PMC5636690.

“And…what am I going to find if…I get through this?”

-Korra, *The Legend of Korra*

“I don’t know. But won’t it be interesting to find out?”

-Katara, *The Legend of Korra*

Utilizing the zebrafish model to investigate the endocannabinoid system, neural signaling, and behavior

Adam David Melgoza

ABSTRACT

The endocannabinoid (eCB) system is a complex network of proteins and ligands primarily found in the central nervous system. Though the eCB system is most notorious for producing psychotropic effects following consumption of the *Cannabis sativa* plant, it also modulates a wide range of physiological processes including neuronal development, neuroinflammation, anxiety, memory, appetite, lipid homeostasis, pain, and immunity. Harnessing the eCB system has been a successful therapeutic strategy for treating diseases, as in the cases of cannabidiol (CBD) for epilepsy treatment, or *Cannabis* as an anti-emetic for patients undergoing chemotherapy. Though there have been great strides in our understanding of the eCB system, unanswered questions remain in regards to its potential for additional therapeutic uses, toxicological considerations for *Cannabis* consumers, and more fundamentally, the mechanistic workings of eCB system signaling in the context of neural circuitry.

One approach to gain insights on the eCB system is through utilization of zebrafish (*Danio rerio*), a powerful model organism used in biological research. Proteins of interest can be easily targeted by both pharmacological agents and genetic alterations within zebrafish, allowing for examination of complex phenotypes resulting from desired perturbations. A diverse panel of zebrafish behavioral assays are available, allowing for examination of memory, addiction, sociability, aggression, and anxiety-like behaviors. Unlike mammalian models, development is relatively fast and breeding produces a large amount of progeny, allowing for

quick generation progression and large sample sizes. Also, unlike mammals, development occurs externally and the brain is transparent, allowing for accessible and clear visualization of neurodevelopment, neuronal activity, and fluorescent markers of interest throughout the whole brain. These attributes make zebrafish an excellent model for studying the eCB system *in vivo*. In this dissertation, we explore the roles of several eCB proteins through utilization of genetic and pharmacological manipulation of the zebrafish model.

We start off in Chapter 1 with an in-depth examination of techniques in zebrafish that have paved the way for gaining insights on neurobiological mechanisms. The techniques we cover include forward and reverse genetic screens, and chemical screens, which have shed light on mechanisms of neuronal subtype differentiation and maintenance, habituation, candidate genes implicated in autism spectrum disorders, genes involved in electrical synapse formation, and regulators of sleep/wake states, to name a few examples.

Next, in Chapter 2, we introduce the known roles of the eCB system in vertebrates, with an emphasis on the zebrafish model. We describe each component of the eCB system, how each eCB protein and ligand work together to facilitate signaling cascades, and the involvement of the eCB system in addiction, development, anxiety, lipid homeostasis, appetite, immunity, and neuroinflammation. We examine spatial expression of two eCB genes, *cb1* and *cnrip1a*, in developing zebrafish larvae, and quantitative expression of 18 eCB genes across 10 developmental stages and 11 organs in adult fish.

In the next two chapters, we use techniques described in Chapter 1 to target eCB genes described in Chapter 2. In Chapter 3, we utilize CRISPR-Cas9 gene editing to produce knockout zebrafish lines of *cb1*, *dagla*, *daglb*, *abhd4*, *mgll*, and *faah*. Following homology analysis, we determined that all 6 of these genes are conserved in zebrafish with amino acid sequence identity ranging from 45-70%. After sequencing each eCB knockout line, we found that all mutant alleles contained a frameshift mutation, suggesting a deleterious effect. We proceeded

to phenotype *dagla* knockout fish and observed in increase in locomotor activity, as well as alterations in mRNA transcript of *dagla*, *gpr55a*, and *fas*. We next examine the effects of pharmacological agents that target CB1 (WIN55212-2, 2-arachadonoylglycerol [2-AG], anandamide [AEA]), MGLL (MJN110, JZL-184) and FAAH (PF-3845) in Chapter 4. Through the light-dark preference assay, we observed changes in dark avoidance (an anxiety-like behavior) and locomotor activity following eCB protein-targeting drug treatment. These genetic and pharmacological studies provide an excellent opportunity for gaining insight on individual gene involvement in behavior and physiological processes.

In Chapter 5, we focus on one gene, *cb1*, and further examine its role in anxiety; in particular, we aim to gain a greater understanding of the neuronal populations that are involved in facilitating eCB-mediated changes in anxiety behavior. Corroborating human and rodent studies, we determine that zebrafish have increased anxiety-like behavior following either pharmacological or genetic inhibition of CB1. By leveraging high resolution *in situ* techniques, we discovered region-specific colocalization of *cb1* mRNA with pallial and hypothalamic glutamatergic and subpallial GABAergic neuronal markers. We produced a transgenic CB1 zebrafish line, allowing access to CB1-expressing cells and visualization of anatomical connectivity throughout the entire brain.

In conclusion, this dissertation reveals the behavioral effects of perturbing eCB genes, furthering our understanding of the roles of each eCB protein, and provides insight on the mechanism by which CB1 modulates anxiety-like behavior. From this work, 7 new eCB zebrafish lines were produced, allowing for further studies to uncover mechanistic roles of *cb1*, *dagla*, *daglb*, *abhd4*, *mgll*, and *faah*. Uncovering the roles of each eCB gene on biological processes not only demystifies this broadly expressed and highly conserved pathway, but also paves the way for insight on potential therapeutic uses and toxicological effects of eCB-targeting pharmacological agents.

Table of Contents

List of Figures

List of Tables

CHAPTER 1: Systematic Screens in Zebrafish Shed Light on Cellular and Molecular Mechanisms of Complex Brain Phenotypes

1.1 ABSTRACT

Next generation sequencing and genome-wide association studies have identified a large number of genetic variants associated with complex brain disorders including autism spectrum disorders (ASD), schizophrenia, anxiety and depression, as well as addiction. Understanding how these variants might contribute to the etiology of diseases remains a daunting challenge and requires a comprehensive knowledge of the genetic basis underlying complex brain phenotypes. In this chapter, we discuss how systematic screening approaches in the vertebrate genetic model organism the zebrafish *Danio rerio*, which use both forward and reverse genetic methods to introduce genetic alterations followed by phenotype-based screening, might provide insights. In addition to induced alterations, naturally existing variations represent another source that can enrich phenotype-based gene discovery.

1.2 INTRODUCTION

The brain, composed of many thousands of different cell types with intricate connections, is arguably the most complex organ. Together with the spinal cord, they constitute the central nervous system (CNS). The vertebrate CNS shares conserved anatomy, including subdivisions such as the forebrain, midbrain, hindbrain, and spinal cord. Studies employing vertebrate genetic model organisms such as zebrafish, xenopus, chick, and mice have shed light on the formation, maintenance, and function of complex brain structures.

The zebrafish is a relatively recent addition to the model organism arena (Grunwald and Eisen, 2002; Guo, 2004). In the 1970s, the late Dr. George Streisinger selected a pair of zebrafish (called A and B respectively) from a local pet shop because of the prolific nature and transparent embryonic and larval stages of this species. Through a series of elegant

experiments, he showed that zebrafish have a diploid genome and could be bred to produce clonal populations (Streisinger et al., 1981). Subsequently, the developmental stages and embryonic brain structures were characterized (Kimmel, 1993; Kimmel et al., 1995), and two large-scale *N*-ethyl-*N*-nitrosourea (ENU) mutagenesis screens were performed that identified thousands of mutations affecting virtually every aspect of visible morphology of a vertebrate embryo (Driever et al., 1996; Haffter et al., 1996). Molecular genetic studies of these mutations have provided valuable insights into vertebrate development.

Despite these advances, the potential of zebrafish to uncover cellular and molecular mechanisms underlying complex brain phenotypes are just beginning to be realized. Morphology-based phenotypic screens cannot detect changes at the cellular or functional levels, and therefore tend to miss the processes that affect specific structures or cell types, or that affect brain function. In recent years, innovative screens targeting these phenotypes were devised, and they will be the subject of review in this chapter.

We will begin the chapter by outlining general strategies used to introduce genetic alterations in the zebrafish. Methods used to produce a library of individuals with random phenotypic variations will be delineated. We will then discuss the results from several screens, with an emphasis on assay development, screen execution, and impacts on our understanding of complex brain phenotypes and related human brain disorders.

1.3 STRATEGIES FOR FORWARD, REVERSE, AND CHEMICAL GENETIC SCREENS

The general strategy for forward, reverse, and chemical genetic screens is outlined in **Figure 1.1**. It starts with a phenotype of interest, which is then developed into an assay with sufficient robustness, sensitivity and throughput suitable for screening. Such assay is then used to screen through a large number of individuals, with either mutagenized genomes (e.g. ENU, insertional

mutagenesis, or genome editing techniques), epigenetic alterations of gene expression (e.g., morpholino antisense oligonucleotide-based, RNAi, over-expression), or treated with small molecules (compound screening). Following the screen, phenotypic traits of interest will be uncovered, and further studies will allow the underlying molecular and cellular mechanisms to be elucidated.

1.4 GENERATION OF A LIBRARY OF INDUCED GENETIC OR EPIGENETIC VARIATIONS

Several methods and technologies can be used to create a library of individuals with random or targeted genetic or epigenetic variations. Some of these methodologies have been broadly used in zebrafish, whereas others have so far only been feasible in cell cultures or invertebrate genetic model organisms, and may be potentially applicable to zebrafish.

1.4.1 N-ethyl-N-nitrosourea mutagenesis

ENU mutagenesis is a classic approach to introduce random mutations throughout the genome. As a highly potent mutagen, ENU introduces random mutations into the genome of exposed individuals. Adult male zebrafish treated with ENU at appropriate doses will harbor random mutations in their germ-line. Upon mating with a wild-type female zebrafish, the next generation (F1) will carry random mutations in heterozygous states. Each F1 individual carries potentially unique mutations. These F1 individuals are then crossed with wild-type fish, producing F2 progeny heterozygous for the same mutation. In the F3 generation, homozygosity of induced mutations will be realized. F3s are used for phenotype-based screening to identify recessive loss-of-function mutations. To uncover dominant mutations, F1 or F2 generations can also be

used. ENU is highly efficient in inducing mutations in the zebrafish genome (Grunwald and Streisinger, 1992; Solnica-Krezel et al., 1994). The induced mutations are non-biased toward specific loci. One limitation with respect to ENU-based screens is its time-consuming nature, which involves three generations of breeding To circumvent this, early pressure induced gynogenesis has been used to uncover homozygosity in F2 generations (**Figure 1.2**) (Guo et al., 1999c).

1.4.2 CRISPR

In recent years, genome-editing technologies, in particular, CRISPR (*clustered regularly interspaced short palindromic repeats)* (Cong et al., 2013; Jinek et al., 2012; Mali et al, 2013), have made it possible to introduce mutations in principally any genes of interest. Double stranded DNA breaks (DSBs) can be induced in a targeted manner by delivering the bacterially derived endonuclease Cas9 and small guide RNA (sgRNA). Targeting specificity is achieved through DNA-RNA base pairing and Cas9 recognition of a short DNA sequence known as the protospacer adjacent motif (PAM). The resulting DSBs are most efficiently repaired by a mechanism known as non-homologous end joining (NHEJ). Due to the error-prone nature of NHEJ, small deletions or insertions are introduced at the site of DSBs, thereby leading to potentially deleterious mutations. While NHEJ is typically used to create a targeted gene knockout, homology directed repair (HDR) is an alternative repair mechanism that can allow for targeted knock-ins of a sequence of interest (Li et al., 2016). This process involves using a template to reconstruct the DSB, which can either come from the sister chromosome or be exogenously introduced.

CRISPR has been successfully applied to introduce mutations into zebrafish genes (Hwang et al., 2013; Jao et al., 2013; Li et al., 2016). The procedure (**Figure 1.3**) involves

micro-injection of the *cas9* gene product (in the form of either mRNA or protein) plus a sequence-specific sgRNA into one-cell stage zebrafish embryos. The injected embryos (F0) often carry single-allele mutations in some but not all cells (called mosaics), although in some cases with highly efficient sgRNAs and Cas9 protein delivery, widespread bi-allelic mutations can be accomplished in the injected embryos. Since the efficacy of sgRNAs vary significantly, it is important to assess the mutagenic efficiency of each sgRNA before proceeding to raise F0s for line propagation. Several methods are available, ranging from T7 endonuclease assay, surveyor assay, to restriction enzyme digestion, and sequencing. These assays are run on a pool of injected F0 embryos. Once the efficacy of sgRNAs is verified, injected F0 embryos can be raised to adulthood and used to produce F1s. Adult F1s (heterozygous for potential mutations) can then be genotyped for the presence and the nature of CRISPR induced mutations. Further breeding of F1s can lead to recovery of homozygous mutations in the F2 generation.

An advantage of using CRISPR is the possibility to create mutations on both chromosomes (bi-allelic targeting). Also, orthologous genes may be targeted simultaneously with ease. Lastly, though CRISPR has been described earlier in the text as a method for reverse genetics, the ease with which CRISPR-based gene targeting is performed may allow this method to be used essentially as a forward genetic approach: targeting a large number of genes and searching for their phenotypic effects.

Although the efficiency of CRISPR in inducing disruptive mutations is high, due to the short nature of the sgRNAs (20 nucleotides), there can be potential off-target effects. This is generally not a major concern in zebrafish, as off-target mutations can be separated from the mutations of interest through outcross breeding. Another limitation of CRISPR-based screening is the need to breed two generations before phenotypes of homozygous mutations can be assessed. This becomes a rather tedious process if a large number of genes are to be

screened. Methods to improve targeting efficiency that enable bi-allelic targeting in injected G0 embryos would circumvent these breeding needs. Another concern is a lack of phenotypes in CRISPR induced mutations (as opposed to morpholino antisense oligonucleotides [MOs] knockdown) due to potential genetic compensation (Rossi et al., 2015). However, a lack of phenotype is not specific to the CRISPR method.

1.4.3 Morpholino antisense oligonucleotides

The MOs are fast and effective tools for knocking down gene activity (Nasevicius and Ekker, 2000). They can be designed through sequence complementarity to interfere with either mRNA translation or splicing. A key limitation with MO is its transient effect that usually lasts several days after delivery into one-cell stage embryos. Its potential off-target effects can be managed through using multiple independent MOs to target the same gene and phenotypic rescue with co-expressing the target gene that is rendered MO-resistant.

1.4.4 RNA interference (RNAi)

RNA interference (RNAi) is a powerful approach to dissect gene function (Fire, 2007; Mello, 2007). It was originally discovered in *Caenorhabditis elegans*, where the observation of gene inactivation by both sense and antisense RNAs (Guo and Kemphues, 1995) led to the finding of dsRNA-mediated gene silencing (Fire et al., 1998). In vertebrates, the effectiveness of RNAi was hindered by the dsRNA-induced interferon response causing non-specific effects (Manche et al., 1992; Stark et al., 1998) until the finding of efficacious small interfering RNAs (siRNAs) (Elbashir et al., 2001). RNAi has proven effective in zebrafish when delivered with the

microRNA (miR-30) backbone and the Gal4/UAS system (Dong et al., 2013), which offers excellent versatility for spatiotemporal control together with amplification of gene expression level. While RNAi is highly effective when transiently expressed, stable transgenic lines so far yield moderate to weak effects, likely due to the presence of low or single copies of the transgene, resulting in insufficient knockdown. The potential off-target effects of RNAi can be ameliorated by designing multiple independent miR-shRNAs targeting the same gene of interest.

1.4.5 Gene overexpression

In addition to interfering with gene activity, over-expression of genes can also be used to assess the impact of genetic alterations on phenotypes. This becomes particularly useful when genetic redundancy is suspected. Gene overexpression-based screens also address the sufficiency of gene activity in generating phenotypes. Successful examples of gene over-expression screens include the early pressure (EP) screens in *Drosophila melanogaster* (Rørth, 1996), CRISPR-mediated gene activation screens in cultured cells (Konermann et al., 2015), and heat shock promoter-driven overexpression screens in zebrafish (Chiu et al., 2016). One caution with gene over-expression induced phenotypes is that sometimes they might not be physiologically relevant, especially when the expression level is too high and when no complementary phenotypes can be observed in loss-of-function studies.

1.4.6 Bioactive small molecules

Another powerful way to perturb gene activity is through the use of small molecules, which can

interact with gene products to either activate or inhibit their activity. Libraries of small molecules, including those with known activities and those composed of diverse and novel entities. Zebrafish, in particular, small sized embryonic and larval zebrafish that can be fit into 96-well plates, are well suited for small molecule screening, since these compounds can be directly added to the medium. Small molecule screening is easy and convenient to carry out. The challenge rests in identifying biological targets of the hit compounds and understanding their mechanisms of actions.

1.5 POSTSCREENING: EFFORTS TO DISCOVER UNDERLYING CELLULAR AND MOLECULAR MECHANISMS

Once a hit that alters the phenotypic trait of interest is uncovered, the next step is to gain insights into the underlying biological processes.

1.5.1 Post-ENU screening

Individual mutations identified from an ENU mutagenesis screen need to be first mapped to a chromosomal location. Such mapping is conducted by using existing genetic linkage maps, which contain many polymorphic markers (Shimoda et al., 1999). A large number of individuals derived from a cross between the mutation-containing strain and a polymorphic strain will be phenotyped and genotyped to uncover linkages. Once a linkage is detected, high resolution mapping within the region of interest can be carried out to pinpoint the gene. Such positional cloning method has been used to successfully map and identify a number of genes (Guo et al., 1999a; Guo et al., 1999b; Guo et al., 2000; Zhang et al., 1998). In recent years, the cost of

sequencing has been precipitously reduced, making it possible to employ whole-genome sequencing to uncover the causal mutations (Leshchiner et al., 2012; Obholzer et al., 2012). Here, pools of mutants and their wild-type siblings are collected for genomic DNA isolation and sequencing. Background polymorphisms unlinked to the mutation will be present equally in both the mutant and the sibling pools, whereas homozygosity for the mutation of interest will be unique to the mutant pool.

Once the causal mutations have been discovered, a variety of cellular molecular and biochemical techniques can be employed to understand how disruption of the particular gene might lead to the observed phenotypes.

1.5.2 Post-target-based screening (e.g., employing MO, RNAi, CRISPR, or overexpression)

Screens employing a library of agents, such as MOs, RNAi, CRISPR, or overexpression constructs, can uncover target gene(s) with ease. By nature, these libraries already have catalogued information on the target gene(s). However, it is worth noting that potential off-target effects are significant concerns with respect to these screens. Therefore, it is important to have multiple independent agents (e.g. two different shRNAs that target the same gene) for functional verification. Additionally, one also needs to bear in mind that different reagents or methods might differentially affect the activity of the same gene, resulting in different phenotypic consequences.

1.5.3 Post-small molecule screens

The result of a small molecule screen is a repertoire of compounds that can alter the phenotype

of interest. Depending on whether the small molecules are known bioactives or novel entities, different challenges lie ahead for target identification.

For known bioactive small molecules, it is relatively easy to uncover their biological targets. However, it is important to bear in mind that the known biological targets might not be the ones that mediate the observed effect. To validate, one shall perform molecular genetic experiments such as knockdown or overexpression of the candidate genes and determine whether it will mimic the effect of the small molecules.

For novel small molecules, it is a considerable challenge to uncover their biological targets. A commonly used method is affinity purification (Wagner and Schreiber, 2016). Also, the Similarity Ensemble Approach (SEA) (Keiser et al., 2007), which takes an organic molecule and compares it to sets of ligands annotated to biological activities/targets, can be used to uncover candidate biological targets for subsequent functional validation.

1.6 EXAMPLES OF SCREENS IN ZEBRAFISH

1.6.1 ENU- and small molecule-based screens to uncover mechanisms of neuronal subtype differentiation and maintenance

Understanding the generation of cellular diversity is a fundamental problem that is particularly daunting in the vertebrate nervous system, which contains many thousands of different neural cell types. To gain insights into the underlying molecular and cellular mechanisms, ENU-based screens have been carried out to uncover genes and pathways that control the differentiation of dopaminergic (DA) neurons (Guo et al., 1999c). DA neurons belong to the catecholaminergic (CA) neuronal groups, and they express the tyrosine hydroxylase (*th*) gene but are devoid of the

expression of dopamine beta-hydroxylase (*dbh*) gene. TH is an enzyme involved in the rate limiting step of the dopamine synthesis pathway, whereas DBH is responsible for conversion of dopamine to noradrenaline. Being present in small numbers and discrete locations in the brain, DA neurons play important roles in movement coordination, reward, and learning and memory. The loss of substantia nigra DA neurons in humans results in Parkinson's disease, the most common movement disorder and the second most common neurodegenerative disorder. After characterizing the distribution of CA neurons in developing zebrafish, an immunohistochemistry-based screen was used to find mutations that affect CA neuron number or identity. Around 700 ENU-mutagenized genomes were screened for these alterations, and five mutations were identified, causing defects in both DA and noradrenergic (NA) neurons. Subsequent molecular characterizations have revealed the identity of the disrupted genes (Guo et al., 1999a; Guo et al., 2000; Lee et al., 2003; Levkowitz et al., 2003; Wang et al., 2006). Three of the five genes encode cell type-specific transcriptional regulators. The other two encode general transcription regulators, one being a component of the mediator complex that controls transcription initiation and the other being a transcription elongation regulator (Guo et al., 2000). Similar screens have revealed additional regulators of DA neuron differentiation (Ryu et al., 2007).

A small molecule screen has uncovered compounds that regulate dopamine neuron maintenance (Sun et al., 2012). In this screen, 5,000 compounds composed of both known bio-actives and novel entities were tested for their effects on DA neuron development and/or survival via high throughput immunostaining in 96-well plates. After drug administration, antibodies against TH were used to visualize DA neurons in search of aberrant neuron number or morphology. One compound named neriifolin was identified; it impaired DA neuron survival but not that of noradrenergic sympathetic neurons. Further mechanistic studies show that its biological target, the Na^+/K^+ ATPase, is critical for maintaining DA neuron integrity.

1.6.2 ENU- and small molecule-based screen to study habituation

Unbiased behavioral screening is a powerful way to reveal novel mechanisms that regulate brain function. To be suitable for a screen, the behavioral assay of interest needs to be sensitive, robust, and can be performed in a relatively high throughput manner. The habituation behavior in larval zebrafish has been a successful example of behavioral screening-based studies. Habituation refers to decreased sensitivity toward repeated delivery of a sensory stimulus and is a fundamental form of behavioral plasticity or nonassociative learning that occurs for virtually all behavioral responses in virtually all organisms (Thompson, 2009). Five-day postfertilization (dpf) larval zebrafish exhibit a highly stereotyped acoustic startle response known as the short latency C-start (SLC). Repetitive acoustic stimuli result in habituation, and the modulation of this phenomenon has been studied via small molecule (Wolman and Granato, 2012) and ENU forward genetic screens (Wolman et al., 2015). Among 1760 known bioactive compounds screened, 11 were found to reduce startle habituation, while 19 increased it. Most targeted neurotransmitter systems were previously reported to affect mammalian startle modulation, suggesting conserved mechanisms between fish and mammals. Compounds previously unknown to be involved in regulating nonassociative learning were also uncovered. For the ENU screen, the same startle habituation assay was used to screen 405 mutagenized F2 families (corresponding to 614 genomes) and identify 14 habituation mutants. Whole genome sequencing was used to uncover the molecular identity of two mutants, one of which encodes a vertebrate specific gene *pregnancy associated plasma protein-aa* (*pappaa*). Further studies revealed a previously unknown role for PAPPAA-regulated IGF signaling in mediating habituation learning.

1.6.3 MO-based screen to uncover the function of candidate genes implicated in autism spectrum disorders (ASD)

MO is a fast and convenient tool to assess gene function during development. Two studies have employed this tool, together with over-expression, to determine which gene(s) might be responsible for ASD in a copy number variation (CNV) involving deletion or duplication of human chromosome 16p11.2 (Blaker-Lee et al., 2012; Golzio et al., 2012). In one study (Blaker-Lee et al., 2012), MOs targeting various zebrafish orthologues were individually micro-injected into early embryos, followed by phenotypic evaluations of morphology and behaviors including spontaneous movement and touch response. Two genes, adolase a and kinesin family member 22, were found to give clear phenotypes when their dosage was reduced by 50%, suggesting that these genes are dosage sensors. In the other study (Golzio et al., 2012), the authors focused on the microcephaly and macrocephaly phenotypes associated with the 16p11.2 duplication and deletion respectively. By gene overexpression studies, they found that one gene named *kctd13*, when over-expressed, led to decreased brain size, whereas MO knockdown of kctd13 led to macrocephaly. In mammalian cell cultures and brain slices, alterations of kctd13 activity affected cell proliferation. Together, MO-based screening help decipher candidate genes involved in complex human brain disorders.

1.6.4 CRISPR-based screen to uncover genes involved in electrical synapse formation

The efficiency of introducing mutations into the genome via CRISPR has been further improved for a candidate gene-based screen to uncover new regulators in electrical synapse formation (Shah et al., 2015). By testing various concentrations of Cas9 and sgRNAs, the authors determined the appropriate doses that resulted in an optimal balance of genome editing

efficiency and embryonic toxicity. Using a column- and row-based pooling strategy, 48 sgRNAs were screened, by microinjection into one-cell stage F0 embryos and imaging of electrical synapses at later stages of development in F0. Two genes with previously undescribed roles in electrical synapse formation were uncovered. Deep sequencing revealed that most target genes were successfully mutated with a frequency of 22% to 85%. Although a small scale, this study showed in principle the feasibility of screening for CRISPR-induced mutations in vivo. Further optimization to reduce mosaicism and increase sgRNA mutagenic efficiency will enable larger scale screens to be carried out.

1.6.5. Overexpression screen to identify regulators of sleep/wake states

The availability of the Tol2 transposon system and Tol2 transposase (Kawakami et al., 2000) makes it possible to perform a primary screen of gene overexpression in the injected embryos/larvae. In a study aimed at identifying regulators of sleep/wake states (Chiu et al., 2016), a publicly available set of human open reading frames (ORF) that encode secreted proteins were cloned into the Tol2 vector under the control of a heat shock promoter. Individual plasmids were injected into one-cell stage embryos together with the transposase mRNA. For each ORF, 32 injected embryos were tested in the sleep/wake assay along with 16 matched controls injected with either hs:EGFP or an empty hs vector. The sleep/wake assay involves tracking larval zebrafish locomotor activity both pre- and post-heat shock, and parameters including number and length of sleep bouts, sleep latency at night, and changes in activity levels were quantified. After 1432 experiments that tested 1286 unique ORFs covering 1126 unique genes (29% of the human Secretome), 60 ORFs were selected to confirm in stable transgenic lines. Ten gave reproducible phenotypes as expected from the primary screen and another two lines gave unexpected phenotypes. Among them, Neuromedin U (Nmu), when over-expressed,

significantly increased locomotor activity. *In situ* hybridization of its orthologue in zebrafish revealed that the *nmu* gene is expressed in the hypothalamus, brainstem, and spinal cord, similar to the reported expression in mammals. Using genome editing technologies, the authors generated mutations in the *nmu* gene, and its receptor encoding genes *nmur1a*, *1b*, and *2*. Analyses of these genetic mutations revealed complementary and at times redundant actions in arousal, activity, and body size. Further mechanistic studies uncovered the brainstem corticotropin releasing factor neurons as a mediator of Nmu function in sleep/wake regulation.

1.7 UNCOVERING CELLULAR AND MOLECULAR MECHANISMS THROUGH STUDYING NATURAL PHENOTYPIC VARIATIONS

Another unique resource to uncover cellular and molecular mechanisms underlying complex brain phenotypes is to study natural phenotypic variations, which already exist in the population and thus obviating the need to perform screens. Often, natural phenotypic variations represent traits that mimic complex human brain disorders.

Studies of natural phenotypic variations in model organisms such as *Caenorhabditis elegans*, *Drosophila melanogaster*, honeybees, and mice have revealed important insights into behavioral regulation (Ben-Shahar et al., 2002; de Bono and Bargmann, 1998; Osborne et al., 1997). Similar studies have not been carried out in zebrafish, except some characterizations with behavioral lateralizations (Facchin et al., 2009).

We have recently discovered a natural behavioral variation in light/dark preference, which is associated with anxiety in larval zebrafish (Wagle et al., 2017). Preference for light or dark environment is an evolutionarily conserved phenomenon (Bourin and Hascoët, 2003; Gong et al., 2010). Adult zebrafish display a natural preference for dark, which is shown to be fear/anxiety-related (Lau et al., 2011; Maximino et al., 2010). Intriguingly, larval zebrafish of

around 1-week of age show opposite preference, dark aversion, which is also fear/anxiety-related (Bai et al., 2016; Chen et al., 2015; Lau et al., 2011; Steenbergen et al., 2011). By testing 200 individual larvae derived from the wild-type laboratory strain AB, we found three phenotypic variations with respect to this behavior: a small subset of individuals displayed strong dark aversion (*sda*) with little variability across four trials, another small subset of individuals displayed variable dark aversion across the four trials (*vda*), whereas the majority showed medium level of dark aversion (*mda*). Selective breeding of these traits uncovered that sda and vda are heritable, with sda being recessive and vda being dominant to the common allele(s). The *sda* individuals also displayed heightened thigmotaxis behavior, another measure of anxiety-like behavior in larval zebrafish. Future molecular genetic studies shall reveal the cellular circuitry and molecular mechanisms underlying this natural behavioral variation.

1.8 CONCLUSION

It is a daunting challenge to understand and treat complex brain disorders including autism, addiction, schizophrenia, anxiety and depression. Molecular genetic studies of complex brain phenotypes employing screening in zebrafish as described in this chapter represent a promising approach that shall reveal important insights into brain development, maintenance, and function, and pave the way for tackling complex brain disorders in humans. The methods as described in this chapter have their own strengths and limitations. For instance, ENU screens are time consuming and labor intensive, so screening has been largely limited to phenotypes that can be very rapidly assessed. Also, mutations in small genes are underrepresented, and identifying the mutated genes requires laborious mapping and positional cloning. CRISPR screens can potentially be carried out with fewer generations to breed. Because labor is reduced,

phenotypes that are relatively subtle or more time consuming to measure can be assayed. Since the target genes are already known, negative results become informative. Also, since genes that affect particular phenotypes are rare, multiple genes can be targeted in the same founder animals to increase throughput and efficiency. Together, the readers shall evaluate and decide which methods to employ based on specific interests. For all screening methods, having a robust, sensitive, and relatively high throughput assay is always an important prerequisite.

1.9 ACKNOWLEDGMENTS

The work in authors' laboratory is supported by the US National Institute of Health (DA035680, NS095734, MH113961, DA044007, 2T32GM007175-41). We thank Michael Munchua, Hongbin Yuan, and Xingnu Zhai for excellent fish care.

1.10 FIGURES

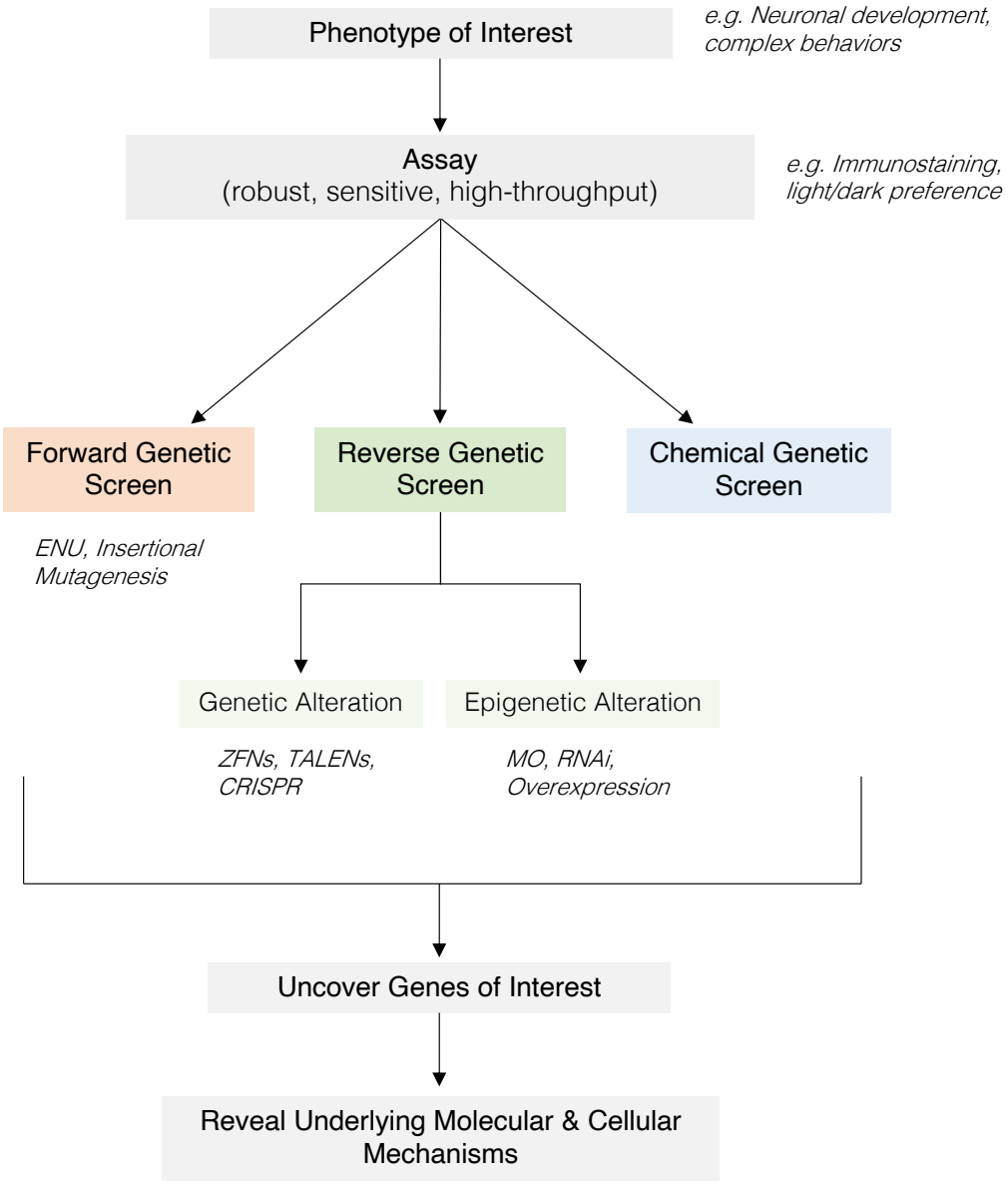

Figure 1.1 Schematic of genetic screening.

The process begins with a phenotype of interest. An assay that is preferably robust, sensitive, and high-throughput must be chosen to test this phenotype. A variety of genetic screens can then be utilized with this assay: forward, reverse, and chemical. Forward genetic screens start by producing many random mutations. Any aberrant phenotypes are identified, then investigated to find the gene responsible (ENU, insertional mutagenesis). Conversely, reverse genetic screens start with specific gene targets in search of an abnormal phenotype. Reverse

genetics can involve either permanent edits to the germ line (CRISPR, ZFNs, TALENs), or transient epigenetic alterations (MO, RNAi, overexpression). Small molecules are administered in chemical genetic screens. The results from these screens help to uncover genes that play a role in modulating the phenotype, providing insight on the molecular and cellular mechanisms at play.

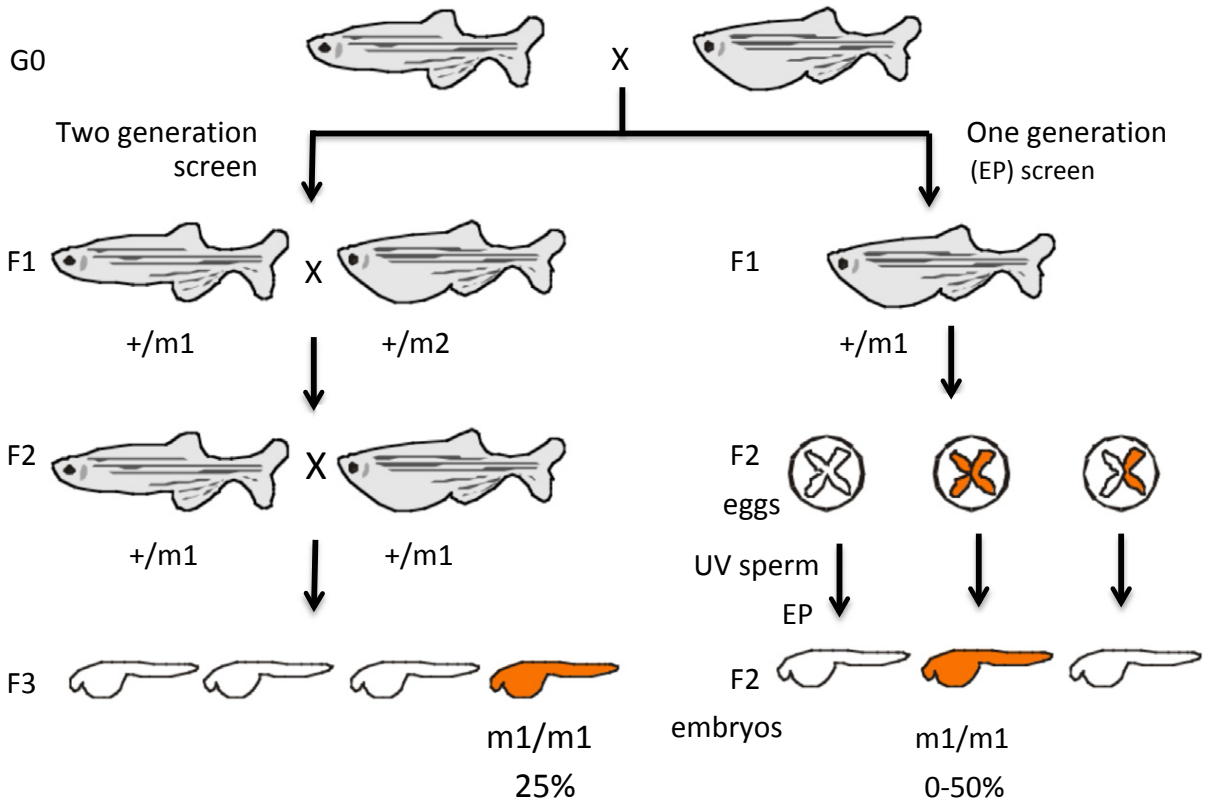

Figure 1.2 Schematic of ENU screening.

Two or one generation breeding can be carried out to screen for recessive mutant phenotypes following ENU mutagenesis. (Left) Standard two-generation breeding to obtain 25% homozygous individuals in the F3 generation. (Right) To shorten the breeding time needed, F2 oocytes can be collected from F1 females, in vitro fertilized with UV-irradiated sperm, resulting in the activation of embryonic development without contributing genetic material. Subsequently, early pressure (EP) is applied to the eggs to prevent second meiosis and enable gynogenetic development. Depending on the location of the mutated loci relative to centromeres, 0%-50% of homozygous mutants can be obtained in the F2 generation.

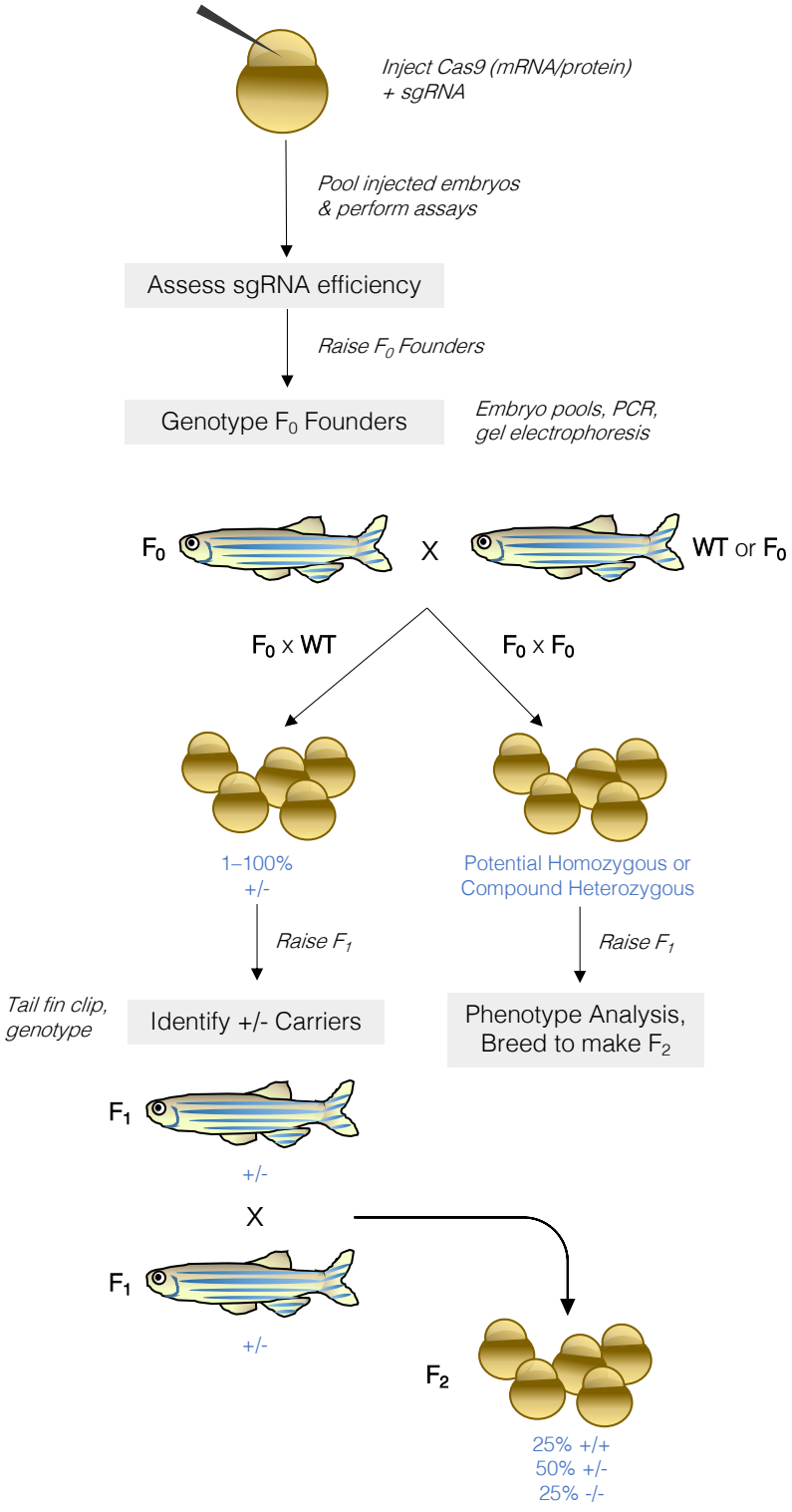

Figure 1.3 Introducing genetic alterations via CRISPR-Cas9.

Using CRISPR technology to produce gene edits begins with injection of both Cas9 (either mRNA or protein) and sgRNA for the gene of interest. The injected embryos are then pooled,

and a variety of assays can be run to determine efficiency of the sgRNA (e.g. T7 endonuclease assay, surveyor assay, sequencing, etc.). Once mutations are confirmed, the F0 generation is raised to adulthood. As adults, they are genotyped to identify any induced genetic alterations. This is done by pooling together a clutch of their embryos, PCR, and gel electrophoresis. When F0 individuals carrying mutations are identified, they can be crossed either with a wild type fish (outcross), or another F0 individual (incross). The outcross results in F1 progeny that are 1-100% heterozygous (due to the mosaicism of the F0 founder). When this F1 generation reaches adulthood, they are genotyped to confirm individuals heterozygous for a mutation in the gene of interest. Two heterozygous fish are then crossed to produce the F2 generation, which is 25% wild type, 50% heterozygous, and 25% homozygous for the mutation. On the other hand, if the F0 fish are incrossed, progeny is produced that are either homozygous for the same mutation or compound heterozygous: containing two different mutations in the gene of interest. These F1 fish can be used for both phenotype analysis and the creation of the F2 generation.

1.11 REFERENCES

Bai, Y., Liu, H., Huang, B., Wagle, M. & Guo, S. Identification of environmental stressors and validation of light preference as a measure of anxiety in larval zebrafish. BMC Neurosci. 17, 63 (2016).

Ben-Shahar, Y., Robichon, A., Sokolowski, M. B. & Robinson, G. E. Influence of gene action across different time scales on behavior. Science 296, 741-744 (2002).

Blaker-Lee, A., Gupta, S., McCammon, J. M., De Rienzo, G. & Sive, H. Zebrafish homologs of genes within 16p11.2, a genomic region associated with brain disorders, are active during brain development, and include two deletion dosage sensor genes. Dis. Model Mech. 5, 834-851 (2012).

Bourin, M. & Hascoët, M. The mouse light/dark box test. . Eur. J. Pharmacol. 463, 55-65 (2003).

Chen, F., Chen, S., Liu, S., Zhang, C. & Peng, G. Effects of lorazepam and WAY-200070 in larval zebrafish light/dark choice test. Neuropharmacology 95, 226-233 (2015).

Chiu, C. N., Rihel, J., Lee, D. A., Singh, C., Mosser, E. A., Chen, S., Sapin, V., Pham, U., Engle, J., Niles, B. J., Montz, C. J., Chakravarthy, S., Zimmerman, S., Salehi-Ashtiani, K., Vidal, M., Schier, A. F. & Prober, D. A. A Zebrafish Genetic Screen Identifies Neuromedin U as a Regulator of Sleep/Wake States. Neuron 89, 842-856 (2016).

Cong, L., Ran, F. A., Cox, D., Lin, S., Barretto, R., Habib, N., Hsu, P. D., Wu, X., Jiang, W., Marraffini, L. A. & Zhang, F. Multiplex genome engineering using CRISPR/Cas systems. Science 339, 819-823 (2013).

de Bono, M. & Bargmann, C. I. Natural variation in a neuropeptide Y receptor homolog modifies social behavior and food response in C. elegans. Cell 94, 679-689 (1998).

Dong, Z., Peng, J. & Guo, S. Stable gene silencing in zebrafish with spatiotemporally targetable RNA interference. Genetics 193, 1065-1071 (2013).

Driever, W., Solnica-Krezel, L., Schier, A. F., Neuhauss, S. C. F., Malicki, J., Stemple, D. L., Stainier, D. Y. R., Zwartkruis, F., Abdelilah, S., Rangini, Z., Belak, J. & Boggs, C. A genetic screen for mutations affecting embryogenesis in zebrafish. Development 123, 37-46 (1996).

Elbashir, S. M., Harborth, J., Lendeckel, W., Yalcin, A., Weber, K. & Tuschl, T. Duplexes of 21-nucleotide RNAs mediate RNA interference in cultured mammalian cells. Nature 411, 494-498 (2001).

Facchin, L., Argenton, F. & Bisazza, A. Lines of Danio rerio selected for opposite behavioural lateralization show differences in anatomical left-right asymmetries. Behav. Brain Res. 197, 157-165 (2009).

Fire, A. Z. Gene silencing by double-stranded RNA. Cell Death Differ. 14, 1998-2012 (2007).

Fire, A., Xu, S., Montgomery, M. K., Kostas, S. A., Driver, S. E. & Mello, C. C. Potent and

specific genetic interference by double-stranded RNA in Caenorhabditis elegans. Nature 391, 806-811 (1998).

Golzio, C., Willer, J., Talkowski, M. E., Oh, E. C., Taniguchi, Y., Jacquemont, S., Reymond, A., Sun, M., Sawa, A., Gusella, J. F., Kamiya, A., Beckmann, J. S. & Katsanis, N. KCTD13 is a major driver of mirrored neuroanatomical phenotypes of the 16p11.2 copy number variant. Nature 485, 363-367 (2012).

Gong, Z., Liu, J., Guo, C., Zhou, Y., Teng, Y. & Liu, L. Two pairs of neurons in the central brain control Drosophila innate light preference. Science 330, 499-502 (2010).

Grunwald, D. J. & Eisen, J. S. Headwaters of the zebrafish-emergence of a new model vertebrate. Nat. Rev. Genet. 3, 717-724 (2002).

Grunwald, D. J. & Streisinger, G. Induction of recessive lethal and specific locus mutations in the zebrafish with ethyl nitrosourea. Genet. Res. 59, 103-116 (1992).

Guo, S. & Kemphues, K. J. par-1, a gene required for establishing polarity in C. elegans embryos, encodes a putative ser/thr kinase that is asymmetrically distributed. Cell 81, 611-620 (1995).

Guo, S. Linking genes to brain, behavior, and neurological diseases: what can we learn from zebrafish? Genes, Brain & Behav. 3, 63-74 (2004).

Guo, S., Brush, J., Teraoka, H., Goddard, A., Wilson, S. W., Mullins, M. C. & Rosenthal, A.

Development of noradrenergic neurons in the zebrafish hindbrain requires BMP, FGF8, and the homeodomain protein Soulless/Phox2a. Neuron 24, 555-566 (1999a).

Guo, S., Driever, W. & Rosenthal, A. Mutagenesis in zebrafish: studying the brain dopamine systems. Handbook of Molecular-Genetic Techniques for Brain and Behavior Research Chapt.2.1.8, 166-176 (1999b).

Guo, S., Wilson, S. W., Cooke, S., Chitnis, A. B., Driever, W. & Rosenthal, A. Mutations in the zebrafish unmask shared regulatory pathways controlling the development of catecholaminergic neurons. Dev. Biol. 208, 473-487 (1999c).

Guo, S., Yamaguchi, Y., Schilbach, S., Wada, T., Goddard, A., Lee, J., French, D., Handa, H. & Rosenthal, A. A regulator of transcriptional elongation, which is required for vertebrate neuronal development. Nature 408, 366-369 (2000).

Haffter, P., Granato, M., Brand, M., Mullins, M. C., Hammerschmidt, M., Kane, D. A., Odenthal, J., Van Eeden, F. J. M., Jiang, Y. J., Heisenberg, C. P., Kelsh, R. N., Furutani-Seiki, M., Vogelsang, E., Beuchle, D., Schach, U., Fabian, C. & Nusslein-Volhard, C. The identification of genes with unique and essential function in the development of the zebrafish, Danio rerio. Development 123, 1-36 (1996).

Hwang, W. Y., Fu, Y., Reyon, D., Maeder, M. L., Tsai, S. Q., Sander, J. D., Peterson, R. T., Yeh, J. R. & Joung, J. K. Efficient genome editing in zebrafish using a CRISPR-Cas system. Nat. Biotechnol. 31, 227-229 (2013).

Jao, L. E., Wente, S. R. & Chen, W. Efficient multiplex biallelic zebrafish genome editing using a CRISPR nuclease system. Proc. Natl. Acad. Sci. 110, 13904-13909 (2013).

Jinek, M., Chylinski, K., Fonfara, I., Hauer, M., Doudna, J. A. & Charpentier, E. A programmable dual-RNA-guided DNA endonuclease in adaptive bacterial immunity. Science 337, 816-821 (2012).

Kawakami, K., Shima, A., Kawakami, N. Idenification of a functional transposase of the Tol2 element, an Ac-like element from the Japanese medaka fish, and its transposition in the zebrafish germ lineage. Proc Natl Acad Sci. 97, 11403-11408 (2000).

Keiser, M. J., Roth, B. L., Armbruster, B. N., Ernsberger, P., Irwin, J. J. & Shoichet, B. K. Relating protein pharmacology by their ligand chemistry. Nat. Biotech. 25, 197-206 (2007).

Kimmel, C. B. Patterning the brain of the zebrafish embryo. Annu. Rev. Neurosci. 16, 707-732 (1993).

Kimmel, C. B., Ballard, W. W., Kimmel, S. R., Ullmann, B. & Schilling, T. F. Stages of embryonic development of the zebrafish. Dev. Dyn. 203, 253-310 (1995).

Konermann, S., Brigham, M. D., Trevino, A. E., Joung, J., Abudayyeh, O. O., Barcena, C., Hsu, P. D., Habib, N., Gootenberg, J. S., Nishimasu, H., Nureki, O. & Zhang, F. Genome-scale transcriptional activation by an engineered CRISPR-Cas9 complex. Nature 517, 583-588 (2015).

Lau, B. Y. B., Mathur, P., Gould, G. G. & Guo, S. Identification of a brain center whose activity discriminates a choice behavior in zebrafish. Proc. Natl. Acad. Sci. U S A 108, 2581-2586 (2011).

Lee, S. A., Shen, E. L., Fiser, A., Sali, A. & Guo, S. The zebrafish forkhead transcription factor Foxi1 specifies epibranchial placode-derived sensory neurons. Development 130, 2669-2679 (2003).

Leshchiner, I., Alexa, K., Kelsey, P., Adzhubei, I., Austin-Tse, C. A., Cooney, J. D., Anderson, H., King, M. J., Stottmann, R. W., Garnaas, M. K., Ha, S., Drummond, I. A., Paw, B. H., North, T. E., Beier, D. R., Goessling, W. & Sunyaev, S. R. Mutation mapping and identification by whole-genome sequencing. Genome Res. 22, 1541-1548 (2012).

Levkowitz, G., Zeller, J., Sirotkin, H. I., French, D., Schilbach, S., Hashimoto, H., Hibi, M., Talbot, W. S. & Rosenthal, A. Zinc finger protein too few controls the development of monoaminergic neurons. Nat. Neurosci. 6, 28-33 (2003).

Li, M., Zhao, L., Page-McCaw, P. S. & Chen, W. Zebrafish Genome Engineering Using the CRISPR-Cas9 System. Trends Genet. 32, 815-827 (2016).

Mali, P., Yang, L., Esvelt, K. M., Aach, J., Guell, M., DiCarlo, J. E., Norville, J. E. & Church, G. M. RNA-guided human genome engineering via Cas9. Science 339, 823-826 (2013).

Manche, L., Green, S. R., Schmedt, C. & Mathews, M. B. Interactions between double-stranded RNA regulators and the protein kinase DAI. Mol. Cell Biol. 12, 5238-5248 (1992).

Maximino, C., Marques de Brito, T., Dias, C. A., Gouveia, A. J. & Morato, S. Scototaxis as anxiety-like behavior in fish. Nat. Protoc. 5, 209-216 (2010).

Mello, C. C. Return to the RNAi world: rethinking gene expression and evolution. Cell Death Differ. 14, 2013-2020 (2007).

Nasevicius, A. & Ekker, S. C. Effective targeted gene "knockdown" in zebrafish. Nat. Genet. 26, 216-220 (2000).

Obholzer, N., Swinburne, I. A., Schwab, E., Nechiporuk, A. V., Nicolson, T. & Megason, S. G. Rapid positional cloning of zebrafish mutations by linkage and homozygosity mapping using whole-genome sequencing. Development 139, 4380-4390 (2012).

Osborne, K. A., Robichon, A., Burgess, E., Butland, S., Shaw, R. A., Coulthard, A., Pereira, H. S., Greenspan, R. J. & Sokolowski, M. B. Natural behavior polymorphism due to a cGMP-dependent protein kinase of Drosophila. Science 277, 834-836 (1997).

Rørth, P. A modular misexpression screen in Drosophila detecting tissue-specific phenotypes. Proc. Natl. Acad. Sci. 93, 12318-12322 (1996).

Rossi, A., Kontarakis, Z., Gerri, C., Nolte, H., Holper, S., Kruger, M. & Stainier, D. Y. R. Genetic compensation induced by deleterious mutations but not gene knockdowns. . Nature 524, 230-233 (2015).

Ryu, S., Mahler, J., Acampora, D., Holzschuh, J., Erhardt, S., Omodei, D., Simeone, A. &

Driever, W. Orthopedia homeodomain protein is essential for diencephalic dopaminergic neuron development. Curr. Biol. 17, 873-880 (2007).

Shah, A. N., Davey, C. F., Whitebirch, A. C., Miller, A. C. & Moens, C. B. Rapid reverse genetic screening using CRISPR in zebrafish. Nat. Methods 12, 535-540 (2015).

Shimoda, N., Knapik, E. W., Ziniti, J., Sim, C., Yamada, E., Kaplan, S., Jackson, D., de Sauvage, F., Jacob, H. & Fishman, M. C. Zebrafish genetic map with 2000 microsatellite markers. Gnomics 58, 219-232 (1999).

Solnica-Krezel, L., Schier, A. F. & Driever, W. Efficient recovery of ENU-induced mutations from the zebrafish germline. Genetics 136, 1401-1420 (1994).

Stark, G. R., Kerr, I. M., Williams, B. R., Silverman, R. H. & Schreiber, R. D. How cells respond to interferons. Annu. Rev. Biochem. 67, 227-264 (1998).

Steenbergen, P. J., Richardson, M. K. & Champagne, D. L. Patterns of Avoidance Behaviours in the Light/Dark Preference Test in Young Juvenile Zebrafish: A Pharmacological Study. Behav. Brain Res. 222, 15-25 (2011).

Streisinger, G., Walker, C., Dower, N., Knauber, D. & Singer, F. Production of clones of homozygous diploid zebra fish (brachydanio rerio). Nature 291, 293-296 (1981).

Sun, Y., Dong, Z., Khodabakhsh, H., Chatterjee, S. & Guo, S. Zebrafish chemical screening reveals the impairment of dopaminergic neuronal survival by cardiac glycosides. PLoS One 7,

e35645 (2012).

Thompson, R. F. Habituation: a history. . Neurobiol. Learn Mem 92, 127-134 (2009).

Wagle, M., Nguyen, J., Lee, S., Zaitlen, N. & Guo, S. Heritable natural variation of an anxiety-like behavior in larval zebrafish. J. Neurogenet. 31, 138-148 (2017).

Wagner, B. K. & Schreiber, S. L. The Power of Sophisticated Phenotypic Screening and Modern Mechanism-of-Action Methods. Cell Chem. Biol. 23, 3-9 (2016).

Wang, X., Yang, N., Uno, E., Roeder, R. G. & Guo, S. A subunit of the mediator complex regulates vertebrate neuronal development. Proc. Natl. Acad. Sci. 103, 17284-17289 (2006).

Wolman, M. & Granato, M. Behavioral genetics in larval zebrafish: learning from the young. Dev. Neurobiol. 72, 366-372 (2012).

Wolman, M. A., Jain, R. A., Marsden, K. C., Bell, H., Skinner, J., Hayer, K. E., Hogenesch, J. B. & Granato, M. A genome-wide screen identifies PAPP-AA-mediated IGFR signaling as a novel regulator of habituation learning. Neuron 85, 1200-1211 (2015).

Zhang, J., Talbot, W. S. & Schier, A. F. Positional cloning identifies zebrafish one-eyed pinhead as a permissive EGF-related ligand required during gastrulation. Cell 92, 241-251 (1998).

CHAPTER 2: Role of the Endocannabinoid System in Vertebrates: Emphasis on the Zebrafish Model

2.1 ABSTRACT

The endocannabinoid (eCB) system, named after the plant *Cannabis sativa,* comprises cannabinoid receptors, endogenous ligands known as “endocannabinoids”, and enzymes involved in the biosynthesis and degradation of these ligands, as well as putative transporters for these ligands. eCB proteins and small molecules have been detected in early embryonic stages of many vertebrate models. As a result, cannabinoid receptors and endogenous as well as exogenous cannabinoids influence development and behavior in many vertebrate species. Understanding the precise mechanisms of action for the eCB system will provide an invaluable guide towards elucidation of vertebrate development and will also help delineate how developmental exposure to marijuana might impact health and cognitive and cognitive/executive functioning in adulthood. Here we review the developmental roles of the eCB system in vertebrates, focusing our attention on the zebrafish model. Since little is known regarding the eCBs in zebrafish, we provide new data on the expression profiles of eCB genes during development and in adult tissue types of this model organism. We also highlight exciting areas for future investigations, including the synaptic regulation of the eCB system, its role in reward and addiction, and in nervous system development and plasticity.

2.2 INTRODUCTION

After the first cannabinoid receptor CB1 was identified as a binding site for psychotropic cannabinoids and cloned for further localization studies (Herkenham et al. 1990; Matsuda et al. 1990), many laboratories started to investigate the phenomenon previously associated with the consumption of cannabinoids, including the feeling of happiness, excitement, dissociation of ideas, spatiotemporal errors, mood fluctuation, illusion, and hallucinations (Moreau 1973).

Researchers explored the physiological roles of this receptor, and in turn discovered anandamide (AEA) (Devane et al. 1992) and 2-arachidonoylglycerol (2-AG) (Mechoulam et al. 1996) as endogenous ligands for CB1. Both ligands specifically interact with CB1 leading to the inhibition of adenylyl cyclase (Howlett et al. 2010). In addition, a second cannabinoid receptor CB2, which shared 48% identity with CB1, was identified. CB2 is mostly expressed in the spleen, suggesting a role in the immune system (Munro et al. 1993). The set of cannabinoid receptors, the two endocannabinoids and the enzymes responsible for their synthesis and degradation are together known as the endocannabinoid (eCB) system.

The eCB system has received considerable attention from the research community. More than 16,000 papers can be found on the NCBI website (PubMed) using keyword searches for “cannabinoid receptor” and “endocannabinoid system”. Despite these advances, the diversity of actions characterizing the stimulation of the two receptors by endogenous and exogenous ligands remains incompletely understood. In particular, the roles of the eCB system in anxiety, reward and addiction, and their impact on embryonic and postnatal development await further investigations.

In this chapter, we will first highlight the eCB system for its known synaptic actions and role in reward and addiction. Evolutionary considerations will then be given by discussing the eCB system in mammals and amphibians. Due to the focus on zebrafish, the current state of knowledge of the eCB system will be subsequently discussed in greater detail in this model organism. Finally, we present new data on the spatiotemporal expression profiles of the eCB system in zebrafish to bridge this knowledge gap.

2.3 ROLE OF THE ENDOCANNABINOID SYSTEM

2.3.1 eCB system signaling at the synapse

The two major cannabinoid receptors, CB1 and CB2, belong to the large family of seven transmembrane-spanning G-protein-coupled receptors (GPCRs) (Matsuda et al. 1990; Munro et al. 1993). Genes encoding orthologues of the mammalian CB1 are found throughout vertebrates including chicken, turtle, frog, and fish (Elphick & Egertova 2001). Within the central nervous system (CNS), the two endocannabinoids are synthesized and released “on demand” into the synaptic cleft, where they work as retrograde synaptic messengers through binding to the CB receptors on the presynaptic terminal of neurons (Elphick & Egertova 2005; Chevaleyre et al. 2006). The activation of cannabinoid receptors in turn inhibits the release of many neurotransmitters (e. g. serotonin, glycine, gamma-aminobutyric acid, glutamate, cholecystokinin). Specific catabolic enzymes are then responsible for the degradation of the ligands. The eCB signaling pathway at the synapse is described in greater detail in **Figure 2.1** and a schematic representation showing gene relationship and function is shown in **Figure 2.2**. Moreover, **Table 2.1** summarizes eCB gene names and function.

2.3.2 Role of the eCBs in Reward and Addiction

The role of the eCB system in reward processing and motivated behaviors has been extensively studied. The ventral tegmental area (VTA) and the nucleus accumbens (NAc) play central roles in the processing of rewarding stimuli and in drug addiction. The VTA also contains at least two additional neuronal phenotypes that are not dopaminergic (DA) (Cameron et al. 1997). DA

neurons produce endogenous cannabinoids to regulate their own activity through the interaction with the afferent neurons: current data support a CB1 receptor-mediated increase in dopamine neuron activity, due to induction of local disinhibitory mechanisms, such as depolarization-induced suppression of inhibition (DSI) or depolarization-induced suppression of excitation (DSE) at inhibitory (i.e., GABAergic) or excitatory (i.e., glutamatergic) synapses, respectively (Zlebnik & Cheer 2016). Previous findings on addiction showed that AEA and its synthetic analog methanandamide are effective reinforcers of intravenous self-administration behavior in squirrel monkeys, an animal model of human drug abuse and suggests that medications that promote the actions of endogenously released cannabinoids could also activate brain reward processes and have the potential for abuse (Justinova et al. 2005). It is important to understand how marijuana can mediate these effects. There is evidence that cannabis is mildly addictive: around 9% of users become dependent on the drug, showing signs of addiction such as developing tolerance or experiencing withdrawal symptoms (Cressey 2015). It has been demonstrated that the psychoactive component of marijuana, Δ^9-tetrahydrocannabinol (THC), alters the activity of central reward pathways in a manner that is consistent with other abused drugs but the cellular mechanisms through which this occurs rely upon the combined regulation of several afferent pathways to the VTA (Lupica et al. 2004). The precise mechanism by which the eCB system facilitates DA burst firing *in vivo* is yet to be fully understood.

2.3.3 The Evolution of the eCBs

The eCB system is widely conserved across organisms, although the patterns of evolution for each protein vary. CB receptor genes appear to be present only in chordates (Elphick 2012). It is believed that CB1 and CB2 arose from a gene duplication event of a common ancestral gene. Remarkably, duplicate CB receptor genes have been found in teleosts. For example, zebrafish

have two cb2 genes, and puffer fish have two cb1 genes (Elphick & Egertova 2001). This may be evidence of a second gene duplication event in a common ancestor of these fish, followed by loss of a gene copy in subsequent families. Unlike CB receptors, DAGLs (2-AG synthesis enzymes) are more widely conserved among bacteria, fungi, plants, and animals (Yuan et al. 2016). However, DAGL substrate selectivity across organisms differs. For example, mammalian DAGL specifically hydrolyzes DAGs, while bacterial DAGL can catalyze hydrolysis of DAG, MAG, and glycerol. It is worth noting that the two isoforms of DAGL, DAGLa and DAGLb, have distinct evolutionary patterns. Yuan et al. compiled a thorough account of the similarities and differences between the evolutions of each isoform. As with DAGL, 2-AG is also largely conserved. 2-AG has been found in animals as primitive as fresh water polyps (De Petrocellis et al. 1999). The 2-AG degradation enzyme MGLL is also largely conserved across many different phyla; it is found in animals such as placozoans and cnidarians. However, several insect species like *Drosophila melanogaster* lost this gene (Elphick 2012). ABHD4 is one of the proteins suggested to be involved in AEA biosynthesis and is also highly conserved, having orthologues in a wide variety of species from fruit flies and lizards to mammals (Ensembl Genome Browser). FAAH and FAAH2, enzymes involved in the degradation of AEA, likely underwent a gene duplication event in an ancestral animal preceding organisms with nervous systems. Though these genes are prevalent across species, certain lineages lost one of these genes. For example, rodents lack FAAH2, and insect species like *Drosophila* lack FAAH (Elphick 2012). Lastly, the cannabinoid receptor interacting protein CRIP1A is thought to originate in the first organisms with nervous systems; this protein is ubiquitous and has been found in species such as *N. vectenses* (cnidaria) and *C. elegans* (nematoda). Even though CRIP1A interacts with CB1, its origins significantly precede CB receptor appearance, suggesting other functions for this protein in addition to interacting with CB receptors (Elphick 2012).

2.3.4 The eCB system in developing mammals

The eCB system, with its metabolic enzymes, receptors, and secondary messenger cascades, plays a major role in development/neurodevelopment. Understanding of the signaling pathways will help reveal the basis of developmental defects that are associated with prenatal drug abuse. The presence of CB1 receptor at early developmental stages suggests that the eCB system contributes to CNS development, such as axonal elongation, myelination, migration, cell proliferation, and synaptogenesis (Fernandez-Ruiz et al. 2000). Multiple studies have shown that mRNA expression of the CB1 receptor is distributed in both the fetal and neonatal rat brain (Romero et al. 1997; Berrendero et al. 1998, 1999). CB1 activity and receptor binding can be identified as early as 14 gestational days old, which overlap with the expression of most neurotransmitters (Insel 1995). In mammals, the CB1 receptor plays a major role in neural progenitor proliferation and survival. The proliferation of neural progenitor cells has been associated with the dependence of the activation of the CB1 receptor in areas such as the cerebellum and hippocampus (Trazzi et al. 2010). Studies using knockout mice demonstrated that inactivation of both the CB1 and CB2 receptor impairs neural progenitor cell proliferation (Aguado et al. 2005; Palazuelos et al. 2006). Also, reduced CB1 function *in vivo* is frequently linked to alterations with regards to hippocampal and cortical development (Aguado et al. 2005; Zurolo et al. 2010). It is shown that mice lacking CB1 receptors have suppressed cortical progenitor proliferation (Aguado et al. 2005; Mulder et al. 2008).

AEA and 2-AG are present throughout prenatal development, but fluctuate and vary with a wide range (Berrendero et al. 1999; Fernandez-Ruiz et al. 2000). In mice, AEA has been associated with the activation of embryo implantation inside the uterus during days 4–6 of pregnancy (Paria et al. 2001). Throughout perinatal development, AEA levels are low at mid-gestation but increase gradually until adulthood (Berrendero et al. 1999). However, fetal 2-AG

levels are approximately the same concentration in young and adult rat brains, with only a distinguishable surge of 2-AG immediately after birth (Berrendero et al. 1999; Fernandez-Ruiz et al. 2000). Overall, it has been observed that in adult brains, the concentrations of 2-AG are much greater than the levels of AEA, a difference of 2000–8000 pmol/g of tissue versus 3–6 pmol/g of tissue, respectively (Berrendero et al. 1999; Fernandez-Ruiz et al. 2000).

In humans, the CB1 receptor is saturated in the cerebellum, hippocampus, caudate nucleus, and cerebral cortex and is evident in the brain as early as prenatal development. At just gestational week 9, the CB1 receptor can be found in Cajal–Retzius cells and in the sub-ventricular zone (Zurolo et al. 2010). During the second trimester of gestation, CB1 receptors can be traced in the hippocampal CA region (Wang et al. 2003). However, the high concentrations of the CB1 receptor in fiber-enriched areas are only detected during prenatal development and are almost non-existent in the adult brain (Mato et al. 2003). Thus, the expression of the CB1 receptor during early development of the nervous system suggests that the endocannabinoid system plays a role on neural development in humans, which ultimately can be associated with possible neuropsychiatric disorders (Galve-Roperh et al. 2009; Jutras-Aswad et al. 2009).

Alterations of the endocannabinoid receptor signaling during early human development can result in changes of the developing brain, for instance, impairment of neuronal maturation, connectivity, or migration, which could play a direct role in adult brain dysfunction (Pang et al. 2008). Indeed, genetic polymorphisms in eCB genes have been associated with functional differences. A missense mutation in the FAAH gene has been associated with problematic drug use (Sipe et al. 2002; Hariri et al. 2009). In 2010, further studies have shown that mutations in the ABHD12 gene (functioning in degradation of AEA) cause the neurodegenerative disease PHARC, with symptoms including polyneuropathy, hearing loss, ataxia, retinitis pigmentosa, and cataracts (Fiskerstrand et al. 2010). Additionally, the inhibition of the CB1 receptor during

cortical neurogenesis resulted in deficits to subcortical projections that impaired proper motor function in adulthood (Diaz-Alonso et al. 2012). Alteration of eCBs signaling also affects the way the brain processes emotion, reward, and threat (Galve-Roperh et al. 2009; Jutras-Aswad et al. 2009). Reduction or enhancement of G-protein mediated signalling due to genetic polymorphisms in the CB1 gene has been linked to psychiatric disorders such as schizophrenia, depression, and psychosis (Ballon et al. 2006). Similarly, polymorphisms in the CB2 gene have also been linked to symptoms of depression and schizophrenia (Onaivi et al. 2008).

2.3.5 The eCBs in amphibians

Under the classification of amphibians, CB1 receptors have been identified within species such as *Taricha granulosa* (Soderstrom et al. 2000), *Xenopus laevis* (Cottone et al. 2003), and *Rana esculenta* (Meccariello et al. 2007). However, *Xenopus tropicalis* is one of the few in which the CB2 gene is present (Elphick & Egertova 2001). *In situ* hybridization experiments conducted on *Xenopus granulosa* have revealed that *cb1* mRNA expression can be detected early during development in the telencephalon, specifically in the nucleus amygdalae, dorso lateralis, and stria terminalis. Additionally, expression of the *cb1* mRNA can be found in the cerebellum, preoptic region, stratum griseum of the hindbrain, and thalamus (Hollis et al. 2006). In *Xenopus laevis*, there has been detection of *cb1* mRNA in the embryos at stage 28. Upon reaching stage 41, *cb1* mRNA is detected in the rhombencephalon and olfactory bulb (Migliarini et al. 2006). During adulthood, Xenopus laevis has CB1 mRNA-positive cells in regions such as amygdala, hypothalamus, cerebellum, spinal cord, mesencephalic tegmentum, dorsal/medial pallium, and cells of the pituitary gland such as the thyrotrophs, lactotrophs, and gonadotrophs (Cesa et al. 2001, 2002; Salio et al. 2002; Cottone et al. 2003).

Similarly, CB1 immunostaining in neurons has been revealed in *Rana esculenta* at high

levels, specifically in the pre-optic regions, hindbrain, hypothalamus, and telencephalic hemispheres (Cottone et al. 2008; Meccariello et al. 2008). There are postulations that gonadal activity is influenced by the eCBs due to fluctuations in *cb1* mRNA expression in regions of the brain associated with the sexual cycle (Meccariello et al. 2006, 2008). During the frog sexual cycle, gonadotropin-releasing hormone I (GnRH-I) mRNA and CB1 levels have an inverse relationship of expression in the diencephalon and telencephalon (Meccariello et al. 2008; Chianese et al. 2012). In these regions, AEA acts as an antagonist to the synthesis of GnRH-I and GnRH-II, which will trigger an increase in *cb1* transcription, suggesting a relationship between GnRH and the eCBs (Meccariello et al. 2008; Chianese et al. 2011, 2012). Additionally, there are speculations of endocannabinoid-mediated responses such as anxiety, stress, and fear due to the *cb1* mRNA *in situ* hybridization staining of the amygdaloid complex in *Taricha granulosa* (Cottone et al. 2003).

2.3.6 The eCB system in zebrafish

As a non-mammalian vertebrate, the zebrafish (*Danio rerio*) is evolutionarily more distant from humans than rodent models but evolutionarily closer to humans than other invertebrate models, such as worms (*C. elegans*) or fruit flies (*D. melanogaster*). Indeed, the eCB system is highly conserved between mammals and zebrafish but not the aforementioned invertebrate model organisms (Elphick 2012). Zebrafish development occurs externally and the transparency of its embryos through larval stages makes it an ideal model to understand the role played by the eCB system in development.

Neural Development. Watson et al. (2008) showed that knockdown of *cb1* gene activity by morpholino anti-sense oligonucleotides resulted in defects of axonal growth and fasciculation.

More recently, Martella et al. (2016a) showed that 2-AG plays a key role in axonal growth and fasciculation, and that the eCBs is critical for the development of functional vision and locomotion.

Anxiety. The eCB system is involved in modulating anxiety across various animal models (Krug & Clark 2015). Low level stimulation of CB receptors commonly causes anxiolytic effects, while high level stimulation is anxiogenic (Viveros et al. 2005). A light/dark preference testing arena was used to see the effects of CB receptor stimulation on fish behavior (Connors et al. 2014). In this assay, zebrafish were placed into a tank with both light and dark regions. Normally, adult zebrafish have a significantly higher preference for dark areas (Serra et al. 1999), but exposure to anxiolytic drugs can increase the time spent in light areas (Guo 2004). Connors et al. showed that supplementing zebrafish food with the potent synthetic CB receptor agonist WIN55212-2 (1 μg/day for 7 days) increases the time spent in light areas, suggesting anxiolytic effects. In contrast, a spatial tank test revealed anxiogenic properties of THC, a CB receptor agonist (Stewart & Kalueff 2014). Zebrafish pre-exposed for 20 min with 30 mg/L or 50 mg/L THC spent less time in the upper half of the tank, suggesting an increase in anxiety-like behavior compared to control fish. Though CB receptor agonists were used in both the light/dark preference assay and the spatial tank test, opposing effects on anxiety are likely due to different amounts of drug dosed, corroborating the idea that the relationship between CB receptor stimulation and anxiety is dosage-dependent and/or due to different routes of administration. Another method of evaluating anxiety involves escape response. Ruhl et al. (2014) measured the response of the fish to a threatening visual stimulus and did not have significant evidence of THC at 100 nmol/L being anxiolytic. However, even though THC at 100 nmol/L did not produce any change in behavioral performance, the same concentration severely impaired spatial memory (Ruhl et al. 2014). Along with differences in concentration, discrepancies in anxiolytic

effects across studies may lie in the fact that different cannabinoids were administered; WIN55212-2 is a full agonist, while THC is a partial agonist. Interestingly, a more recent threat experiment using the same concentration of THC as Ruhl et al. yielded different results; THC administration appeared to have some anxiolytic properties (THC treated fish spent less time at the bottom of the tank), yet did not reduce other behaviors indicative of anxiety (freezing and erratic movements) (Ruhl et al. 2016). The fear stimulus in this experiment was a pheromone, and a possible explanation for the conflicting results may be that CB stimulation distinctly affects different sensory inputs. Lastly, social interactions may also be indicative of nervous behavior. Fish treated with 1mg/L WIN55212-2 swam longer with a stranger fish than controls, suggesting anxiolytic activity (Barba-Escobedo & Gould 2012). Though most evidence from zebrafish experiments agree with conclusions from other animal models, some conflicting evidence calls for more experiments to have a clearer understanding of the connection between the eCBs and anxiety in zebrafish.

Lipid Homeostasis and Appetite. Zebrafish have become a common and relevant model for the study of lipid homeostasis, and the eCBs has been associated with changes in lipid homeostasis and food intake (Krug & Clark 2015). In rodent models, CB1 stimulation in the liver has been shown to induce fatty acid synthesis, increase appetite, and promote obesity, while CB1 downregulation produces opposite effects (Osei-Hyiaman et al. 2005; Wiley et al. 2005; Gary-Bobo et al. 2007). Similar results were seen in zebrafish. Liu et al. (2016) reported the importance of the eCBs in the liver; *cb1* and *cb2* double mutant fish have impaired liver development and function. Specifically the authors showed that inhibition of CB receptor activity disrupts liver development and metabolic function in zebrafish, impacting hepatic differentiation and liver size due to fewer hepatocytes and reduced liver-specific gene expression and proliferation (Liu et al. 2016). In contrast, when *cb1* is overexpressed in zebrafish liver, the

expression levels of genes involved in the fatty acid production, transport, and storage are consequently increased, resulting in hepatosteatosis (Pai et al. 2013). Addition of Cb1 antagonist AM251 rescued this phenotype, suggesting the role of Cb1 in stimulating lipid accumulation. Additionally, AEA administration to zebrafish has been shown to increase expression of Srebp, a transcription factor involved in sterol synthesis (Migliarini & Carnevali 2008). In another study, Fraher et al. showed that alteration of the activity of the eCBs and Retinoic Acid (RA) pathways have additive function in lipid abundance during zebrafish development (zebrafish embryos were exposed to chemical treatments WIN55212-2, Rimonabant, 4-diethylaminobenzaldehyde, BMS 753, BMS 614, BMS 961, CD 2665, oleamide, AM 630, bisphenol A diglycidyl ether, and Rosiglitazone) (Fraher et al. 2015).

A study by Martella et al. (2016b) determined that bisphenol A (BPA) stimulates hepatosteatosis in zebrafish via upregulation of the eCB system. While stimulation of CB receptors appears to increase lipid synthesis, not all cannabinoids facilitate this process. A study showed that phytocannabinoids cannabidiol (CBD) and D9-tetrahydrocannabivarin (THCV) reduce lipid levels in zebrafish, agreeing with studies done in rodent models (Silvestri et al. 2015). Unlike THC, THCV is a Cb1 receptor antagonist, and CBD has minimal affinity for either CB receptor. Therefore, the effects on lipid homeostasis by these particular cannabinoids likely occur through either Cb1 downregulation or interaction with receptors outside of the eCB system. It is worth noting that this experiment measured lipid metabolism *in vivo* by quantifying the amount of yolk in zebrafish embryos over time. Therefore, further studies must be done to see if these phytocannabinoids can protect against hepatosteatosis in adult fish. CB receptors have also been shown to modulate fish appetite. In an experiment done by Piccinetti et al. (2010), the administration of melatonin reduced zebrafish food intake. These melatonin-treated fish consequently had reduced Cb1 expression, suggesting that Cb1 has a role in stimulating hunger in zebrafish. Additionally, downregulation of Cb1 in zebrafish has been shown to reduce

appetite in a dose dependent manner (Shimada et al. 2012). Nishio et al. (2012) conclude that Cb1 downregulates the expression of cocaine- and amphetamine-related transcript (CART)-3 to induce hunger in zebrafish. A schematic representation of the eCB system's role in zebrafish hepatocytes is shown in **Figure 2.3**.

Immune System and Neuroinflammation. The eCB system is also associated with immune system processes such as inflammation. As in mammals, zebrafish Cb2 receptors are highly expressed in white blood cells (Krug & Clark 2015). Administration of various Cb2 agonists in zebrafish reduced leukocyte migration to a tail wound (Liu et al. 2013). Conversely, knocking out *cb2* resulted in increased leukocyte migration compared to control fish. These studies suggest that Cb2 is a critical component in the modulation of inflammation responses, agreeing with other animal model studies. Cb2 activation is thought to inhibit leukocyte migration by downregulating arachidonate 5-lipoxygenase (Alox5) through the JNK/c-Jun/Alox5 pathway. Additionally, Cb2 plays a role in neuroinflammation; in experimental allergic encephalomyelitis (EAE), a mouse model of brain inflammation, Cb2 is upregulated 200-fold in resting microglial cells (Maresz et al. 2005). The reduction of Cb2 receptors on invading T-cells is shown to facilitate neurodegenerative disease progression (Maresz et al. 2007). Experiments with neurodegenerative zebrafish models are needed to test whether Cb2 has a similar role in regulating neuroinflammatory disease progression in zebrafish.

2.4 METHODS

2.4.1 Zebrafish husbandry

Wild type of the AB strain adult (1 year old) and larval zebrafish (*Danio rerio*, of either sex) were used in this study. The animals were raised at the University of California, San Francisco zebrafish facility at 28°C under a 14/10 hour light/dark cycle in accordance with National Institutes of Health and University of California, San Francisco guidelines.

2.4.2 Quantitative polymerase chain reaction (qPCR) analysis

Total RNA was prepared from isolated adult tissues (skin, brain, muscles, kidney, heart, intestine, liver, spleen, eyes, ovary, testis) and representative developmental embryo stages (1 hpf to 120 hpf dechorionated embryos) of zebrafish using TRIzol reagent (Invitrogen) by homogenization and purified using RNeasy Mini Kit (Qiagen). cDNAs were synthesized from 500 ng of purified RNA using qScript cDNA SuperMix (Quanta Biosciences) and used as templates. qPCR was performed using Applied Biosystems SYBR Green PCR Master Mix and the ABI7900HT machine. Forward and Reverse primers were designed using NCBI/primer-BLAST software with exon-exon junction parameters and *Danio rerio* RefSeq for off targets. *elf1α* primers were used as standard CT (McCurley & Callard 2008) to generate Ct values.

2.4.3 Whole mount in situ *hybridization*

cb1 and *cnrip1a* sense and anti-sense *in situ* probes were created by cloning PCR products

from zebrafish embryos' cDNA template into commercial TOPO vector pCR4-TOPO cloning kit (Invitrogen). After checking the directionality of the PCR products by sequencing (Quintara Biosciences), linearization of the vector by specific restriction enzymes was performed. Digoxigenin labeled RNA probes for *in situ* hybridization (ISH) were generated using the DIG labeling kit (Roche) according to the manufacturer's instructions using either T3 or T7 RNA polymerases (depending on directionality). DNA template was removed using DNase. Hybridization of embryos collected at 30, 50 and 72 hpf (incubation step performed at 68°C) and detection with anti-digoxigenin was done as previously described (Guo et al. 1999). After staining, embryos were cleared with glycerol, and whole-mounted for viewing. Images were taken using Zeiss Axioskop 2 plus microscope, Canon EOS DS126431 camera and MicroManager software.

2.5 RESULTS

2.5.1 Zebrafish cb1 *and* cnrip1a *transcripts are detected in the developing zebrafish brain*

Whole-mount *in situ* hybridization revealed enriched *cb1* expression in discrete brain regions of zebrafish embryos. Similarly to what was previously described in (Lam et al. 2006), *cb1* transcript was detected in the preoptic area at 30 hpf (**Figure 2.4A,B**) and extends to other areas of the telencephalon, diencephalon, and midbrain at 50 hpf (**Figure 2.4C,D**). At 72 hpf, *cb1* transcript was detected in the olfactory bulb and weakly in the midbrain (**Figure 2.4E,F**).

We next analyzed the expression pattern of *cnrip1a* transcript. *cnrip1a* transcript is highly expressed in the head region and in the brain at 30 hpf (**Figure 2.4I,J**) showing an enrichment in the telencephalon, midbrain, hindbrain, and eyes. At 50 hpf, cnrip1a transcript is detected in

the brain, retina, pectoral fins, and potentially in digestive organs which they are not easily demarcated due to the strong signal of the probe (**Figure 2.4K,L**). At 72 hpf *cnrip1a* expression is reduced but was still detectable in the mid- and hind-brain regions (**Figure 2.4M,N**). For both cb1 and cnrip1a there was no detectable staining with the sense control probes at all stages analyzed (50 hpf stages are shown as an example in **Figure 2.4G,H,O,P**).

2.5.2 Expression profile of zebrafish eCBs genes during embryogenesis

Next we used qPCR analysis to investigate the expression profiles of zebrafish eCB genes during embryogenesis using cDNAs prepared from 10 zebrafish embryonic developmental stages (between 1 hour and 120 h post-fertilization). *cb1* expression was low during development although a very clear maternal-zygotic transition phase was detected (**Figure 2.5A**). These data were consistent with *in situ* hybridization analysis shown in **Figure 2.4**. Similar low expression was seen for orphan receptor *gpr55a* (**Figure 2.5A**). *cb2* was expressed at higher levels and its expression seemed to be paired with the onset of peripheral organogenesis (**Figure 2.5A**). Expression analysis of *cnrip1a* showed high level of expression starting at 24 hpf in concomitance with brain development (**Figure 2.5B**). High levels of expression were detected in later stages, too. Its maternal expression also suggested a role at very early stages (**Figure 2.5B**). The expression levels of genes encoding Mgll and Abhd6a and b (enzymes involved in 2-AG degradation) were relatively low during zebrafish development (**Figure 2.5C**) while *abhd12* showed high maternal mRNA levels, which continues throughout organogenesis (**Figure 2.5C**). *dagla* showed a similar expression profile to *daglb*, even though *daglb* seemed required during initial phases of embryonic development (**Figure 2.5D**). *faah* and *faah2a* gene expression levels were very similar during development and fairly weak (**Figure 2.5E**). A similar expression profile was seen for *nape-pld* and *gde1* (**Figure 2.5F**) but not for

abhd4 of which the maternal expression was higher (**Figure 2.5F**), suggesting a role during embryo early stages and a potential requirement for AEA synthesis during these stages. Expression of other eCBs related genes is shown in **Figure 2.5G**. Of these genes, *naaa1a*, showed elevated relative expression mRNA levels before 24 hpf (**Figure 2.5G**).

2.5.3 Expression profiles of zebrafish eCBs genes in adult tissue types

We also analyzed the expression of zebrafish eCBs genes in adult tissues by qPCR. *cb1* mRNA was present at very high levels in the brain while very little is detected in the eyes and testis (**Figure 2.6A**); *cb2* was detected in the brain, kidney, spleen and testis (**Figure 2.6A**); *gpr55A* was predominant in the brain, spleen and testis (**Figure 2.6A**). The expression of *cnrip1a* was extremely high in the brain, eyes and testis (**Figure 2.6B**). The highest expression for *mgll* was detected in the brain, kidney, spleen and eyes (**Figure 2.6C**). While *abhd6b* appeared to be expressed at levels barely detectable, *abhd6a* was mostly expressed in the intestine, liver and testis (**Figure 2.6C**). *abhd12* showed variable expression within different tissues, and it was found more abundant in the brain, muscles, eyes and reproductive organs with a lower level in kidney, heart and intestine (**Figure 2.6C**). The different expression levels of these serine hydrolases in the brain are explainable by their respective activity in the brain: indeed MGLL accounts for 85% of 2-AG hydrolysis, ABHD6 accounts for approx. 4% of brain 2-AG hydrolase and ABHD12 for 9% (Savinainen et al. 2012). *dagla* and *daglb* showed a similar pattern of expression in the brain, muscles, kidney, eyes and testis; in the spleen, *dagla* showed higher levels of expression compared to *daglb* (**Figure 2.6D**). *faah* and *faah2a* were expressed at comparable levels in the brain (**Figure 2.6E**); *faah* was also moderately expressed in the skin and testis (**Figure 2.6E**) while *faah2a* was also detected intestine, eyes and testis (**Figure 2.6E**). *nape-pld*, *gde1* and *abhd4* were widely expressed in almost all organs with similar mRNA levels in the brain (**Figure 2.6F**); *abhd4* was found more abundant in the spleen and testis

(**Figure 2.6F**). *ptgs2a* was predominantly expressed in the skin, spleen and eyes (**Figure 2.6G**); *naaa1a* was greatly expressed in the reproductive organs (**Figure 2.6G**), this was consistent with its high levels of maternal mRNA (**Figure 2.5G**). *pparab* and *pparg* showed similar expression in muscles and spleen (**Figure 2.6G**); *pparab* expression was greater in the brain, heart and eyes while *pparg* seemed to be enriched in the testis (**Figure 2.6G**).

2.6 DISCUSSION

Although the eCB system has been studied in various animal models and humans, there are still many unknown features of this system. For example, it is not clear how activity regulates the availability of endogenous eCB ligands to specific synapses. The circuit mechanisms underlying eCB system's role in reward, addiction, and anxiety remain to be elucidated. How endogenous and exogenous CB ligands impact nervous system development and plasticity is also an important question for which deep mechanistic insights can be gained.

Zebrafish (*Danio rerio*) has become a prominent vertebrate model organism to study biological processes in vivo (Stern & Zon 2003; Hill et al. 2005; Santoriello & Zon 2012). This is due to a combination of salient properties for elucidating embryonic development, physiology and diseases. Though a vertebrate, it has the strengths of invertebrate model systems, such as small size, high fecundity, and a relatively short generation time (Lieschke & Currie 2007). Moreover, its rapid and synchronous embryonic development greatly facilitates phenotypic analysis and high throughput experimental approaches. Its transparent and easily accessible embryos and larvae make zebrafish ideally suited for cell-type specific gene activity alterations and subsequent in vivo observations.

Despite the clear advantages in using this model, limited functional studies of the eCBs

have been carried out using zebrafish. Here we present expression profiles of all genes known to be involved in endocannabinoid signaling in zebrafish at different developmental stages and in individual adult organs. Our observational gene expression studies contribute to the existing data about the endocannabinoid system and emphasize the benefit of this model in providing new insights. Using *in situ* hybridization and qPCR to assess spatial and temporal expression in zebrafish embryos respectively, we found that *cb1* transcript is restricted to very specific areas of the brain while *cnrip1a* is highly and widely expressed within the CNS; it is possible that Crip1A has an independent role from Cb1, which has already been suggested by Guggenhuber and colleagues (Elphick 2012; Guggenhuber et al. 2016). Consequently, despite the initial exclusive characterization of Crip1A protein as Cb1 interacting protein, it would be interesting to investigate further.

Another interesting finding is that, despite the proposed role for Cb1 in the liver, in our studies zebrafish *cb1* does not show detectable levels of mRNA expression in the adult liver. This is consistent with what has been previously stated in Alswat et al.: “in the normal liver, the expression of CB1 and CB2 receptors is modest, which probably explains why the focus of research on the role of eCBs in the liver pathophysiology has come only recently. Indeed, early studies of brain CB1 receptors used the liver as a negative control” (Galiegue et al. 1995; Alswat 2013).

The manipulation and analysis of the eCB system in zebrafish (i.e. the creation of zebrafish knock-out models) could bridge existing knowledge gaps on their function. Zebrafish studies could also contribute to a better understanding of the toxicological effects of exogenous cannabinoids. Through the employment of knockout models and well controlled assays, the effects of acute and chronic phytocannabinoid administration on development and behavior can be assessed.

The eCB system has the potential to be used in various therapeutic strategies. Previous

studies have given evidence that activation or inhibition of the eCBs could alleviate the symptoms of various disease states, including multiple sclerosis, Alzheimer's disease, Parkinson's disease, Huntington's disease, obesity, anxiety, and depression (Di Marzo et al. 2015; Krug & Clark 2015). On the other hand, exposure to exogenous CB ligands such as marijuana may have unwanted consequences on development and health. Further exploration of the eCB system, in particular by harvesting the strength of model organisms such as zebrafish, will allow for its exploitation in therapeutic contexts while avoiding the side effects of modulating eCB signaling.

2.7 ACKNOWLEDGMENTS

We would like to thank the Guo lab members for the helpful discussions and Michael Munchua, Hongbin Yuan, and Xingnu Zhai for excellent fish care.

2.8 FIGURES

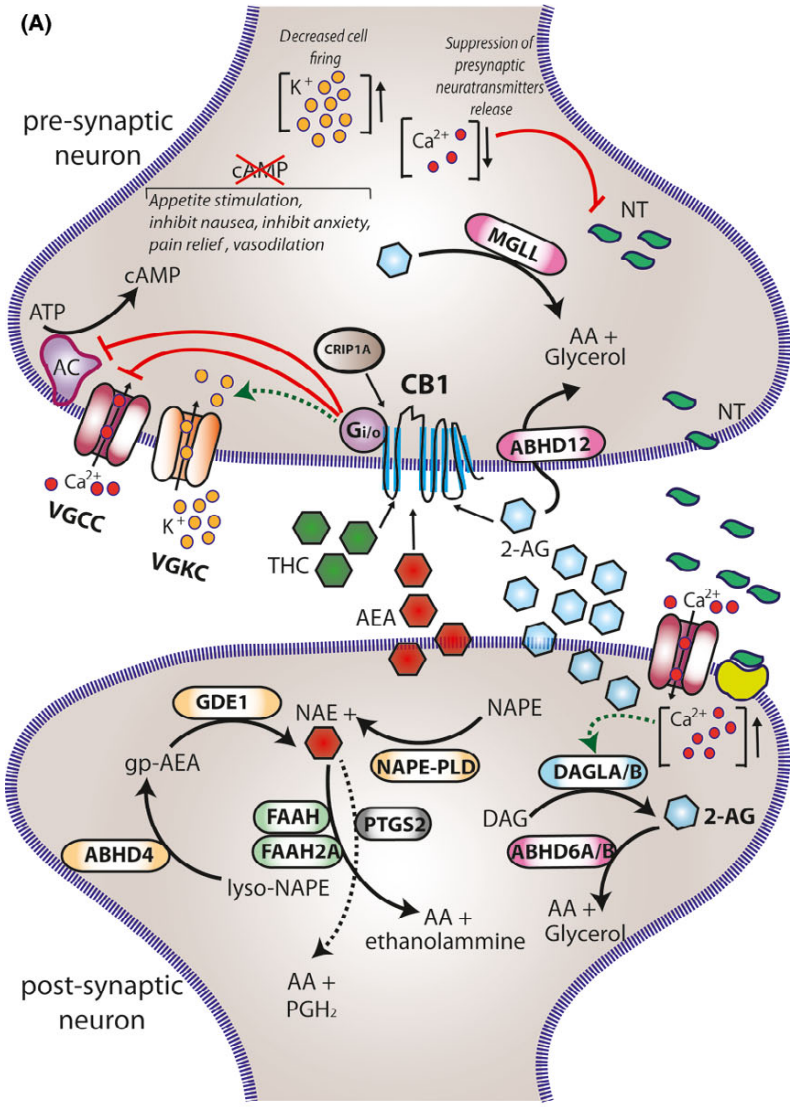

Figure 2.1 eCB system signaling in neurons.

(A) Within the brain, the endocannabinoids AEA and 2-AG are biosynthesized from different membrane phospholipid families, both esterified with arachidonic acid (AA). Several possible biosynthetic routes for the formation of AEA in the post-synaptic neuron have been suggested with multiple enzymes implicated: N-acylphosphatidylethanolamine specific phospholipase D (NAPE-PLD), ab-Hydrolase domain-containing 4 (ABHD4), and glycerophosphodiesterase-1 (GDE1). The biosynthetic precursors of 2-AG are converted to 2-AG by the action of sn-1-diacylglycerol lipases a and b (DAGLa and DAGLb). Endogenous AEA and 2-AG and exogenous D9-THC (THC) activate the CB1 receptor, exposed on the pre-synaptic neuron, causing (1) G-protein mediated inactivation of voltage-gated calcium channels (VGCC) which results in a transient reduction of neurotransmitter (NT) release, (2) G-protein mediated

activation of voltage-gated potassium channels (VGKC), which decreases cell firing, and (3) G-protein mediated inhibition of adenylate cyclase (AC) with consequent reduction of cAMP levels. 2-AG is then degraded by three serine hydrolases, MGLL (monoglyceride lipase), ABHD6 (ab-Hydrolase domain-containing 6) and ABHD12 (ab-Hydrolase domain-containing 12), that account for approximately 99% of 2-AG hydrolysis in the CNS (Savinainen et al. 2012). MGLL is responsible for approx. 85% of 2-AG hydrolysis and co-localizes with CB1 in axon terminals (Savinainen et al. 2012). ABHD6 accounts for approximately 4% of brain 2-AG hydrolase activity; in neurons it resides post-synaptically, often juxtaposed with CB1 where it regulates intracellular pools of 2-AG at the site of generation. ABHD12 is highly expressed in microglia and accounts for approx. 9% of total brain 2-AG hydrolysis. AEA is generally degraded by the fatty acid amide hydrolases FAAH and FAAH2A. Prostaglandin-Endoperoxide Synthase 2 PTGS2 (COX-2) possesses the capacity to metabolize AEA in vivo and can compete with FAAH for AEA in several brain regions (Glaser & Kaczocha 2010). The cannabinoid receptor interacting protein CRIP1A, transiently interacting with CB1 can stabilize and regulate the inactive state of the receptor (Niehaus et al. 2007). In contrast with this conclusion, Guggenhuber and colleagues proposed that CRIP1A regulates CB1 activity in an agonist-dependent manner (Guggenhuber et al. 2016).

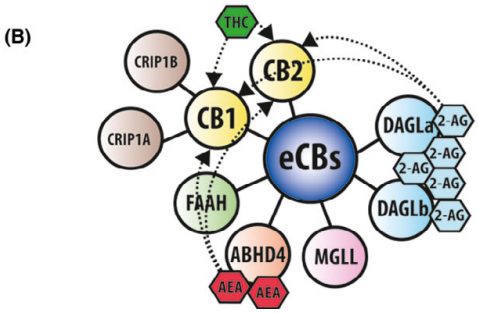

Figure 2.2 Relationship between eCB proteins and ligands.

Schematic representation of the main proteins belonging to the eCB system. CB1 and CB2 receptors get activated by endogenous (2-AG and AEA) and exogenous (THC) cannabinoids; 2-AG is synthesized by DAGLa and DAGLb and degraded by MGLL; AEA is mainly synthesized by ABHD4 and degraded by FAAH. CRIP1A and CRIP1B are known interaction partners of CB1; Levels of 2-AG in the brain are higher than those of AEA.

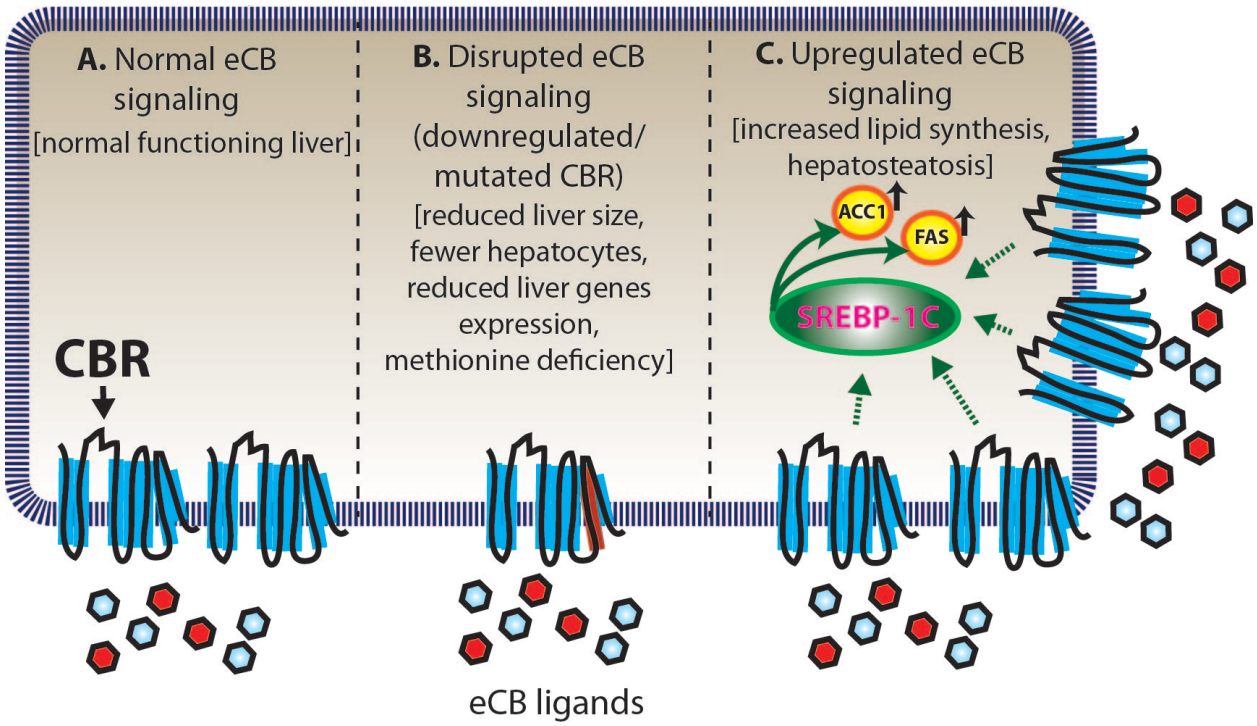

Figure 2.3 The eCB system in zebrafish liver.

Proper liver function in zebrafish appears to be dependent on a normal, functioning eCBs in hepatocytes. (A) Zebrafish liver functions regularly when eCB signaling is unaltered. (B) Mutation of cb1 and cb2 impair liver development and function (Liu et al. 2016). Loss of CB1 and CB2 function results in a smaller liver with less hepatocytes and reduced expression of liver-specific genes in zebrafish. Additionally, methionine levels are irregular, which is known to cause a variety of metabolic problems, including hepatosteatosis. (C) Overexpression of CB1 results in fish with hepatosteatosis (Pai et al. 2013). Increased CB1 receptor signaling stimulates SREBP-1c, a transcription factor which upregulates the expression of ACC1 and FAS (genes involved in fatty acid synthesis). ACC1, acetyl coenzyme-A carboxylase-1; CBR, cannabinoid receptor; FAS, fatty acid synthase; SREBP-1c, sterol regulatory element-binding protein 1c.

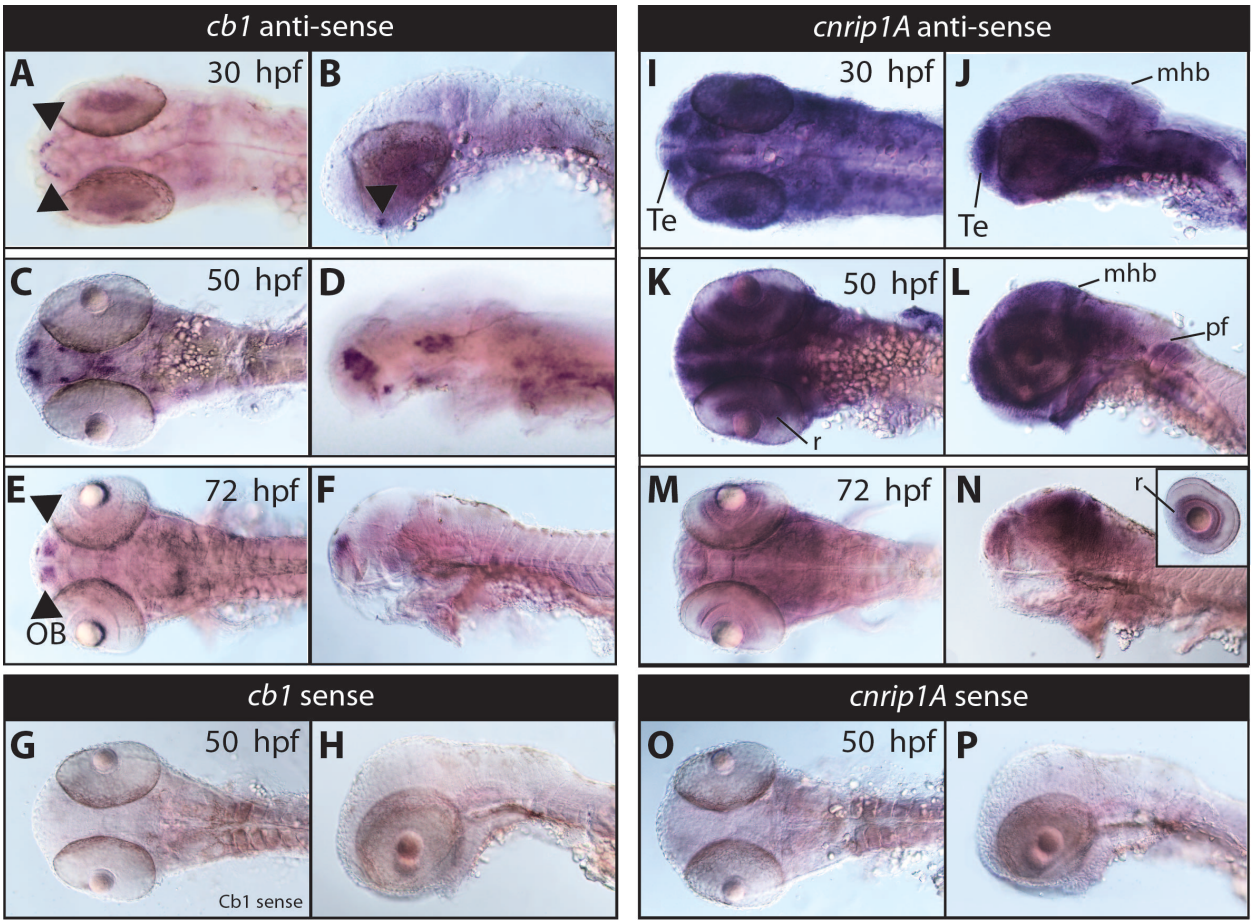

Figure 2.4 Whole mount *in situ* hybridization analysis of *cb1* and *cnrip1a* genes.

cb1 (A–H) and *cnrip1a* (I–P) expression in developing zebrafish (30, 50 and 72 hpf). *cb1* expression was examined using whole-mount *in situ* hybridization in wild type embryos at the 30 hpf (A, B; dorsal and lateral respectively), 50 hpf (C, D; dorsal and lateral respectively), and 72 hpf (E,F dorsal and lateral respectively) stages. By 30 hpf, *cb1* expression is highly restricted to the pre-optic area (A, B). At 50 hpf, *cb1* expression was prominent in very specific areas of the brain including the olfactory bulbs, telencephalon, optic tectum and hypothalamus (C, D). At 72 hpf, *cb1* expression was further restricted to the telencephalon in the olfactory bulbs and weakly in the midbrain area (E, F). No signal was detected using *cb1* sense probes at all stages, 50 hpf is shown (G, H). cnrip1a expression was examined using whole-mount *in situ* hybridization in wild type embryos at the 30 hpf (I, J; dorsal, lateral respectively), 50 hpf (K, L; dorsal, lateral respectively), and 72 hpf (M, N; dorsal, lateral respectively) stages. By 30 hpf, *cnrip1a* expression is highly expressed in the head region showing an enrichment in the telencephalon, mid- brain, midbrain-hindbrain boundary and eyes (I, J). At 50 hpf, strong *cnrip1a* expression was prominent in specific areas of the brain, eyes retina, pectoral fins, and potentially in digestive organs (K, L). At 72 hpf, *cnrip1a* expression was further restricted to the retina, telencephalon, midbrain, midbrain-hindbrain boundary (M, N). No signal was detected using *cnrip1a* sense probes at all stages, 50 hpf is shown (O, P). Te, telencephalon; pf, pectoral fins; r, retina; mhb, midbrain-hindbrain boundary, OB, olfactory bulbs.

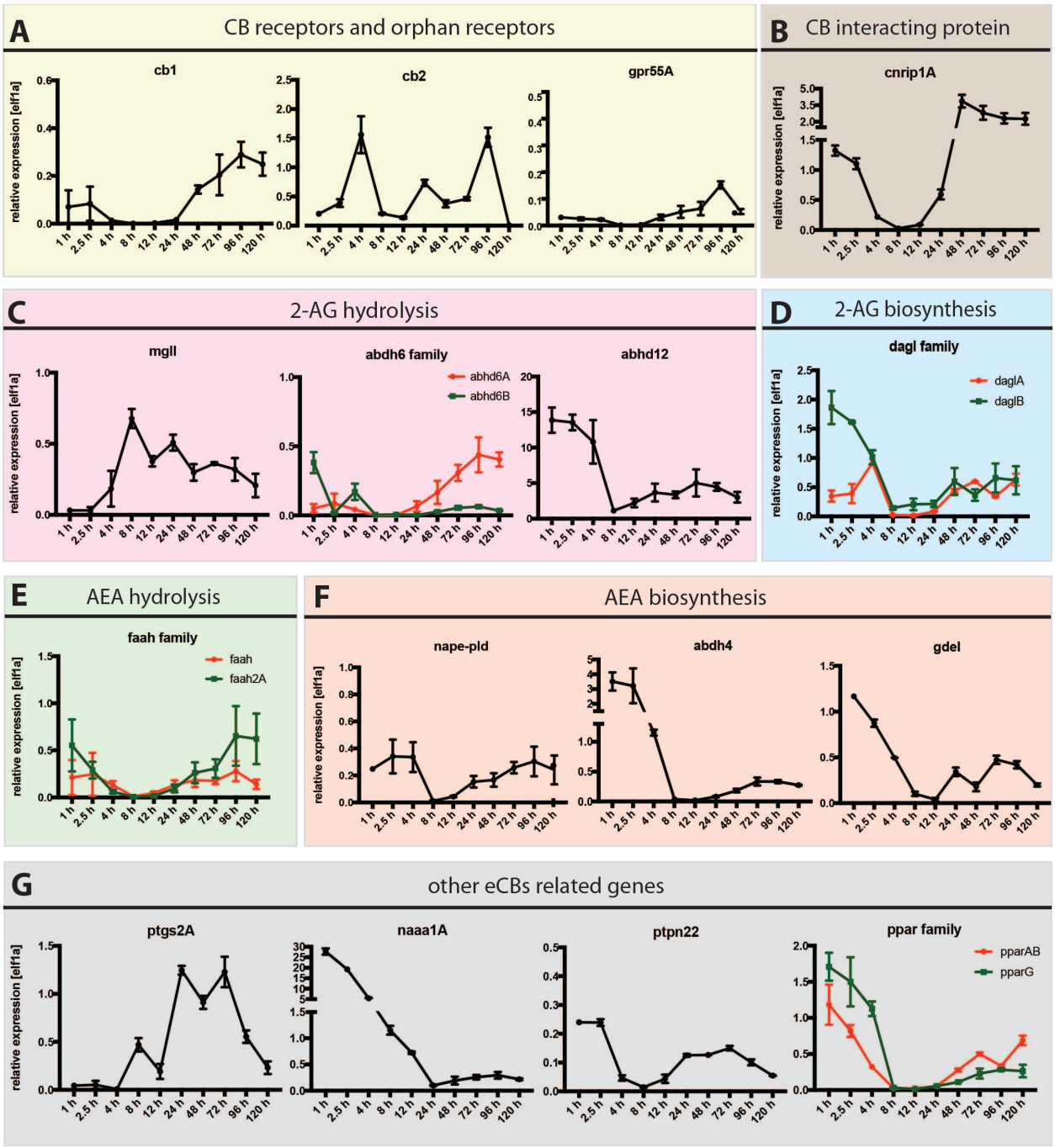

Figure 2.5 Developmental expression of zebrafish eCB genes.

qPCR analysis of mRNA prepared at ten embryonic developmental stages of WT embryos (X axis: 1–120 h postfertilization, hpf) using primers against (A) Cannabinoid Receptors, *cb1* and *cb2* and putative orphan receptor *gpr55a* (B) cannabinoid receptor interacting protein, *cnrip1a*, (C) enzymes responsible for 2-AG hydrolysis *mgll*, *abhd6a* and *abhd6b* and *abhd12*, (D) enzymes responsible for 2-AG synthesis, *dagla* and *daglb*, (E) enzymes responsible for AEA hydrolysis *faah* and *faah2a* (F) enzymes responsible for AEA synthesis *nape-pld*, *abhd4* and *gde1* (G) genes associated with the eCB system, *ptgs2a*, *naaa1a* (*asah1A*), *ptpn22*, *pparab* and

pparg. *elf1a* was used as internal control to determine the relative mRNA expression. Relative average expression +/ SEM (qPCR results are representative of two experimental repeats, two repeats/experiment). GraphPad Prism 7 software was used for statistical analysis.

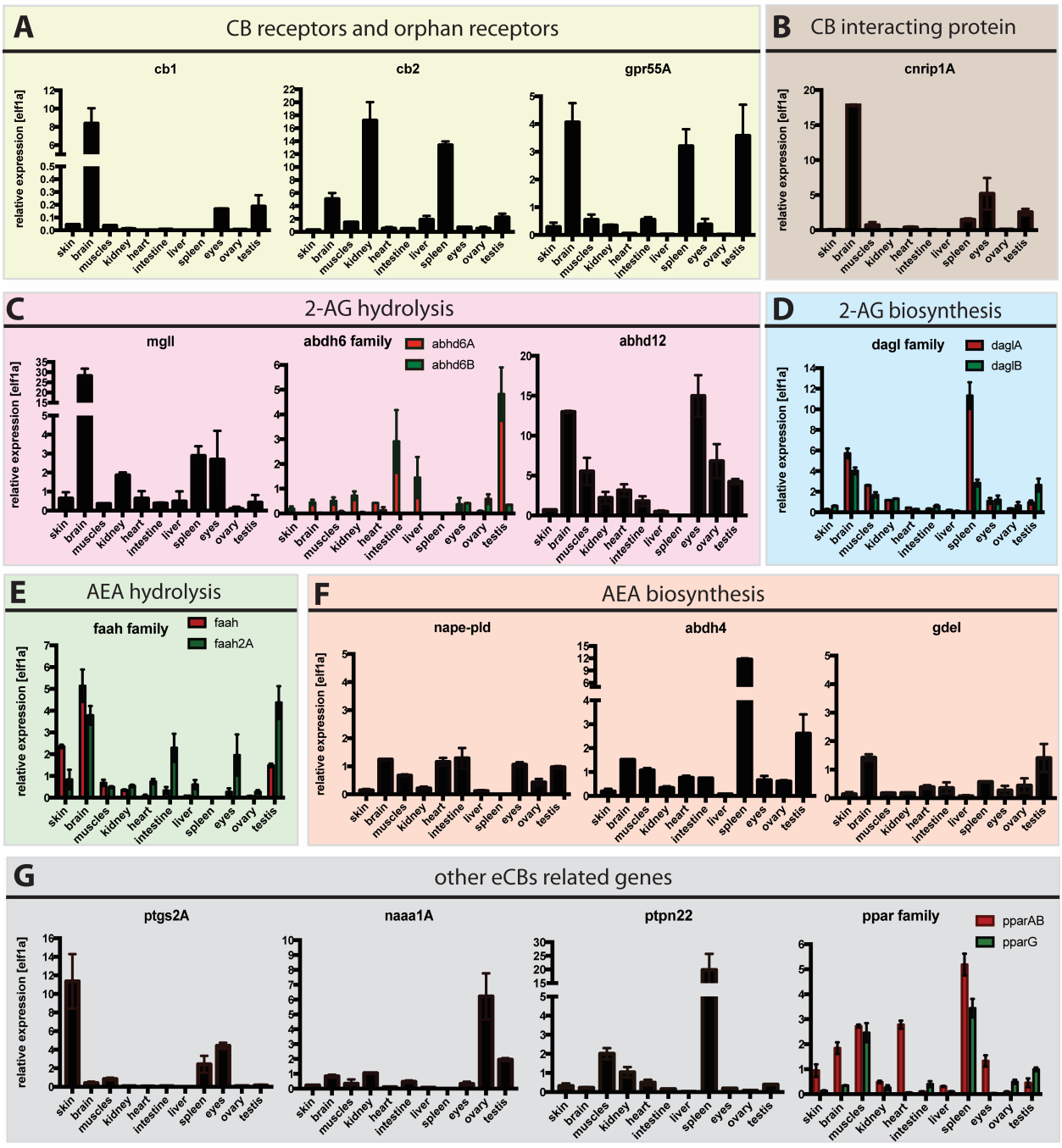

Figure 2.6 WT zebrafish adult tissue types expression of zebrafish eCB genes.

qPCR detection of zebrafish eCBs genes in zebrafish tissues (X axis: skin, brain, muscles, kidney, heart, intestine, liver, spleen, eyes, ovary, testis) using primers against (A) Cannabinoid Receptors, *cb1* and *cb2* and putative orphan receptor *gpr55a* (B) cannabinoid receptor interacting protein, *cnrip1a*, (C) enzymes responsible for 2-AG hydrolysis *mgll*, *abhd6a* and *abhd6b* and *abhd12*, (D) enzymes responsible for 2-AG synthesis, *dagla* and *daglb*, (E) enzymes responsible for AEA hydrolysis *faah* and f*aah2a* (F) enzymes responsible for AEA synthesis *nape-pld*, *abhd4* and *gde1* (G) genes associated with the eCB system, *ptgs2A*,

naaa1a (*asah1a*), *ptpn22*, *pparab* and *pparg*. *elf1a* was used as internal control to determine the relative mRNA expression. Relative average expression +/ SEM (qPCR results are representative of two experimental repeats and two repeats/ experiment). GraphPad Prism 7 software was used for statistical analysis.

2.9 TABLES

Table 2.1 eCB system protein names and functions.

Description of protein names, standard abbreviations, conventional zebrafish names (https://zfin.org) and function of endocannabinoid related genes investigated in this study.

Protein name	Standard abbreviation	Zfin gene name	Function
Cannabinoid receptor 1	CB1	cnr1	G-protein coupled receptor located primarily in the CNS; activated by endogenous and exogenous cannabinoids
Cannabinoid receptor 2	CB2	cnr2	G-protein coupled receptor located primarily in peripheral organs of the immune system and in the brain; activated by endogenous and exogenous cannabinoids
G protein-coupled receptor 55a	GPR55A	gpr55a	G- protein coupled receptor widely expressed in the brain; recently found to be activated by endogenous and exogenous cannabinoids; its activation leads to stimulation of rhoA, cdc4 and rac1
Cannabinoid receptor interacting protein 1a	CRIP1A	cnrip1a	CB1 receptor interacting protein that interacts with the distal C-terminus of CB1 altering/modulating CB1 interactions with G-protein
Monoglyceride lipase	MGLL (MAGL)	mgll	Member of the serine hydrolases superfamily; it catalyzes the hydrolysis of 2-AG to AA and Glycerol
αβ-hydrolase domain containing 6b	ABHD6A	abhd6b	Member of the serine hydrolases superfamily; it catalizes the hydrolysis of 2-AG to AA and Glycerol
αβ-hydrolase domain containing 12	ABHD12	abhd12	Member of the serine hydrolases superfamily; it catalyzes the hydrolysis of 2-AG to AA and Glycerol in the CNS
Diacylglycerol lipase, alpha	DAGLα	dagla	Diacylglycerol lipase; it catalyzes the hydrolysis of diacylglycerol (DAG) to the most abundant endocannabinoid 2-AG
Diacylglycerol lipase, beta	DAGLβ	daglb	Diacylglycerol lipase; it catalyzes the hydrolysis of diacylglycerol (DAG) to the most abundant endocannabinoid 2-AG
Fatty acid amide hydrolase	FAAH	faah	Fatty acid amide hydrolase with a single N-terminal transmembrane domain; principal catabolic enzyme for a clas of lipids known as fatty acid amides (FAAs) of which AEA belongs to
Fatty acid amide hydrolase 2a	FAAH2A	faah2a	Fatty acid amide hydrolase; it degrades bioactive fatty acid amides, including AEA (AEA = arachidonic acid + ethanolamine)
N-acyl phosphatidylethanolamine phospholipase D	NAPE-PLD	napepld	Member of the metallo-beta-lactamase family with phosphodiesterase activity; it releases NAE from NAPE to for AEA
αβ-hydrolase domain containing 4	ABHD4	abhd4	Hydrolase that acts on either NAPE or lyso-NAPE to generate the glycerophospho-arachidonoyl ethanolamide which is subsequently cleavaged to give AEA
Glycerophosphodiester phosphodiesterase 1	GDE1 (MIR16)	gde1	Phosphodiesterase with glycerophospho-NAE phosphodiesterase activity; it hydrolyses the phosphodiester bond of GP-NArE to release free AEA
Prostaglandin-endoperoxide synthase 2a	PTGS2A (COX-2; COX-2A)	ptgs2a	Cycloxigenase involved in AEA (and 2-AG?) metabolism
N-acylsphingosine amidohydrolase (acid ceramidase) 1a	NAAA1A (ASAH1A)	asah1a	Member of the choloylglycine hydrolase family with similar structure to faah. Unlike faah, naaa1a operates in acidic environments (pH 4.5)
Protein tyrosine phosphatase, non-receptor type 22	PTPN22	ptpn22	Protein tyrosine phosphase highly expressed in the immune system; it dephosphorylates pAEA to yield AEA
Peroxisome proliferator-activated receptor alpha b	PPARαβ	pparab	Nuclear receptor transcription factor protein suggested as a binding target of endocannabinoids
Peroxisome proliferator-activated receptor gamma	PPARγ (ARF6)	pparg	Nuclear receptor transcription factors protein suggested as a binding target of endocannabinoids

2.10 REFERENCES

Aguado T, Monory K, Palazuelos J, Stella N, Cravatt B, et al. 2005. The endocannabinoid system drives neural progenitor proliferation. FASEB journal : official publication of the Federation of American Societies for Experimental Biology 19: 1704-6

Ahmed MH, Kellogg GE, Selley DE, Safo MK, Zhang Y. 2014. Predicting the molecular interactions of CRIP1a-cannabinoid 1 receptor with integrated molecular modeling approaches. Bioorg Med Chem Lett 24: 1158-65

Alswat KA. 2013. The role of endocannabinoids system in fatty liver disease and therapeutic potentials. Saudi J Gastroenterol 19: 144-51

Ballon N, Leroy S, Roy C, Bourdel MC, Charles-Nicolas A, et al. 2006. (AAT)n repeat in the cannabinoid receptor gene (CNR1): association with cocaine addiction in an African-Caribbean population. Pharmacogenomics J 6: 126-30

Barba-Escobedo PA, Gould GG. 2012. Visual social preferences of lone zebrafish in a novel environment: strain and anxiolytic effects. Genes Brain Behav 11: 366-73

Berrendero F, Garcia-Gil L, Hernandez ML, Romero J, Cebeira M, et al. 1998. Localization of mRNA expression and activation of signal transduction mechanisms for cannabinoid receptor in rat brain during fetal development. Development 125: 3179-88

Berrendero F, Sepe N, Ramos JA, Di Marzo V, Fernandez-Ruiz JJ. 1999. Analysis of

cannabinoid receptor binding and mRNA expression and endogenous cannabinoid contents in the developing rat brain during late gestation and early postnatal period. Synapse 33: 181-91

Cameron DL, Wessendorf MW, Williams JT. 1997. A subset of ventral tegmental area neurons is inhibited by dopamine, 5-hydroxytryptamine and opioids. Neuroscience 77: 155-66

Cesa R, Guastalla A, Cottone E, Mackie K, Beltramo M, Franzoni MF. 2002. Relationships between CB1 cannabinoid receptors and pituitary endocrine cells in Xenopus laevis: an immunohistochemical study. Gen Comp Endocrinol 125: 17-24

Cesa R, Mackie K, Beltramo M, Franzoni MF. 2001. Cannabinoid receptor CB1-like and glutamic acid decarboxylase-like immunoreactivities in the brain of Xenopus laevis. Cell Tissue Res 306: 391-8

Chevaleyre V, Takahashi KA, Castillo PE. 2006. Endocannabinoid-mediated synaptic plasticity in the CNS. Annu Rev Neurosci 29: 37-76

Chianese R, Ciaramella V, Fasano S, Pierantoni R, Meccariello R. 2011. Anandamide modulates the expression of GnRH-II and GnRHRs in frog, Rana esculenta, diencephalon. Gen Comp Endocrinol 173: 389-95

Chianese R, Ciaramella V, Scarpa D, Fasano S, Pierantoni R, Meccariello R. 2012. Anandamide regulates the expression of GnRH1, GnRH2, and GnRH-Rs in frog testis. Am J Physiol Endocrinol Metab 303: E475-87

Connors KA, Valenti TW, Lawless K, Sackerman J, Onaivi ES, et al. 2014. Similar anxiolytic effects of agonists targeting serotonin 5-HT1A or cannabinoid CB receptors on zebrafish behavior in novel environments. Aquat Toxicol 151: 105-13

Cottone E, Guastalla A, Mackie K, Franzoni MF. 2008. Endocannabinoids affect the reproductive functions in teleosts and amphibians. Mol Cell Endocrinol 286: S41-5

Cottone E, Salio C, Conrath M, Franzoni MF. 2003. Xenopus laevis CB1 cannabinoid receptor: molecular cloning and mRNA distribution in the central nervous system. J Comp Neurol 464: 487-96

Cressey D. 2015. The cannabis experiment. Nature 524: 280-3

De Petrocellis L, Melck D, Bisogno T, Milone A, Di Marzo V. 1999. Finding of the endocannabinoid signalling system in Hydra, a very primitive organism: possible role in the feeding response. Neuroscience 92: 377-87

Devane WA, Hanus L, Breuer A, Pertwee RG, Stevenson LA, et al. 1992. Isolation and structure of a brain constituent that binds to the cannabinoid receptor. Science 258: 1946-9

Di Marzo V, Stella N, Zimmer A. 2015. Endocannabinoid signalling and the deteriorating brain. Nat Rev Neurosci 16: 30-42

Diaz-Alonso J, Aguado T, Wu CS, Palazuelos J, Hofmann C, et al. 2012. The CB(1) cannabinoid receptor drives corticospinal motor neuron differentiation through the Ctip2/Satb2

transcriptional regulation axis. J Neurosci 32: 16651-65

Elphick MR. 2012. The evolution and comparative neurobiology of endocannabinoid signalling. Philos Trans R Soc Lond B Biol Sci 367: 3201-15

Elphick MR, Egertova M. 2001. The neurobiology and evolution of cannabinoid signalling. Philos Trans R Soc Lond B Biol Sci 356: 381-408

Elphick MR, Egertova M. 2005. The phylogenetic distribution and evolutionary origins of endocannabinoid signalling. Handb Exp Pharmacol: 283-97

Fernandez-Ruiz J, Berrendero F, Hernandez ML, Ramos JA. 2000. The endogenous cannabinoid system and brain development. Trends Neurosci 23: 14-20

Fiskerstrand T, H'Mida-Ben Brahim D, Johansson S, M'Zahem A, Haukanes BI, et al. 2010. Mutations in ABHD12 cause the neurodegenerative disease PHARC: An inborn error of endocannabinoid metabolism. Am J Hum Genet 87: 410-7

Fraher D, Ellis MK, Morrison S, McGee SL, Ward AC, et al. 2015. Lipid Abundance in Zebrafish Embryos Is Regulated by Complementary Actions of the Endocannabinoid System and Retinoic Acid Pathway. Endocrinology 156: 3596-609

Galiegue S, Mary S, Marchand J, Dussossoy D, Carriere D, et al. 1995. Expression of central and peripheral cannabinoid receptors in human immune tissues and leukocyte subpopulations. Eur J Biochem 232: 54-61

Galve-Roperh I, Palazuelos J, Aguado T, Guzman M. 2009. The endocannabinoid system and the regulation of neural development: potential implications in psychiatric disorders. Eur Arch Psychiatry Clin Neurosci 259: 371-82

Gary-Bobo M, Elachouri G, Gallas JF, Janiak P, Marini P, et al. 2007. Rimonabant reduces obesity-associated hepatic steatosis and features of metabolic syndrome in obese Zucker fa/fa rats. Hepatology 46: 122-9

Glaser ST, Kaczocha M. 2010. Cyclooxygenase-2 mediates anandamide metabolism in the mouse brain. J Pharmacol Exp Ther 335: 380-8

Guggenhuber S, Alpar A, Chen R, Schmitz N, Wickert M, et al. 2016. Cannabinoid receptor-interacting protein Crip1a modulates CB1 receptor signaling in mouse hippocampus. Brain Struct Funct 221: 2061-74

Guo S. 2004. Linking genes to brain, behavior and neurological diseases: what can we learn from zebrafish? Genes Brain Behav 3: 63-74

Guo S, Wilson SW, Cooke S, Chitnis AB, Driever W, Rosenthal A. 1999. Mutations in the zebrafish unmask shared regulatory pathways controlling the development of catecholaminergic neurons. Developmental biology 208: 473-87

Hariri AR, Gorka A, Hyde LW, Kimak M, Halder I, et al. 2009. Divergent effects of genetic variation in endocannabinoid signaling on human threat- and reward-related brain function. Biol

Psychiatry 66: 9-16

Herkenham M, Lynn AB, Little MD, Johnson MR, Melvin LS, et al. 1990. Cannabinoid receptor localization in brain. Proc Natl Acad Sci U S A 87: 1932-6

Hill AJ, Teraoka H, Heideman W, Peterson RE. 2005. Zebrafish as a model vertebrate for investigating chemical toxicity. Toxicological sciences : an official journal of the Society of Toxicology 86: 6-19

Hollis DM, Coddington EJ, Moore FL. 2006. Neuroanatomical distribution of cannabinoid receptor gene expression in the brain of the rough-skinned newt, Taricha granulosa. Brain Behav Evol 67: 135-49

Howlett AC, Blume LC, Dalton GD. 2010. CB(1) cannabinoid receptors and their associated proteins. Curr Med Chem 17: 1382-93

Insel T. 1995. The Fourth Generation of Progress. Raven Press, New York: 683-94

Justinova Z, Solinas M, Tanda G, Redhi GH, Goldberg SR. 2005. The endogenous cannabinoid anandamide and its synthetic analog R(+)-methanandamide are intravenously self-administered by squirrel monkeys. J Neurosci 25: 5645-50

Jutras-Aswad D, DiNieri JA, Harkany T, Hurd YL. 2009. Neurobiological consequences of maternal cannabis on human fetal development and its neuropsychiatric outcome. Eur Arch Psychiatry Clin Neurosci 259: 395-412

Krug RG, 2nd, Clark KJ. 2015. Elucidating cannabinoid biology in zebrafish (Danio rerio). Gene 570: 168-79

Lam CS, Rastegar S, Strahle U. 2006. Distribution of cannabinoid receptor 1 in the CNS of zebrafish. Neuroscience 138: 83-95

Lieschke GJ, Currie PD. 2007. Animal models of human disease: zebrafish swim into view. Nat Rev Genet 8: 353-67

Liu LY, Alexa K, Cortes M, Schatzman-Bone S, Kim AJ, et al. 2016. Cannabinoid receptor signaling regulates liver development and metabolism. Development 143: 609-22

Liu YJ, Fan HB, Jin Y, Ren CG, Jia XE, et al. 2013. Cannabinoid receptor 2 suppresses leukocyte inflammatory migration by modulating the JNK/c-Jun/Alox5 pathway. J Biol Chem 288: 13551-62

Lupica CR, Riegel AC, Hoffman AF. 2004. Marijuana and cannabinoid regulation of brain reward circuits. Br J Pharmacol 143: 227-34

Maresz K, Carrier EJ, Ponomarev ED, Hillard CJ, Dittel BN. 2005. Modulation of the cannabinoid CB2 receptor in microglial cells in response to inflammatory stimuli. J Neurochem 95: 437-45

Maresz K, Pryce G, Ponomarev ED, Marsicano G, Croxford JL, et al. 2007. Direct suppression of CNS autoimmune inflammation via the cannabinoid receptor CB1 on neurons and CB2 on

autoreactive T cells. Nat Med 13: 492-7

Martella A, Sepe RM, Silvestri C, Zang J, Fasano G, et al. 2016a. Important role of endocannabinoid signaling in the development of functional vision and locomotion in zebrafish. FASEB journal : official publication of the Federation of American Societies for Experimental Biology 30: 4275-88

Martella A, Silvestri C, Maradonna F, Gioacchini G, Allara M, et al. 2016b. Bisphenol A Induces Fatty Liver by an Endocannabinoid-Mediated Positive Feedback Loop. Endocrinology 157: 1751-63

Mato S, Del Olmo E, Pazos A. 2003. Ontogenetic development of cannabinoid receptor expression and signal transduction functionality in the human brain. Eur J Neurosci 17: 1747-54

Matsuda LA, Lolait SJ, Brownstein MJ, Young AC, Bonner TI. 1990. Structure of a cannabinoid receptor and functional expression of the cloned cDNA. Nature 346: 561-4

McCurley AT, Callard GV. 2008. Characterization of housekeeping genes in zebrafish: male-female differences and effects of tissue type, developmental stage and chemical treatment. BMC Mol Biol 9: 102

Meccariello R, Chianese R, Cacciola G, Cobellis G, Pierantoni R, Fasano S. 2006. Type-1 cannabinoid receptor expression in the frog, Rana esculenta, tissues: a possible involvement in the regulation of testicular activity. Mol Reprod Dev 73: 551-8

Meccariello R, Chianese R, Cobellis G, Pierantoni R, Fasano S. 2007. Cloning of type 1

cannabinoid receptor in Rana esculenta reveals differences between genomic sequence and cDNA. FEBS J 274: 2909-20

Meccariello R, Franzoni MF, Chianese R, Cottone E, Scarpa D, et al. 2008. Interplay between the endocannabinoid system and GnRH-I in the forebrain of the anuran amphibian Rana esculenta. Endocrinology 149: 2149-58

Mechoulam R, Ben Shabat S, Hanus L, Fride E, Vogel Z, et al. 1996. Endogenous cannabinoid ligands--chemical and biological studies. J Lipid Mediat Cell Signal 14: 45-9

Migliarini B, Carnevali O. 2008. Anandamide modulates growth and lipid metabolism in the zebrafish Danio rerio. Mol Cell Endocrinol 286: S12-6

Migliarini B, Marucci G, Ghelfi F, Carnevali O. 2006. Endocannabinoid system in Xenopus laevis development: CB1 receptor dynamics. FEBS Lett 580: 1941-5

Moreau J. 1973. Hashish and Mental Illness. Raven Press, New York

Mulder J, Aguado T, Keimpema E, Barabas K, Ballester Rosado CJ, et al. 2008. Endocannabinoid signaling controls pyramidal cell specification and long-range axon patterning. Proc Natl Acad Sci U S A 105: 8760-5

Munro S, Thomas KL, Abu-Shaar M. 1993. Molecular characterization of a peripheral receptor for cannabinoids. Nature 365: 61-5

Niehaus JL, Liu Y, Wallis KT, Egertova M, Bhartur SG, et al. 2007. CB1 cannabinoid receptor activity is modulated by the cannabinoid receptor interacting protein CRIP 1a. Mol Pharmacol 72: 1557-66

Nishio S, Gibert Y, Berekelya L, Bernard L, Brunet F, et al. 2012. Fasting induces CART down-regulation in the zebrafish nervous system in a cannabinoid receptor 1-dependent manner. Mol Endocrinol 26: 1316-26

Onaivi ES, Ishiguro H, Gong JP, Patel S, Meozzi PA, et al. 2008. Brain neuronal CB2 cannabinoid receptors in drug abuse and depression: from mice to human subjects. PLoS One 3: e1640

Osei-Hyiaman D, DePetrillo M, Pacher P, Liu J, Radaeva S, et al. 2005. Endocannabinoid activation at hepatic CB1 receptors stimulates fatty acid synthesis and contributes to diet-induced obesity. J Clin Invest 115: 1298-305

Pai WY, Hsu CC, Lai CY, Chang TZ, Tsai YL, Her GM. 2013. Cannabinoid receptor 1 promotes hepatic lipid accumulation and lipotoxicity through the induction of SREBP-1c expression in zebrafish. Transgenic Res 22: 823-38

Palazuelos J, Aguado T, Egia A, Mechoulam R, Guzman M, Galve-Roperh I. 2006. Non-psychoactive CB2 cannabinoid agonists stimulate neural progenitor proliferation. FASEB journal : official publication of the Federation of American Societies for Experimental Biology 20: 2405-7

Pang T, Atefy R, Sheen V. 2008. Malformations of cortical development. Neurologist 14: 181-91

Paria BC, Song H, Wang X, Schmid PC, Krebsbach RJ, et al. 2001. Dysregulated cannabinoid signaling disrupts uterine receptivity for embryo implantation. J Biol Chem 276: 20523-8

Piccinetti CC, Migliarini B, Olivotto I, Coletti G, Amici A, Carnevali O. 2010. Appetite regulation: the central role of melatonin in Danio rerio. Horm Behav 58: 780-5

Romero J, Garcia-Palomero E, Berrendero F, Garcia-Gil L, Hernandez ML, et al. 1997. Atypical location of cannabinoid receptors in white matter areas during rat brain development. Synapse 26: 317-23

Ruhl T, Prinz N, Oellers N, Seidel NI, Jonas A, et al. 2014. Acute administration of THC impairs spatial but not associative memory function in zebrafish. Psychopharmacology (Berl) 231: 3829-42

Ruhl T, Zeymer M, von der Emde G. 2016. Cannabinoid modulation of zebrafish fear learning and its functional analysis investigated by c-Fos expression. Pharmacol Biochem Behav 153: 18-31

Salio C, Cottone E, Conrath M, Franzoni MF. 2002. CB1 cannabinoid receptors in amphibian spinal cord: relationships with some nociception markers. J Chem Neuroanat 24: 153-62

Santoriello C, Zon LI. 2012. Hooked! Modeling human disease in zebrafish. J Clin Invest 122: 2337-43

Savinainen JR, Saario SM, Laitinen JT. 2012. The serine hydrolases MAGL, ABHD6 and

ABHD12 as guardians of 2-arachidonoylglycerol signalling through cannabinoid receptors. Acta Physiol (Oxf) 204: 267-76

Serra EL, Medalha CC, Mattioli R. 1999. Natural preference of zebrafish (Danio rerio) for a dark environment. Braz J Med Biol Res 32: 1551-3

Shimada Y, Hirano M, Nishimura Y, Tanaka T. 2012. A high-throughput fluorescence-based assay system for appetite-regulating gene and drug screening. PLoS One 7: e52549

Silvestri C, Paris D, Martella A, Melck D, Guadagnino I, et al. 2015. Two non-psychoactive cannabinoids reduce intracellular lipid levels and inhibit hepatosteatosis. J Hepatol 62: 1382-90

Sipe JC, Chiang K, Gerber AL, Beutler E, Cravatt BF. 2002. A missense mutation in human fatty acid amide hydrolase associated with problem drug use. Proc Natl Acad Sci U S A 99: 8394-9

Soderstrom K, Leid M, Moore FL, Murray TF. 2000. Behaviroal, pharmacological, and molecular characterization of an amphibian cannabinoid receptor. J Neurochem 75: 413-23

Stern HM, Zon LI. 2003. Cancer genetics and drug discovery in the zebrafish. Nature reviews. Cancer 3: 533-9

Stewart AM, Kalueff AV. 2014. The behavioral effects of acute Delta(9)-tetrahydrocannabinol and heroin (diacetylmorphine) exposure in adult zebrafish. Brain Res 1543: 109-19

Trazzi S, Steger M, Mitrugno VM, Bartesaghi R, Ciani E. 2010. CB1 cannabinoid receptors

increase neuronal precursor proliferation through AKT/glycogen synthase kinase-3beta/beta-catenin signaling. J Biol Chem 285: 10098-109

Viveros MP, Marco EM, File SE. 2005. Endocannabinoid system and stress and anxiety responses. Pharmacol Biochem Behav 81: 331-42

Wang X, Dow-Edwards D, Keller E, Hurd YL. 2003. Preferential limbic expression of the cannabinoid receptor mRNA in the human fetal brain. Neuroscience 118: 681-94

Watson S, Chambers D, Hobbs C, Doherty P, Graham A. 2008. The endocannabinoid receptor, CB1, is required for normal axonal growth and fasciculation. Mol Cell Neurosci 38: 89-97

Wiley JL, Burston JJ, Leggett DC, Alekseeva OO, Razdan RK, et al. 2005. CB1 cannabinoid receptor-mediated modulation of food intake in mice. Br J Pharmacol 145: 293-300

Yuan D, Wu Z, Wang Y. 2016. Evolution of the diacylglycerol lipases. Prog Lipid Res 64: 85-97

Zlebnik NE, Cheer JF. 2016. Drug-Induced Alterations of Endocannabinoid-Mediated Plasticity in Brain Reward Regions. J Neurosci 36: 10230-38

Zurolo E, Iyer AM, Spliet WG, Van Rijen PC, Troost D, et al. 2010. CB1 and CB2 cannabinoid receptor expression during development and in epileptogenic developmental pathologies. Neuroscience 170: 28-41

CHAPTER 3: Genetic Manipulation of the Endocannabinoid System in Zebrafish

3.1 ABSTRACT

The endocannabinoid (eCBs) system contains several proteins involved in eCB signaling, synthesis, and degradation. Perturbing eCB protein function through genetic knockouts can uncover valuable information regarding its role in biological processes. Here, we utilize CRISPR Cas9-mediated gene editing to produce 6 endocannabinoid gene knockout zebrafish lines: *cb1*, *dagla*, *daglb*, *abhd4*, *mgll*, and *faah*. The *dagla* knockout larvae and adults do not exhibit altered light-dark preference behavior, but knockout larvae do demonstrate an increase in locomotor activity when both parents are also *dagla* knockouts. The *dagla* knockout fish demonstrated an 85% increase in *gpr55a*, 44% reduction in *dagla*, and 99% reduction in *fas* mRNA transcripts. Future work includes further examination of *dagla* phenotypes, phenotyping the rest of the knockout lines, and producing double mutants.

3.2 INTRODUCTION

As mentioned in the previous chapter, the endocannabinoid (eCB) system is a complex signaling pathway involved in a broad range of biological processes, including neural development (Burggren et al., 2019; Mechoulam and Parker, 2013), anxiety (Lisboa et al., 2017; Lutz et al., 2015; Mechoulam and Parker 2013), lipid homeostasis (Pai et al., 2013), immune function (Almogi-Hazan and Or, 2020; Cabral et al., 2015), and neuroinflammation (Cheung et al., 2019; Cooray et al., 2020). The eCB system is comprised of ligands and proteins that work together to facilitate endocannabinoid signaling (for a list of eCB proteins, ligands, and their respective functions, see **Table 2.1**, p.63). Inhibiting a protein via genetic perturbation – gene knockouts – can help us learn new information about eCB gene function. For example, Leishman et al. (2016) examined changes in lipid levels following genetic disruption of N-acyl-

phosphatidylethanolamine phospholipase D (NAPE-PLD) in mice. They discovered that NAPE-PLD deletion results in changes in prostaglandin levels, suggesting a broader role of the NAPE-PLD on lipid modulation than previously thought. Another study (Fin et al., 2017) examined genetic perturbation of Cannabinoid receptor interacting protein (Cnrip1) isoforms in zebrafish. Though these eCB proteins are strongly conserved across species dating back 400 million years, *cnrip1a* and *cnrip1b* knockout fish did not exhibit any deleterious phenotypes, revealing that these proteins are not necessary for viability, morphological development, or fertility.

In this chapter, we produce 6 new zebrafish knockout lines: Cannabinoid Receptor 1 (*cb1*), Diacylglycerol lipase alpha (*dagla*), Diacylglycerol lipase beta (*daglb*), Alpha beta hydrolase domain containing 4 (*abhd4*), Monoglyceride lipase (*mgll*), and Fatty acid amide hydrolase (*faah*). These knockout lines can aid in furthering our knowledge of eCB proteins and their individual roles in the biological processes that are modulated by the eCB system.

3.3 METHODS

3.3.1 Zebrafish husbandry

Zebrafish were raised at the University of California, San Francisco zebrafish facility at 28°C under a 14/10 hour light/dark cycle per National Institutes of Health and University of California, San Francisco, and treated according to IACUC regulations. On day -1, adult zebrafish were placed into breeding chambers. On day 0, the divider of the breeding chambers were removed and embryos were collected. Freshly collected embryos were sorted into 100mm petri dishes with 30 mL blue egg water (0.12 g of $CaSO_4$, 0.2 g of Instant Ocean Salts, 30 uL of methylene blue in 1 L of H_2O) and stored in a 28 °C incubator. On day 2, embryos were moved onto a blue

pad (VWR underpad #82020-845) in a room with 14/10 hour light/dark cycle to allow for proper vision development.

3.3.2 Sequence alignment

Sequences of endocannabinoid genes and proteins were taken from the Ensembl database (https://uswest.ensembl.org/index.html). Sequences were aligned using the Clustal Omega 1.2.4 sequence alignment tool (https://www.ebi.ac.uk/Tools/msa/clustalo/).

3.3.3 sgRNA design and synthesis

sgRNAs targeting the *cb1*, *dagla*, *daglb*, *abhd4, mgll*, and *faah* loci were designed using CRISPRscan (https://www.crisprscan.org), CCtop (https://cctop.cos.uni-heidelberg.de), and CHOPCHOP (https://chopchop.cbu.uib.no) web tools (sgRNA sequences are found in **Table 3.S1**). Phusion Flash High-Fidelity PCR Master Mix (ThermoFisher, #F548L) was added to 10 μM forward primer containing T7 promotor with sgRNA sequence and 10 μM reverse primer containing standard stem loop backbone (Jinek et al., 2012; Varshney, et al. 2015) and PCR was run. PCR product was purified with MinElute PCR Purification kit (Qiagen, #28006) and used for *in vitro* transcription with T7 RNA polymerase (Jiang et al. 2019). Transcription product was incubated in DNaseI (ThermoFisher, #EN0521), extracted with phenol/chloroform, and precipitated with ethanol. Ethanol was left to evaporate for 10 min, and precipitate was resuspended in nuclease free water. To produce Cas9 RNA, the template DNA pT3Ts-nls-zCas9-nls (from Wenbiao Chen, Addgene plasmid #46757) was linearized by XbaI digestion and purified with QIAprep column (Qiagen, #27115). Cas9 RNA was synthesized using mMESSAGE mMACHINE T3 Transcription kit (Invitrogen, #AM148) and purified using

MEGAclear Transcription Cleanup kit (Invitrogen, #AM1908).

3.3.4 Microinjections

To produce knockouts, a solution of 200 ng/μL sgRNA and 100 ng/μL Cas9 RNA was injected into a clutch of AB wild-type zebrafish embryos at the 1-cell stage using a microinjector (NARISHIGE IM 300). Roughly half of the embryos were set aside as uninjected controls.

3.3.5 Sequencing

Injected F0 fish were raised to adulthood and bred with ABWT fish to produce the F1 generation. Genotyping primers were designed to flank the sgRNA target sequence of each gene (sequences are found in **Table 3.S2**). Genomic DNA was extracted from fins clipped from the F1 generation. PCR was run on a solution of 0.4 μM primers, genomic DNA, and GoTaq Green Master Mix (Promega, #M7123). PCR product was purified using Monarch DNA Gel Extraction Kit (New England BioLabs, #T1020L), and sequenced by QuintaraBio. Sequencing results were deconvoluted using the TIDE web tool (https://tide.nki.nl) to determine the number of base pairs that were inserted or deleted. F1 fish heterozygous for the same allele were bred together, and their progeny were sequenced as described above. Sequencing results for the knockout fish allowed for determination of the precise mutation sequence.

3.3.6 Allele-specific polymerase chain reaction (ASPCR)

Once the nature of the mutation is found and the mutant sequence is determined, ASPCR can be performed: a method of genotyping that is faster and lower cost than sequencing (Gaudet et

al. 2009). In this technique, several sets of primers are designed (these can only be made when the mutant sequence is known). One primer set specifically recognizes the wild-type allele, and another primer set is designed for specific recognition of each mutant allele. Primers sets were designed for wild-type and mutant alleles of *cb1* and *dagla* (see **Table 3.S3** for ASPCR primer sequences). To increase specificity of each primers set for its intended allele, primers sets were designed ensuring that one primer (either the forward or reverse) includes the mutation location at or near the 3' end. Primers were used to run PCR, and PCR product was run on a gel to view results.

3.3.7 Light-dark preference assay

For larval experiments, 5 dpf zebrafish were randomly distributed into 100 mm petri dishes with 30 mL of blue egg water at 8 larvae per dish. Behavioral recording of light-dark choice was carried out as described by Wagle et al. (2017). Larvae in petri dishes or adults in fish tanks were placed on a blue pad at 27.1°C for a one hour habituation period before testing. For larval experiments, a plastic transfer pipette was used to individually transfer 8 larvae to the center of light/dark chambers containing 10 mL of blue egg water. The larval chambers were placed on a trans-illuminator (Stratagene light box) covered with acrylic strips that obscured the dark side of the chamber and simultaneously allowed the light side to be illuminated. For adult experiments, fish were netted into adult light/dark chambers made of plastic with white and dark plastic lining and filled with system water. The larval and adult chambers were recorded from above using two cameras (Panasonic) with infrared filters (ACRYLITE IR acrylic 11460) and Noldus MPEG 2.1 software.

For the baseline light-dark preference experiments, recording duration was 8 minutes, and fish were recorded twice a day (AM trial: 10:00am-11:50am, PM trial: 3:30pm-5:00pm) for

two consecutive days (5dpf and 6dpf for larvae). For light-dark preference with habituation, recording duration was extended to 45 minutes and one recording was done for each larvae.

Videos collected from the light/dark preference assay were analyzed using Noldus Ethovision XT 13 video tracking software. Larvae were tracked and the following output parameters were collected: duration in the light zone, duration in the dark zone, and velocity. Any larvae that were frozen for the duration of the experiment were excluded. Choice index was calculated by subtracting the duration in the light from the duration in the dark then dividing by the total time. Choice index and velocity were averaged per larvae and adults that underwent multiple trials.

3.3.8 Quantitative polymerase chain reaction (qPCR) analysis

qPCR was performed as described in Chapter 2 (section 2.4.2, p.47) on 3 dpf zebrafish larvae. See **Table 3.S4** for qPCR primer sequences.

3.4 RESULTS

3.4.1 eCB proteins are conserved between human and zebrafish orthologues

Each of the human eCB proteins CB1, DAGLA, DAGLB, ABHD4, MGLL, and FAAH have zebrafish orthologues. For CB1, human (peptide ID: ENSP00000358513) and zebrafish (ENSDARP00000007647) proteins consist of 472 and 475 amino acids, respectively, and share 70% amino acid sequence identity (**Figure 3.S1**). For DAGLA, human (ENSP00000257215) and zebrafish (ENSDARP00000146636) proteins consist of 1042 and 1076 amino acids,

respectively, and share 66% amino acid sequence identity (**Figure 3.S2**). For DAGLB, human (ENSDARP00000106821) and zebrafish (ENSP00000297056) proteins consist of 672 and 668 amino acids, respectively, and share 56% amino acid sequence identity (**Figure 3.S3**). For ABHD4, human (ENSP00000414558) and zebrafish (ENSDARP00000137303) proteins consist of 342 and 394 amino acids, respectively, and share 62% amino acid sequence identity (**Figure 3.S4**). For MGLL, human (ENSP00000265052) and zebrafish (ENSDARP00000053462) proteins consist of 313 and 300 amino acids, respectively, and share 45% amino acid sequence identity (**Figure 3.S5**). For FAAH, human (ENSP00000243167) and zebrafish (ENSDARP00000100787) proteins consist of 579 and 590 amino acids, respectively, and share 52% amino acid sequence homology (**Figure 3.S6**).

3.4.2 Production of eCB zebrafish mutants

CRISPR Cas9-mediated genetic modification was used to produce eCB gene knockout fish lines (see **Figure 1.3**, p.22 for an overview of CRISPR-mediated genetic alterations in zebrafish). sgRNAs that target the *cb1*, *dagla, daglb, abhd4, mgll,* and *faah* loci were designed. Sequences for each sgRNA can be found in **Table 3.S1**. *cb1* sgRNA targets exon 1 of 2, *dagla* sgRNA targets exon 3 of 20, *daglb* sgRNA targets exon 4 of 15, *abhd4* sgRNA targets exon 4 of 8, *mgll* sgRNA targets exon 2 of 7, and *faah* sgRNA targets exon 4 of 15 (**Figure 3.1**). sgRNAs were injected along with Cas9 RNA into AB wild-type fish. Subsequent generations of each line were produced, and sequencing revealed the nature of each mutation (**Figure 3.2**). All introduced mutations were insertions or deletions that are not divisible by 3, suggesting deleterious frameshift mutations. Two *cb1* mutant lines were produced, one containing an 8 base pair deletion and another with a 1 base pair deletion (**Figure 3.2A**). Two *dagla* mutant lines were produced, one containing a 5 base pair deletion and another with a 7 base pair

insertion (along with 2 base pair changes) (**Figure 3.2B**). For the knockouts, one mutant line was produced: the *daglb* mutation had a 4 base pair deletion (**Figure 3.2C**), the *abhd4* mutation had a 1 base pair deletion (along with 1 base pair change) (**Figure 3.2D**), the *mgll* mutation had a 13 base pair insertion (**Figure 3.2E**), and the *faah* mutation had a 1 base pair insertion (along with 1 base pair change) (**Figure 3.2F**). Sequences of genotyping primers can be found in **Tables 3.S2** and **3.S3**.

3.4.3 Light-dark preference behavior is unchanged in dagla *knockout fish*

After the knockout lines were established, our next aim was to examine phenotypes that occur due to the eCB gene perturbations. For the rest of this chapter, we will focus on the *dagla* 5 base pair deletion mutant, which will be denoted as Tg(*dagla*$^{-5/-5}$). We first examined baseline light-dark preference behavior in Tg(*dagla*$^{-5/-5}$) larvae and adults. Compared to wild-type and heterozygous siblings, Tg(*dagla*$^{-5/-5}$) larvae exhibited no change in light-dark preference nor locomotor activity, as seen by the choice index and velocity measured in the light-dark preference assay (**Figure 3.3A**). Tg(*dagla*$^{-5/-5}$) adults also did not show any significant changes in choice index nor velocity compared to wild-type controls (**Figure 3.3B**).

We followed up these experiments with an alternative version of the light-dark preference assay that examines habituation. Habituation, or the reduction in response to a stimuli following repeated or prolonged exposure, can be examined by extending the duration of the assay from the standard 8 minutes to 45 minutes. We first compared wild-type and knockout *dagla* siblings, whose parents were both heterozygous for the -5 base pair allele (as in **Figure 3.3**). As expected, the choice index increased over time in both wild-type and knockout larvae as they habituated to the light-dark chamber, though there was no significant difference between genotypes (**Figure 3.4A**). There was also no significant change in velocity between

genotypes (**Figure 3.4A**).

One possible explanation for the similarity between the phenotypes of Tg(*dagla*$^{-5/-5}$) and wild-type siblings is maternal contribution of mRNA or protein; because the mother is heterozygous, maternal mRNA/protein that is exposed to the larvae during early stages of development could mask any phenotypes that the knockout would present (Burgess et al., 2002; Zhang et al., 2020). To overcome this caveat of using siblings, we next performed the light-dark preference habituation assay comparing wildtype and knockout cousins. Parents of the wild-type larvae were both wild-type for *dagla*, and parents of the knockout larvae were both knockout for *dagla*, removing the possibility of maternal *dagla* mRNA or protein contribution to the Tg(*dagla*$^{-5/-5}$) larvae. Though there was no change in choice index compared to controls, we observed a significant increase in velocity at the 1.5min–3min ($p = 0.014245$), 4.5min–6min ($p = 0.025776$), 9mi –10.5min ($p = 0.027814$), and 10.5min–12min ($p = 0.027814$) time bins (**Figure 3.4B**).

3.4.4 Effects of dagla *knockout on mRNA expression of eCB-, dopamine-, lipid-related genes*

After determining a change in phenotype when using genetic cousins instead of siblings, we continued our phenotyping of the *dagla* mutant by comparing wild-type and knockout cousins. The next assay we performed was qPCR, in order to determine if mRNA levels of eCB-, dopamine- or lipid- related genes are altered in Tg(*dagla*$^{-5/-5}$) larvae. Notable mRNA alterations include G protein-coupled receptor 55a (*gpr55a*), which increased 85%, *dagla*, which decreased 44%, and Fatty acid synthase (*fas*), which decreased 99% in Tg(*dagla*$^{-5/-5}$) fish (**Figure 3.5**).

3.5 DISCUSSION

In this chapter, we discussed 6 newly produced genetic knockouts of the endocannabinoid genes *cb1*, *dagla*, *daglb*, *abhd4*, *mgll*, and *faah*. Following genotyping, we were able to propagate mutant lines for each gene containing frameshift mutations (**Figure 3.2**).

We next sought to phenotype the *dagla* knockout. We determined that there was no difference in light-dark preference between Tg(*dagla*$^{-5/-5}$) and wild-type larvae and adults (**Figure 3.3**). Similarly, we observed no change in light-dark preference between wild-type and knockout larvae when examining light-dark preference habituation. (**Figure 3.4**). We did find a significant increase in velocity in Tg(*dagla*$^{-5/-5}$) mutants compared to wildtype cousins that was not seen when performing the same assay using siblings (**Figure 3.4**), suggesting that maternal compensation of *dagla* mRNA or protein could be playing a role in masking phenotypes (**Figure 2.5D**, p.59, shows that *dagla* maternal mRNA is present between 1 hour and 8 hours post fertilization). This finding suggests that it may be worthwhile to examine the phenotypes between wild-type and knockout siblings, as well as wild-type and knockout cousins, when phenotyping the eCB mutants. Regarding the velocity phenotype, change in locomotor activity was also seen by Martella et al. (2016) when perturbing *dagla* in larval zebrafish, though interestingly, they observed a *decrease* in locomotor activity that was partially rescued by the CB1 agonist noladin. A possible explanation for the discrepancy in results could be that Martella et al. used morpholinos to transiently knockdown *dagla*, whereas here we are examining the effects of a germline *dagla* mutation. Differing phenotypes between knockdowns and knockouts have been observed before (Place and Smith, 2017), and can be due to off-target effects of the morpholino (Gerety and Wilkinson, 2011; Kok et al., 2015; Robu et al., 2007), or by genetic compensatory effects in knockouts (Rossi et al., 2015). Follow-up studies could involve administering a Cb1 agonist to *dagla* knockouts to see if this reduces the locomotor phenotype

back to wild-type levels, performing RNA-seq on *dagla* knockouts to see if any genes have altered expression, or injecting *dagla* morpholino into *dagla* knockouts to determine if the *dagla* morpholino induces off-target effects.

Lastly, we observed an 85% increase in *gpr55a*, 44% reduction in *dagla*, and 99% reduction in *fas* mRNA transcripts in *dagla* knockout larvae (**Figure 3.5**). The reduction in *dagla* transcript is in line with the phenomenon of nonsense-mediated decay, which can occur in mRNA with aberrant sequences (Garneau et al., 2007; Lykke-Andersen and Jensen, 2015; Tuladhar et al., 2019). Furthermore, the reduction in *fas* with *dagla* knockouts corroborates a previous study that demonstrated an increase in *fas* expression following Cb1 overexpression in zebrafish larvae (Pai et al., 2013).

It would be worthwhile to follow up on the interaction between *dagla* and *gpr55a*, as well as *dagla* and *fas*. More assays can be done to examine the role of *dagla* on behavior and other biological processes that the eCB system is invovled with. Furthermore, phenotyping the other mutants could provide new information on the roles of *cb1*, *daglb*, *abhd4*, *mgll*, and *faah*. Lastly, double mutants such as *cb1 & cb2*, *dagla & daglb*, and *mgll & faah* can now be produced and phenotyped, allowing more possibilities to uncover mechanisms of endocannabinoid proteins.

3.6 ACKNOWLEDGMENTS

I would like to thank Dr. Francesca Oltrabella for producing the eCB lines and being an incredible mentor. I would also like to thank Brian Nguyen, Fatima Murad, Sacha Salphati, and Amelia Dahlén for helping with line maintenance.

3.7 FIGURES

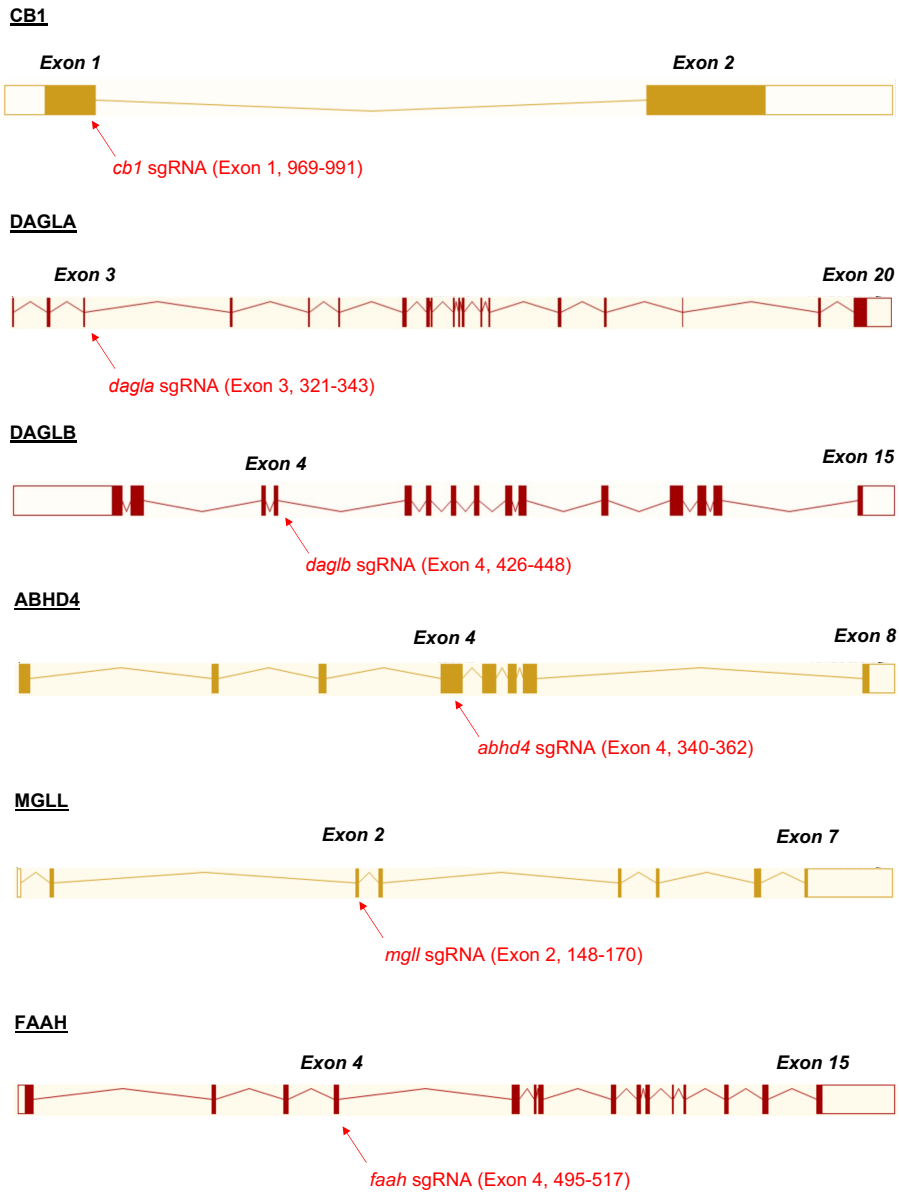

Figure 3.1 Schematic of all eCB sgRNA targets.

Red arrows point to the region of each loci that is targeted by the sgRNA and nucleotide position of the sgRNA sequence is provided. Exon schematics are from Ensembl (https://uswest.ensembl.org/index.html). CB1 – Cannabinoid receptor 1; DAGLA – Diacylglycerol lipase alpha; DAGLB – Diacylglycerol lipase beta; ABHD4 - Alpha beta hydrolase domain containing 4; MGLL – Monoglyceride lipase; FAAH – Fatty acid amide hydrolase.

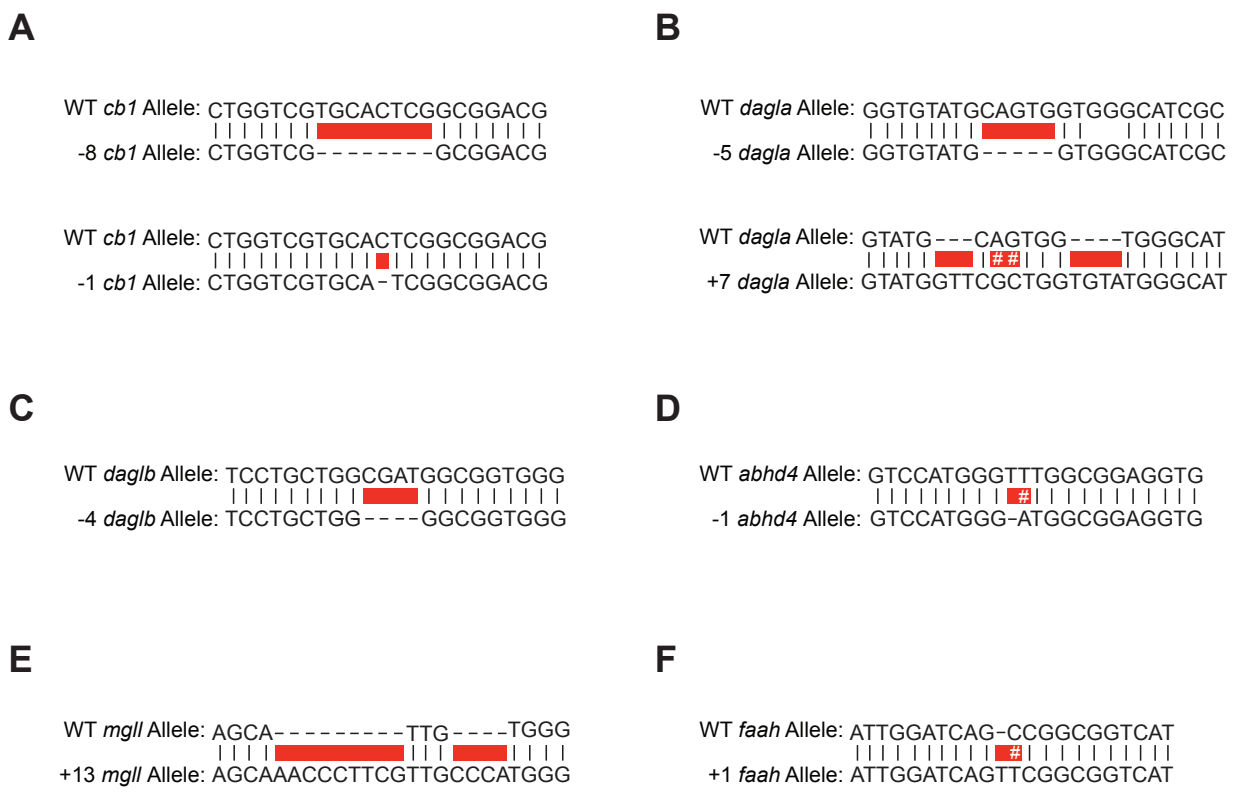

Figure 3.2 Nature of each eCB gene mutation.

(A-F) Sequences of wild-type alleles compared to mutant alleles at the sgRNA site for *cb1* (A), *dagla* (B), *daglb* (C), *abhd4* (D), *mgll* (E), and *faah* (F). All indels are not multiples of three, suggesting a deleterious frameshift mutation.

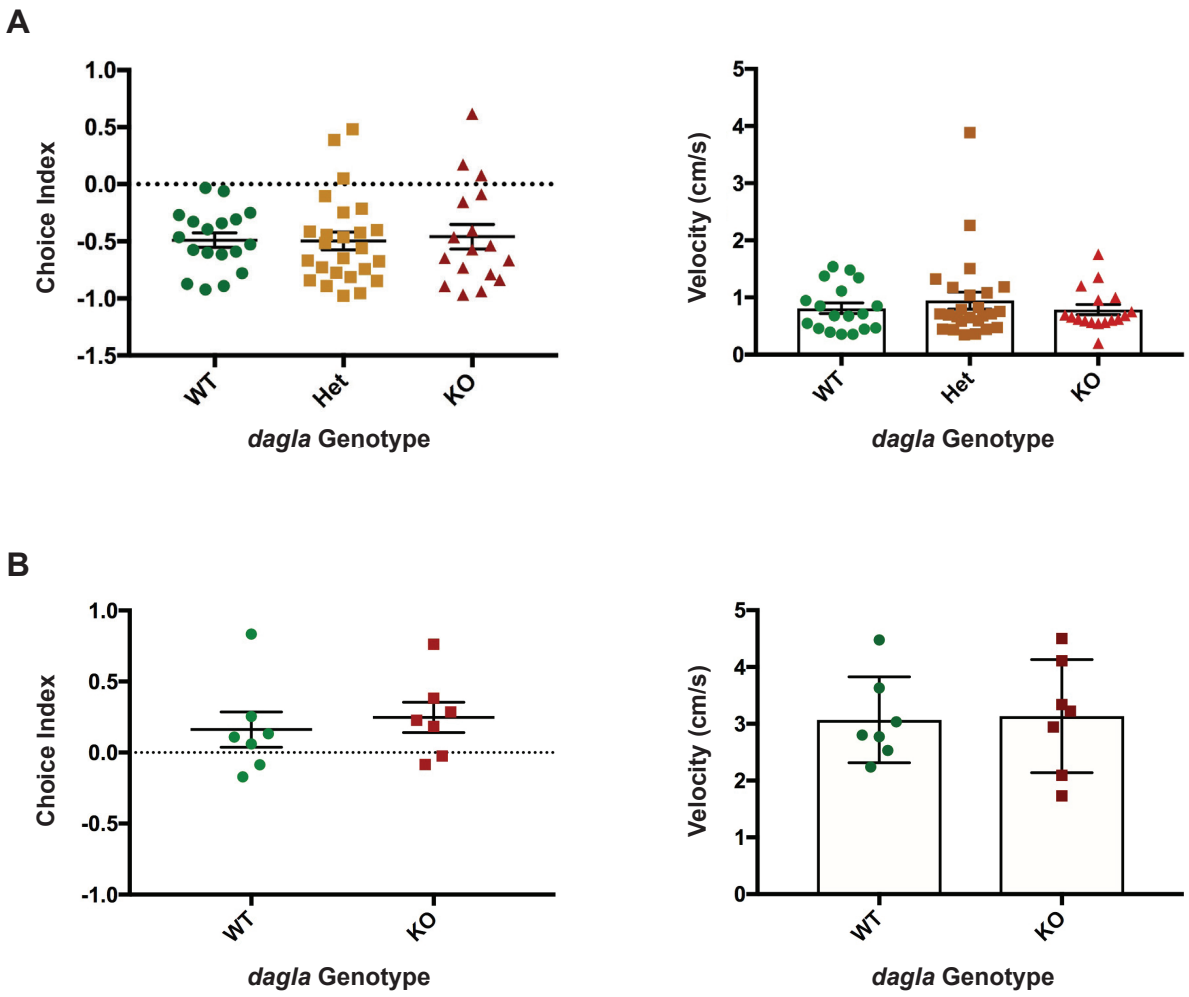

Figure 3.3 Baseline light-dark preference behavior is unchanged in *dagla* knockout fish.

(A) No difference in light-dark preference behavior (left) nor velocity (right) was observed between larvae that were wild-type, heterozygous, and knockout for the *dagla* gene. Larvae were 5-6dpf siblings, n = 18 wild-type; n = 25 heterozygous; n = 17 knockout.
(B) No difference in light-dark preference behavior (left) nor velocity (right) was observed between adult fish that were wild-type and knockout for the *dagla* gene. Adults were approximately 8 month old siblings, n = 7 wild-type; n = 7 knockout.
All data represented as mean +/ SEM. Each data point represents the average of 4 trials for one fish. Student's t-test was performed to assess statistical significance.

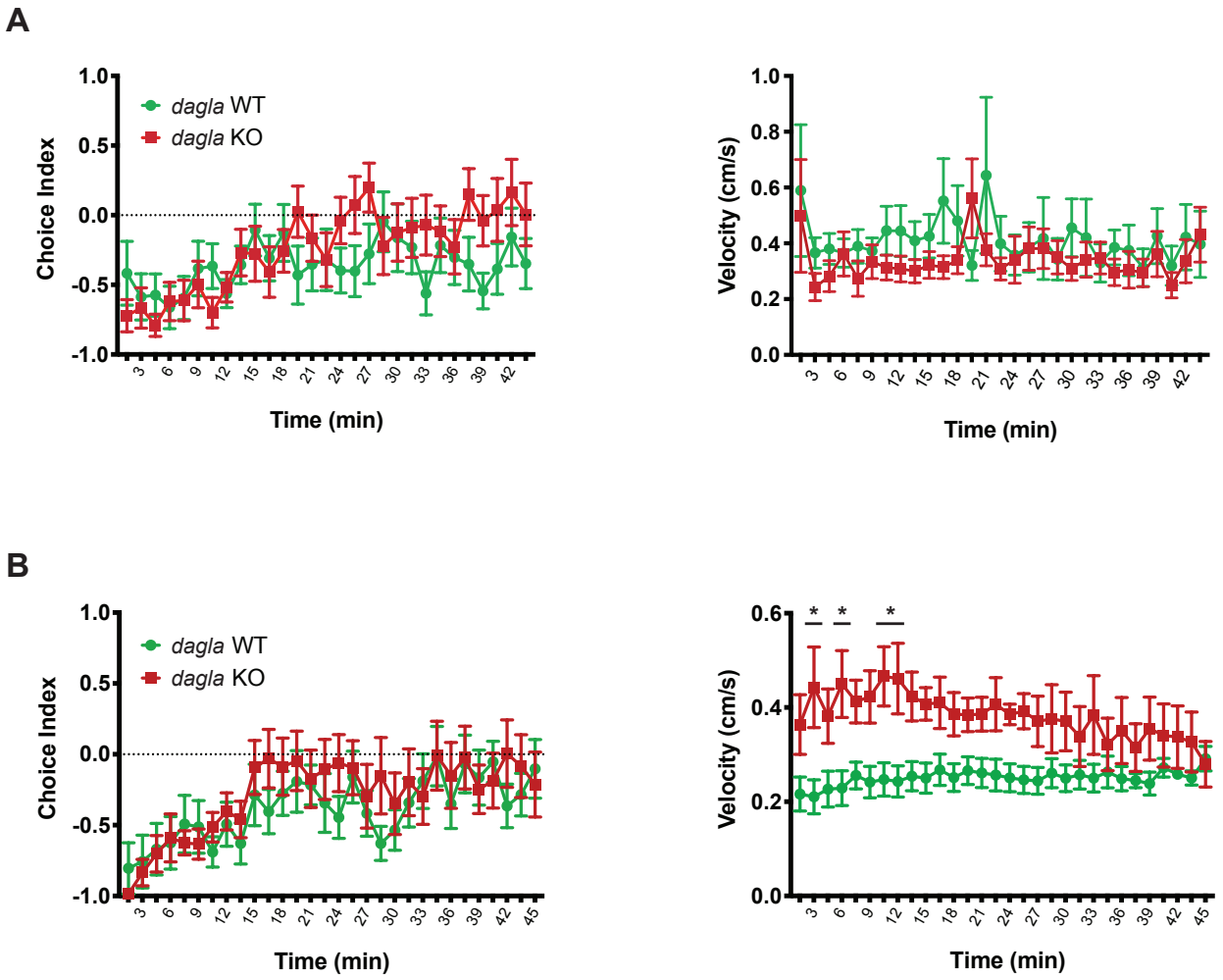

Figure 3.4 Effects of *dagla* knockout on Light-dark preference habituation.

(A) Choice index (left) and velocity (right) of *dagla* WT (n=13) and *dagla* KO (n=14) 5 dpf larval siblings in the light-dark preference habituation assay.
(B) Choice index (left) and velocity (right) of *dagla* WT (n=11) and *dagla* KO (n=11) 6 dpf larval cousins in the light-dark preference habituation assay.
All data represented as mean +/ SEM. Each data point represents a population of *dagla* WT or *dagla* KO separated into 1.5-minute time bins. *p < 0.05, multiple t-tests were performed to assess statistical significance.

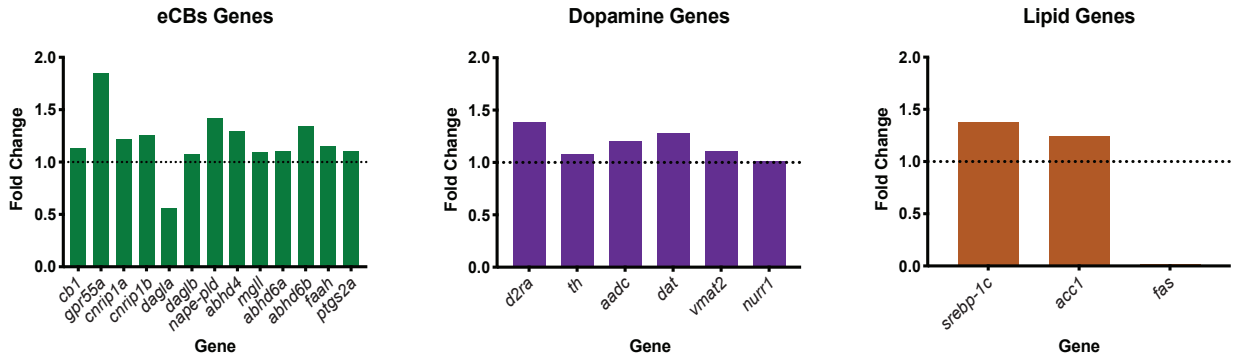

Figure 3.5 Effects of *dagla* knockout on mRNA expression of eCB-, dopamine-, lipid-related genes.

qPCR results examining mRNA levels of eCB genes (left), dopamine-related genes (middle), and lipid-related genes (right) in 3 dpf Tg(*dagla*$^{-5/-5}$) compared to age-matched wild-type cousins. Each bar represents the average of 3 technical replicates of 1 biological replicate comparing the fold change in mRNA quantity of knockouts (n=13) to wild-type (n=13). Values were standardized to elongation factor 1 alpha (*elf1a*). *cb1* – Cannabinoid receptor 1; *gpr55a* – G protein-coupled receptor 55a; *cnrip1a* – Cannabinoid receptor interacting protein 1a; *cnrip1b* – Cannabinoid receptor interacting protein 1a; *dagla* – Diacylglycerol lipase, alpha; *daglb* – Diacylglycerol lipase, beta; *nape-pld* – N-acyl phosphatidylethanolamine phospholipase D; *abhd4* – Alpha beta - hydrolase domain containing 4; *mgll* – Monoglyceride lipase; *abhd6a* – Alpha beta - hydrolase domain containing 6a; *abhd6b* – Alpha beta - hydrolase domain containing 6b; *faah* – fatty acid amide hydrolase; *ptgs2a* – Prostaglandin-endoperoxide synthase 2a; *d2ra* – Dopamine receptor 2a; *th* – Tyrosine hydroxylase; *aadc* – Aromatic L-amino acid decarboxylase; *dat* – Dopamine transporter; *vmat2* – Vesicular monoamine transporter 2; *nurr1* – Nuclear receptor related 1; *srebp-1c* – Sterol regulatory element-binding protein 1; *acc1* – acetyl-CoA carboxylase 1; *fas* – Fatty acid synthase.

3.8 SUPPLEMENTAL FIGURES AND TABLES

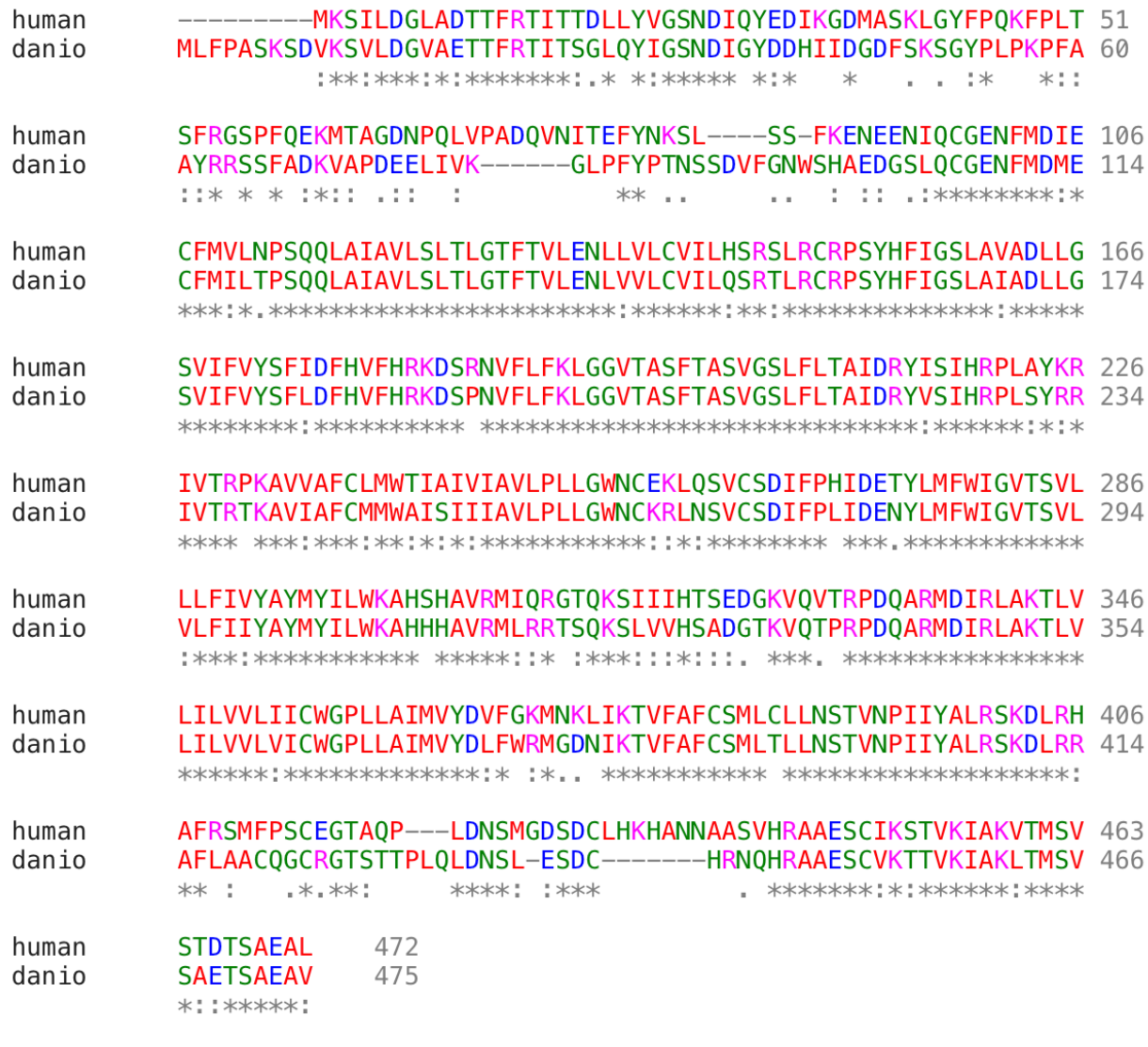

Figure 3.S1 Alignment between human and zebrafish homologs of CB1.

Amino acid sequence comparison between human CB1 and zebrafish cnr1.

Figure 3.S2 Alignment between human and zebrafish homologs of DAGLA.

Amino acid sequence comparison between human DAGLA and zebrafish dagla.

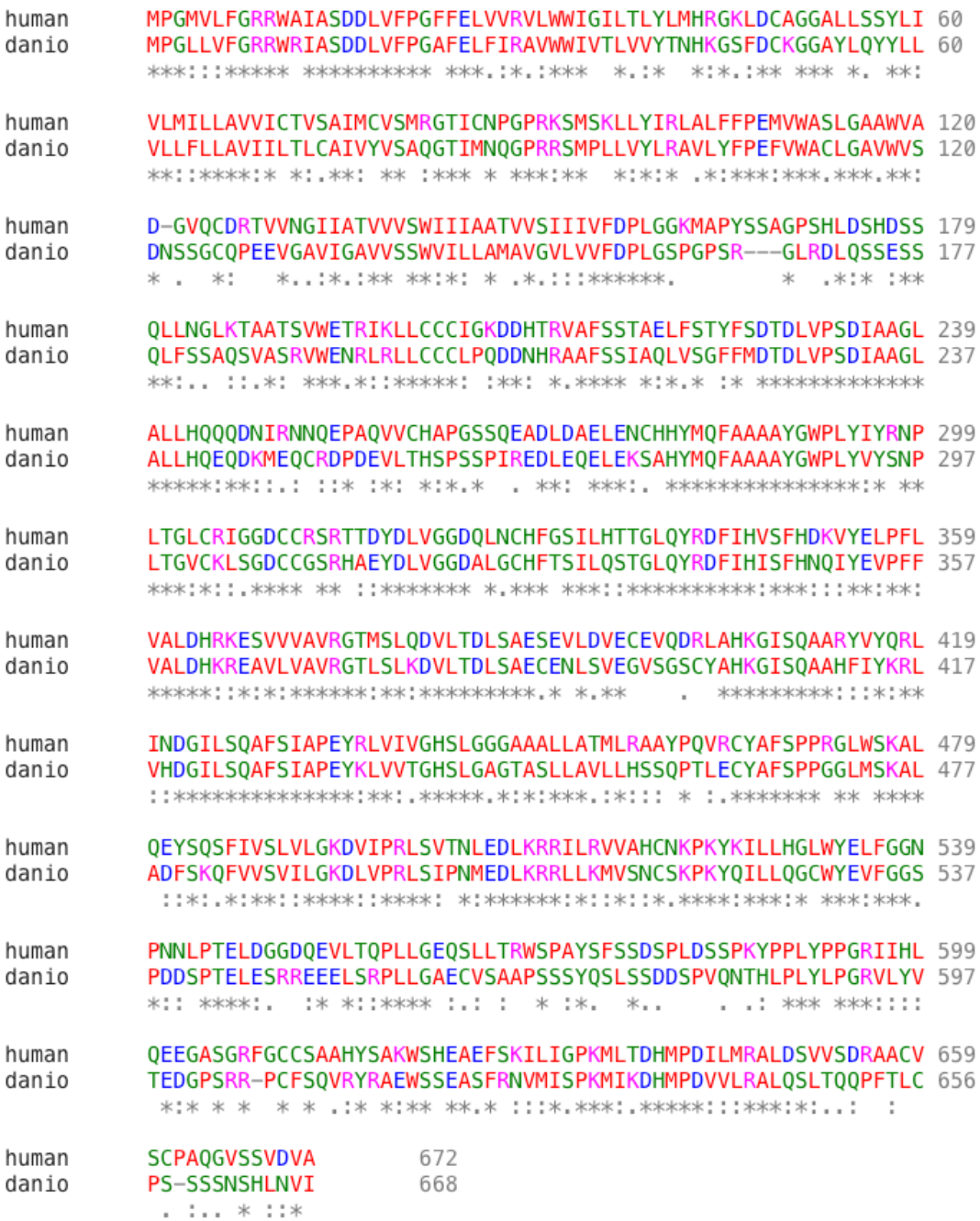

Figure 3.S3 Alignment between human and zebrafish homologs of DAGLB.

Amino acid sequence comparison between human DAGLB and zebrafish daglb.

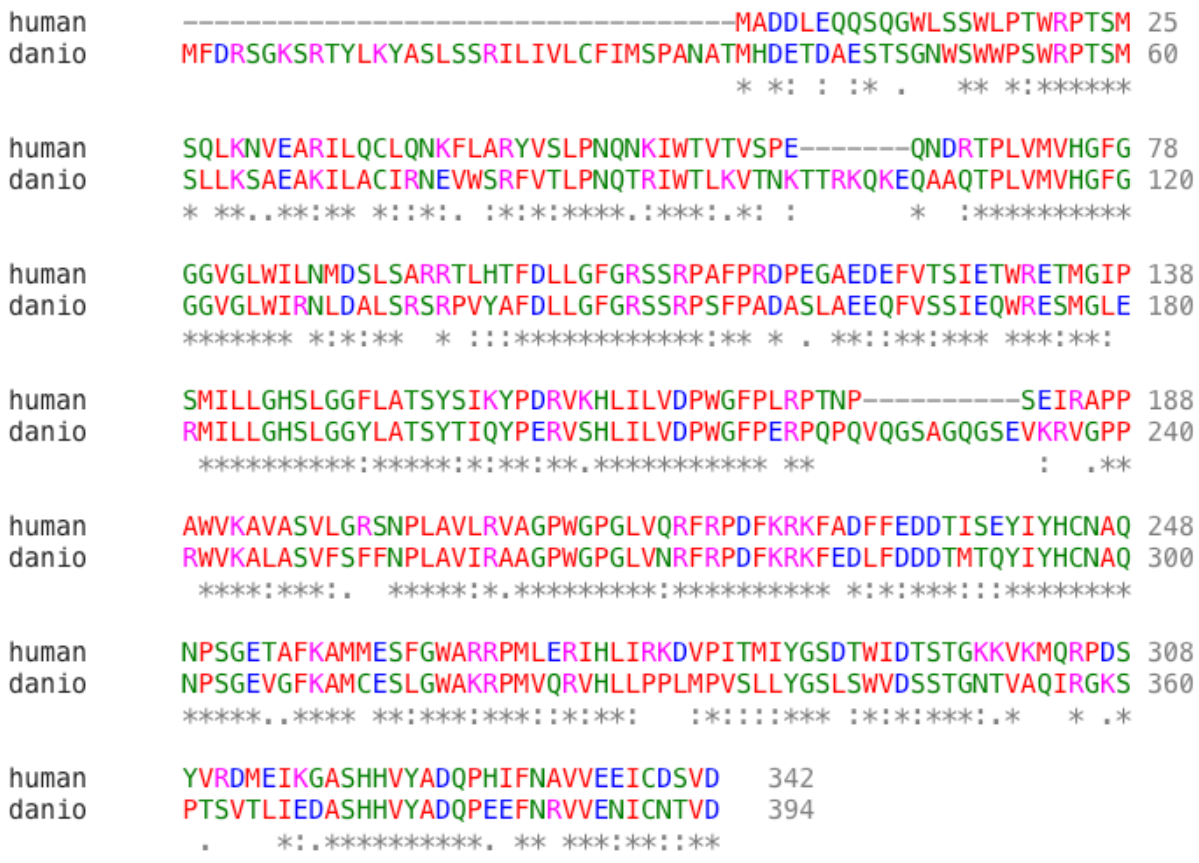

Figure 3.S4 Alignment between human and zebrafish homologs of ABHD4.

Amino acid sequence comparison between human ABHD4 and zebrafish abhd4.

Figure 3.S5 Alignment between human and zebrafish homologs of MGLL.

Amino acid sequence comparison between human MGLL and zebrafish magl.

Figure 3.S6 Alignment between human and zebrafish homologs of FAAH.

Amino acid sequence comparison between human FAAH and zebrafish faah.

Table 3.S1 sgRNA sequences for eCBs gene knockout zebrafish line production.

The zebrafish eCB gene, target location, and sequence of each sgRNA is shown. Protospacer adjacent motif (PAM) sequences are in parentheses.

GENE	TARGET (Exon & Nucleotides)	SEQUENCE
cb1	Exon 1, 969-991	GAGCCTGGTCGTGCACTCGG(CGG)
dagla	Exon 3, 321-343	GGAGCTGGTGTATGCAGTGG(TGG)
daglb	Exon 4, 426-448	GGTCATCCTGCTGGCGATGG(CGG)
abhd4	Exon 4, 340-362	GTGATGGTCCATGGGTTTGG(CGG)
mgll	Exon 2, 148-170	GAGTAAATTGGATCAGCCGG(CGG)
faah	Exon 4, 495-517	GAGTAAATTGGATCAGCCGG(CGG)

Table 3.S2 Genotyping primer sequences for eCB lines.

The following primers were designed to flank the sgRNA target locations to allow for sequencing and genotyping of the eCB zebrafish lines.

GENE	FORWARD PRIMER	REVERSE PRIMER
cb1	GATCTCCTCGGCAGTGTTAT	CAATAGTGATATATCGTGCTAACG
dagla	TTCAGTGCTATTATTCGCTGC	CACAAAGTGTCCCAGTTTAGC
daglb	GGGACATACTGGCAATTTGATTA	GTGGTTATCATCCTGAGGCA
abhd4	CATTCCATGTCTAGTCCCATC	CGACTTTATGAGGCATAATTCTC
mgll	TCAACTTCAGACATTGTAGGTT	CTGTCATTTCTCAACTCCATCC
faah	CCAACCATCACAGGAGACG	TTGAGAAGACCTTGTGGTATGT

Table 3.S3 Allele-specific PCR primer sequences for *cb1* and *dagla*.

The following primers were designed to specifically recognize either the wild-type or mutant alleles for *cb1* and *dagla*, allowing for quick genotyping.

GENE	ALLELE	FORWARD PRIMER	REVERSE PRIMER
cb1	WT	TTCTGCATGATGTGGGCGA	CCGTCCGCCGAGTGC
	-8	CTGCATGATGTGGGCGATCTCTATT	GTGCCGTCCGCCGACCA
dagla	WT	TGTTTTGCTCTGTTTGCTCTGGCG	CCAGGCGATGCCCACCACTG
	-5	TGTTTTGCTCTGTTTGCTCTG	CCAGCGATGCCACCATAC
	+7	TGTTTTGCTCTGTTTGCTCTGGCG	CGATGCCCATACACCAGCGAAC

Table 3.S4 qPCR primer sequences.

The following primers were designed to examine mRNA expression of eCB-, dopamine- and lipid-related genes in zebrafish.

GENE	FORWARD PRIMER	REVERSE PRIMER
cb1	GACGGCACAAAGGTGCAGA	TTGATGTTGTCCCCCATCCG
gpr55a	GAACTCCTCCAACTCATCGACA	AGCCCAGGATCAAAGGGATG
cnrip1a	CATCGAGTTCAAAGACGCCG	TTGGGTTTGGCCTCGTACTC
cnrip1b	AGGTCAGCATACAGTTCACTC	ATACTCGATGCTGTTGAAGCT
dagla	CAGCCATCTTGGATCAGGCAA	ATAAACGGGCCAGCCATATGC
daglb	CTTCATGGACACAGATCTGGT	TATGGGAGAGGACGGACTG
nape-pld	CACATCGCAGGTGTTTGTGC	TGCCAAGTTGACCAAGGGTT
abhd4	AGTATGCCAGTCTGTCGTCG	TCCAGAAGTGGACTCGGCG
mgll	GGGATCCCAAACAGGTGGAG	AAAGGGCCACCTGATGTCTG
abhd6a	CGATTCTGTTACTCTCACAGAG	AGGGAGAAACTTCACCACC
abhd6b	CGGAGAACTCTGGGTCTGC	TGGGAAGGTACTTCAGCATGG
faah	GTGGCCGTCTTAACAGTGCT	GAAGAGTTTGTCCCACGGGT
ptgs2a	CCTTTGAGGAGATGACAGGAGAC	GGCCAGGATACAGCTCAACC
d2ra	ACGGAAACGTGTCAACACCA	CGGGATGGGTGCATTTCTTTA
th	GCTCTCAGCACGCGATTTTT	ATGGACGCAATCCGGTTCAG
aadc	CAAAGGAGGTGGGGTCATCC	CACCGATGAGTGTGCCTGAT
dat	TGCTACAAGAATGGCGGAGG	GTAGGAGCCCACATACAGCG
vmat2	TCTTCTGTGGCAGGTATGGG	CCTCCCAGTGCAATCCCAAT
nurr1	CAGGTCCAACCCGATGGAAA	TCCGTGTCTCTCTGTGACCA
srebp-1c	TCGGCTTCACCAATCCTGAC	GTCACGTCCGGTTTCAGAGT
acc1	AATCAGGTGGTACGGATGGC	GGATGTTCCCTCTGTTGGGG
fas	GACTCAGGAGGGCGAGAGTA	CTTCTTGAATCTGAACGCGGG
elf1a	TTCTCAGGCTGACTGTGC	CCGCTAGCATTACCCTCC

3.9 REFERENCES

Almogi-Hazan, O. and Or, R. (2020). *Cannabis*, the endocannabinoid system and immunity – the journey from the bedside to the bench and back. Int J Mol Sci. *21*, 4448.

Burgess, S., Reim, G., Chen, W., Hopkins, N., and Brand, M. (2002). The zebrafish spiel-ohne-grenzen (spg) gene encodes the POU domain protein Pou2 related to mammalian Oct4 and is essential for formation of the midbrain and hindbrain, and for pre-gastrula morphogenesis. Development. *129*, 905-916.

Burggren, A.C., Shirazi, A., Ginder, N., and London, E.D. (2019). Cannabis effects on brain structure, function, and cognition: considerations for medical uses of cannabis and its derivatives. Am J Drug Alcohol Abuse. *45*, 563-579.

Cabral, G.A., Rogers, T.J., and Lichtman, A.H. (2015). Turning over a new leaf: cannabinoid and endocannabinoid modulation of immune function. J Neuroimmune Pharmacol. *10*, 193-203.

Cheung, K.A.K., Peiris, H., Wallace, G., Holland, O.J., and Mitchell, M.D. (2019). The interplay between the endocannabinoid system, epilepsy, and cannabinoids. Int J Mol Sci. *20*, 6079.

Cooray, R., Gupta, V., and Suphioglu, C. (2020). Current aspects of the endocannabinoid system and targeted THC and CBD phytocannabinoids as potential therapeutics for Parkinson's and Alzheimer's diseases: a review. Mol Neurobiol. *57*, 4878-4890.

Fin, L., Bergamin, G., Steiner, R.A., and Hughes, S.M. (2017). The cannabinoid receptor

interacting proteins 1 of zebrafish are not required for morphological development, viability, or fertility. Sci Rep. *7*, 4858.

Garneau, N.L., Wilusz J., and Wilusz, C.J. (2007). The highways and byways of mRNA decay. Nat Rev Mol Cell Biol. *8*, 113–126.

Gaudet, M., Fara, A.G., Beritognolo, I., and Sabatti, M. (2009). Allele-specific PCR in SNP genotyping. Methods Mol Biol. *578*, 415–424.

Gerety, S.S. and Wilkinson, D.G. (2011). Morpholino artifacts provide pitfalls and reveal a novel role for pro-apoptotic genes in hindbrain boundary development. Dev Biol. *350*, 279-289.

Kok, F.O., Shin, M., Ni, C.W., Gupta, A., Grosse, A.S., van Impel, A., Kirchmaier, B.C., Peterson-Maduro, J., Kourkoulis, G., Male, I., DeSantis, D.F., Sheppard-Tindell, S., Ebarasi, L., Betsholtz, C., Schulte-Merker, S., Wolfe, S.A., and Lawson, N.D. (2015). Reverse genetic screening reveals poor correlation between morpholino-induced and mutant phenotypes in zebrafish. Dev Cell. *32*, 97–108.

Leishman, E., Mackie, K., Luquet, S., and Bradshaw, H.B. (2016). Lipidomics profile of a NAPE-PLD KO mouse provides evidence of a broader role of this enzyme in lipid metabolism in the brain. Biochim Biophys Acta. *1861*, 491-500.

Lisboa, S.F., Gomes, F.V., Terzian, A.L.B., Aguiar, D.C., Moreira, F.A., Resstel, L.B.M., and Guimarães, F.S. (2017). The endocannabinoid system and anxiety. Vitam Horm. *103*, 193-279.

Lutz, B., Marsicano, G., Maldonado, R., and Hillard, C.J. (2015). The endocannabinoid system in guarding against fear, anxiety, and stress. Nat Rev Neurosci. *16*, 705-718.

Lykke-Andersen S. and Jensen T.H. (2015). Nonsense-mediated mRNA decay: an intricate machinery that shapes transcriptomes. Nat Rev Mol Cell Biol. *16*, 665–677.

Martella, A., Sepe, R.M., Silvestri, C., Zang, J., Fasano, G., Carnevali, O., De Girolamo, P., Neuhauss, S.C.F., Sordino, P., and Di Marzo, V. (2016). Important role of endocannabinoid signaling in the development of functional vision and locomotion in zebrafish. FASEB J. *30*, 4275-4288.

Mechoulam, R., and Parker, L.A. (2013). The endocannabinoid system and the brain. Annu. Rev. Psychol. *64*, 21-47.

Pai, W.Y., Hsu, C.C., Lai, C.Y., Chang, T.Z., Tsai, Y.L., and Her, G.M. (2013). Cannabinoid receptor 1 promotes hepatic lipid accumulation and lipotoxicity through the induction of SREBP-1c expression in zebrafish. Transgenic Res. *22*, 823–838.

Place, E.S. and Smith J.C. (2017). Zebrafish *atoh8* mutants do not recapitulate morpholino phenotypes. PLoS One. *12*, e0171143.

Robu, M.E., Larson, J.D., Nasevicius, A., Beiraghi, S., Brenner, C., Farber, S.A., and Ekker, S.C. (2007). p53 activation by knockdown technologies. PLoS Genet. *3*, e78.

Rossi, A., Kontarakis, Z., Gerri, C., Nolte, H., Hölper, S., Krüger, M., and Stainier, D.Y.R.

(2015). Genetic compensation induced by deleterious mutations but not gene knockdowns. Nature. *524*, 230-233.

Tuladhar, R., Yeu, Y., Piazza, J.T., Tan, Z., Clemenceau, J.R., Wu, X., Barrett, Q., Herbert, J., Mathews, D.H., Kim, J., Hwang, T.H., and Lum, L. (2019). CRISPR-Cas9-based mutagenesis frequently provokes on-target mRNA misregulation. Nat Commun. *10*, 4056.

Wagle, M., Nguyen, J., Shinwoo, L., Zaitlen, N., and Guo, S. (2017). Heritable natural variation of an anxiety-like behavior in larval zebrafish. J Neurogenet. *31*, 138-148.

Zhang, F., Li, X., He, M., Ye, D., Xiong, F., Amin, G., Zhu, Z., and Sun, Y. (2020). Efficient generation of zebrafish maternal-zygotic mutants through transplantation of ectopically induced and Cas9/gRNA targeted primordial germ cells. J Genet Genomics. *47*, 37–47.

CHAPTER 4: Pharmacological Manipulation of the Endocannabinoid System in Zebrafish

4.1 ABSTRACT

Targeting the endocannabinoid (eCB) system through pharmacological administration can uncover valuable information regarding its role in biological processes and potential therapeutic strategies. Here, we examine the effects of various eCB protein-modulating drugs on light-dark preference and locomotor activity. High doses of cannabinoid agonist WIN55212-2 (0.3 – 4 mg/L) increased dark avoidance behavior and decreased locomotor activity. Of the two main endocannabinoids, anandamide (AEA) reduced dark avoidance behavior (1 μM and 4 μM), while 2-arachadonoylglycerol (2-AG) displayed a tend of increasing dark avoidance behavior at the highest tested dose (4 μM). Of the two monoacylglycerol lipase (MGLL) inhibitors tested, MJN110 significantly decreased dark avoidance behavior and locomotor activity (2 μM), while JZL-184 had no observable effects. Lastly, the fatty acid amide hydrolase (FAAH) inhibitor PF-3845 reduced dark avoidance behavior (1 μM) and had a biphasic effect on locomotor activity (0.25 μM – 4 μM). Effects of PF-3845 were lost when tested on *faah* mutants. Future work includes examining phenotypes from additional assays (including adult behavior), and phenotyping using drugs that target other proteins in the eCB system.

4.2 INTRODUCTION

As stated in the previous chapter, perturbing endocannabinoid (eCB) proteins can reveal new information regarding their roles in various physiological processes. In addition to genetic perturbations, pharmacological agents have been used not only to reveal eCB protein functions, but also discover therapeutics for a diverse range of diseases (Cristino et al., 2020; Kaur et al., 2016; Pacher et al., 2006). One of the most recent eCB compounds to successfully become a novel therapeutic is cannabidiol (CBD), a well-tolerated drug used to treat epileptic disorders

(Devinsky, et al. 2014; Chen et al. 2019; Silvestro et al., 2019). The cannabis plant, whose main psychotropic component is Δ^9-tetrahydrocannabinol (THC) – a cannabinoid receptor 1 (CB1) partial agonist – has been approved for treatment of nausea, anorexia, muscle spasms, pain, and has even shown beneficial effects in patients with Tourette syndrome (Amin and Ali, 2019; Müller-Vahl, 2013). Studies have also shown that targeting the eCB system may have the potential to treat mood disorders, Parkinson's disease, Alzheimer's disease, Huntington disease, multiple sclerosis, traumatic brain injury, stroke, and glioblastoma. (Cristino et al. 2020; Cooray et al., 2020; Han et al., 2020; Lisboa et al., 2017). Indeed, given the potential of the eCB system as a targetable therapeutic strategy for a diverse set of diseases, examining the effects of eCB-targeting drugs provides an exciting opportunity to advance our understanding of the eCB system from both a basic science and therapeutic perspective.

One way to gain insight on the effects of eCB-targeting drugs is through the light-dark preference assay. The light-dark preference assay is a well-established paradigm used to examine anxiety-like behaviors in model organisms including larval zebrafish (Bai et al., 2016; Chen et al., 2015; Lara and Vasconcelos, 2021; Steenbergen et al., 2011; Wagle et al., 2017). In short, following pre-adaptation to a well-controlled luminance background, a zebrafish larva is placed in the center of a chamber that is half illuminated and half dark. Immediately after the fish is placed, recording starts and the larva is able to swim freely throughout the chamber for the duration of the 8-minute experiment. While untreated wild-type zebrafish larvae show a baseline preference for spending their time in the light zone of the chamber, anxiogenic/anxiolytic drugs, mutations, and experiences have been shown to adjust this preference, with an increase in dark avoidance being associated with an increase in anxiety-like behavior, and the opposite occurring with reduced anxiety-like behavior (Bai et al., 2016; Lara and Vasconcelos, 2021; Steenbergen et al., 2011; Wagle et al., 2017). Here, we utilize drugs targeting CB1, monoglyceride lipase (MGLL), and fatty acid amide hydrolase (FAAH) to determine how

pharmacological modulation of these proteins affects both light dark preference behavior and locomotor activity.

4.3 METHODS

4.3.1 Zebrafish husbandry

Zebrafish were handled as described in Chapter 3 (section 3.3.1, p.79). All larvae used in this study were of the AB wild-type genetic background, except for **Figure 4.5**, which uses the +13 base pair *mgll* knockout line, and **Figures 4.6** and **4.S1**, which uses the -1 base pair *faah* knockout line, (see **Figure 3.2,** p.90, for *mgll* and *faah* knockout details).

4.3.2 Light-dark preference assay

The baseline light-dark preference assay was performed on 6 dpf zebrafish larvae as described in Chapter 3 (section 3.3.6, p.82) with the following modifications: one recording was collected for each larvae, and larvae were incubated in pharmacological agent for a duration of either 20 minutes or 1 hour prior to testing. All behavior tests were performed between the hours of 8:00am and 1:00pm. See **Table 4.1** for all of pharmacological agents used, their targets, and properties. Data was analyzed as described in Chapter 3 (section 3.3.6, p.82), with Choice Index measuring light-dark preference behavior, and average velocity or distance travelled for the duration of the assay measuring locomotor activity.

4.4 RESULTS

4.4.1 Effects of CB1 agonists on light-dark preference behavior and locomotor activity

We first examined the effects of the cannabinoid receptor 1 (CB1) agonist WIN55212-2 on light-dark preference behavior and locomotor activity. After incubating larvae in WIN55212-2 for one hour in concentrations ranging from 0.000048 mg/L – 4 mg/L, we found a significant reduction of choice index with the following concentrations: 0.03-, 0.16-, 0.8-, and 4 mg/L (0.03 mg/L: $p = 0.0493$; 0.16 mg/L: $p = 0.0387$; 0.8 mg/L: $p = 0.0183$ middle panel, $p = 0.0210$ right panel; and 4 mg/L: $p = 0.0168$) (**Figure 4.1A**). We also saw a significant decrease in velocity with 0.0012-, 0.03-, 0.16-, 0.8-, and 4 mg/L WIN55212-2 (0.0012 mg/L: $p = 0.0170$; 0.03 mg/L: $p < 0.0001$; 0.16 mg/L: $p = 0.003$; 0.8 mg/L: $p < 0.0001$ middle panel, $p = 0.003$ right panel; and 4 mg/L: $p < 0.0001$) (**Figure 4.1B**).

We next examined the effects of the two most prevalent eCBs: 2-arachodonoylglycerol (2-AG) and anandamide (AEA). For each eCB, we tested a series of concentrations ranging from 0.5 μM – 4 μM incubated groups of larvae in each concentration for 20 minutes. We observed a trend of reduced choice index in larvae treated with 4 uM 2-AG ($p = 0.0825$), and conversely found a significant increase in choice index in larvae treated with 4 uM AEA ($p = 0.0108$) (**Figure 4.2A**). The higher doses tested of each endocannabinoid resulted in a decrease in locomotor activity: 4 μM 2-AG ($p < 0.0001$), and 2- and 4 μM AEA (2 μM: $p = 0.0004$; 4 μM: $p < 0.0001$) (**Figure 4.2B**).

We followed up our 2-AG and AEA experiments by changing the incubation time to 1 hour and choosing the concentration of each eCB that did not affect locomotor activity – 2 μM 2-AG and 1 μM AEA. With these conditions, we observed no significant change in choice index with 2 μM 2-AG, but again found an increase in choice index with 1 μM AEA ($p = 0.0197$)

(**Figure 4.3A**). Consistent with the 20 minute incubations, 1 hour incubation in 2 μM 2-AG or 1 μM AEA had no effect on locomotor activity compared to controls (**Figure 4.3B**).

4.4.2 Effects of MGLL inhibitors on light-dark preference behavior and locomotor activity

Next, we examined the effects of MJN110 and JZL-184, inhibitors of monoglyceride lipase (MGLL). We tested a range of 0.25 μM – 2 μM MJN110, and 1 μM – 20 μM JZL-184 with a 1 hour incubation period for each dose. We observed a significant increase in choice index with 2 μM MJN110 ($p = 0.0009$), but no changes in choice index at any concentrations of JZL-184 tested (**Figure 4.4A**). Similarly, we found a significant reduction in locomotor activity at the highest concentrations of MJN110 tested (1 μM: $p = < 0.0001$; 2 μM: $p < 0.0001$), but no observable differences at any concentration of JZL-184 tested. When administering 1 μM MJN110 to *mgll*$^{-/-}$ larvae, we observed no significant difference in choice index between knockout-treated and wild-type treated larvae, but did see a loss of change in locomotor activity compared to wild-type controls (**Figure 4.5**).

4.4.3 Effects of FAAH inhibitor PF-3845 on light-dark preference behavior and locomotor activity

Lastly, we examined the effects of PF-3845, an inhibitor of fatty acid amide hydrolase (FAAH). We tested 0.25 μM, 1 μM, and 4 μM of this drug with a 1 hour incubation period for each dose. We observed a significant increase in choice index at 1 μM, and a trend of increased choice index at 4 μM (1 μM: $p = 0.0151$; 4 μM: $p = 0.0729$) (**Figure 4.6A**). Interestingly, we observed a biphasic effect of PF-3845 on locomotor activity; there was an increase in distance travelled in larvae that were administered 0.25- or 1 μM PF-3845, but a decrease in distance travelled in

larvae that were administered 4 μM (0.25 μM: p = 0.0156; 1 μM: 0.0006; 4 μM: p < 0.0001) (**Figure 4.6B**). When administering PF-3845 to *faah*$^{-/-}$ larvae, we observed a loss of change in choice index and locomotor activity compared to wild-type controls (**Figure 4.7**).

4.5 DISCUSSION

In this chapter, we examined changes in light-dark preference and locomotor activity in larvae treated with eCB protein-modulating pharmacological agents. We first examined the effects of drugs that target CB1: the synthetic cannabinoid agonist WIN55212-2, and the endocannabinoids 2-AG and AEA. We found that concentrations of WIN55212-2 ranging from 0.03 μM – 4 μM significantly reduce larval choice index, as well as reduce locomotor activity (**Figure 4.1**). We observed distinct effects between 2-AG and AEA on light dark preference behavior: 2-AG showed a trend of reducing choice index at 4 μM (20-min incubation), while AEA significantly increased choice index at 1 μM (1-hour incubation) and 4 μM (20-minute incubation) (**Figures 4.2 & 4.3**). Both endocannabinoids reduced locomotor activity at higher concentrations tested (4 μM 2-AG at 20 minute incubation, 2- and 4 μM AEA at 20 minute incubation) (**Figure 4.2**). Though the results appear conflicting, particularly the effects of the two endocannabinoids on light-dark preference, a biphasic effect on anxiety-like behavior has been observed before with CB1 agonists (Viveros et al., 2005). It is possible that WIN55212-2 and 2-AG increase dark avoidance, and thus anxiety-like behavior, at the concentrations tested due to their nature as full agonists, while AEA reduces anxiety-like behavior due to its nature as a partial CB1 agonist. To gain a clearer picture on how these compounds affect light dark preference behavior in zebrafish, a broader range of drug concentrations should be tested.

It is worth noting that one of the limitations of using pharmacological agents is polypharmacology (Chaudhari et al., 2020); it is possible that the effects we observe in drug-

treated animals is a consequence of an unintended target rather than the protein-target of interest. To confirm that effects are indeed caused by modulation of the intended target, more than one drug that modulates the protein of interest can be tested (preferably with distinct chemical structures to prevent any repeated off target effects). For this study, WIN55212-2 and 2-AG are both full agonists of CB1, and both demonstrated the same effect of increasing dark avoidance behavior and reducing locomotor activity in zebrafish larvae. It would be worthwhile to examine the effects of another CB1 partial agonist, such as THC, to confirm the reduction in dark avoidance behavior seen with AEA.

When examining the effects of MGLL inhibition, two drugs were used: MJN110 and JZL-184. Interestingly, each drug had a distinct effect on light dark preference behavior and locomotor activity; MJN110 reduced dark avoidance behavior and locomotor activity, while JZL-184 had no observable effects on either behavior (**Figure 4.4**). Previous findings have shown MJN110 as being more potent, selective, and effective in raising concentrations of 2-AG in the brain compared to JZL-184 (Ignatowska-Jankowska et al., 2015; Niphakis et al., 2013), which may account for the distinct effects on choice index and locomotion.

Another strategy to verify pharmacological effects is to use genetic knockout animals. Though knocking out a gene and observing the same phenotype as the corresponding drug treatment could help verify drug effects, phenotypes are not always observed in genetic knockouts due to genetic compensatory mechanisms (Rossi et al., 2015). Another approach to utilize genetic knockouts would be to treat the knockout animal with drug; if the effect is no longer seen when the knockout is treated, this helps provide evidence that the protein of interest is necessary for the observed effect. This was the case for both MGLL inhibitor MJN110 and FAAH inhibitor PF-3845. When 1 μM of MJN110 was administered to both WT and *mgll* knockout larvae (**Figure 4.5B**), the severe effects on locomotor activity were lost, providing evidence that MGLL is indeed necessary for the phenotype to be observed. It is worth noting

that no significant change in choice index was observed in either the wild-type nor the *mgll* knockout treated larvae; as shown in **Figure 4.4**, 1 hour incubation of 1 μM MJN110 does not appear to have any significant effect on choice index. Thus a next step to verify the on-target effect of MJN110 would be to treat *mgll* larvae with 2 μM MJN110 and examine choice index.

For PF-3845, when tested on wild-type fish, we observed an increase in choice index (1- and 4 μM), and alterations in locomotor activity (increase at 0.25- and 1 μM, decrease at 4 μM) (**Figure 4.6**). To verify these effects, we utilized a *faah* genetic knockout fish line. Though this line does not show a difference in light-dark preference compared to wild-type controls (**Figure 4.S1**), PF-3845-mediated changes in choice index and locomotor activity are lost when administered to the *faah* knockout line (**Figure 4.7**), providing further evidence that FAAH is necessary for both phenotype to be observed.

Overall, we observed a wide range of effects on light-dark preference behavior and locomotion in eCB drug-treated larvae (A summary of all results can be seen in **Table 4.2**.) CB1 agonists showed opposing effects on dark avoidance, while MGLL and FAAH inhibitors demonstrated a decrease in dark avoidance (or no effect). As dark avoidance is a known anxiety-like behavior, these results have implications for the roles of CB1, MGLL, and FAAH on anxiety state, with CB1-modulating drugs having the ability to both increase and decrease anxiety levels, and MGLL and FAAH inhibitors having anxiolytic properties. Indeed, previous studies using other animal models have also observed a CB1's biphasic effect on anxiety (Moreira et al., 2009; Rey et al. 2012; Rubino et al. 2008), as well as anxiolytic properties of inhibitors targeting MGLL (Busquets-Garcia et al., 2011; Kinsey et al., 2011; Lomazzo et al., 2015; Shonesy et al., 2014) and FAAH (Kathuria, et al., 2003; Moreira et al., 2008; Patel and Hillard, 2006). As our study is the first record of examining dark avoidance behavior in larval zebrafish using these drugs, our results provide an exciting foundation for continued investigation into the roles of CB1, FAAH, and MGLL in anxiety-like behavior using zebrafish. To

gain insight on the neuronal populations that are involved with each eCB gene's ability to modulate anxiety-like behavior, brain-wide calcium imaging can be done following drug administration. Additionally, more assays can be done in fish to examine the effects of eCB-modulating drugs on other behaviors (i.e. memory, addiction, sociability, and aggression), offering more opportunities to demystify eCB system involvement in behavior.

4.6 ACKNOWLEDGMENTS

I would like to thank Sacha Salphati for his hard work running behavioral assays, optimizing protocols, and overall being a determined mentee.

4.7 FIGURES

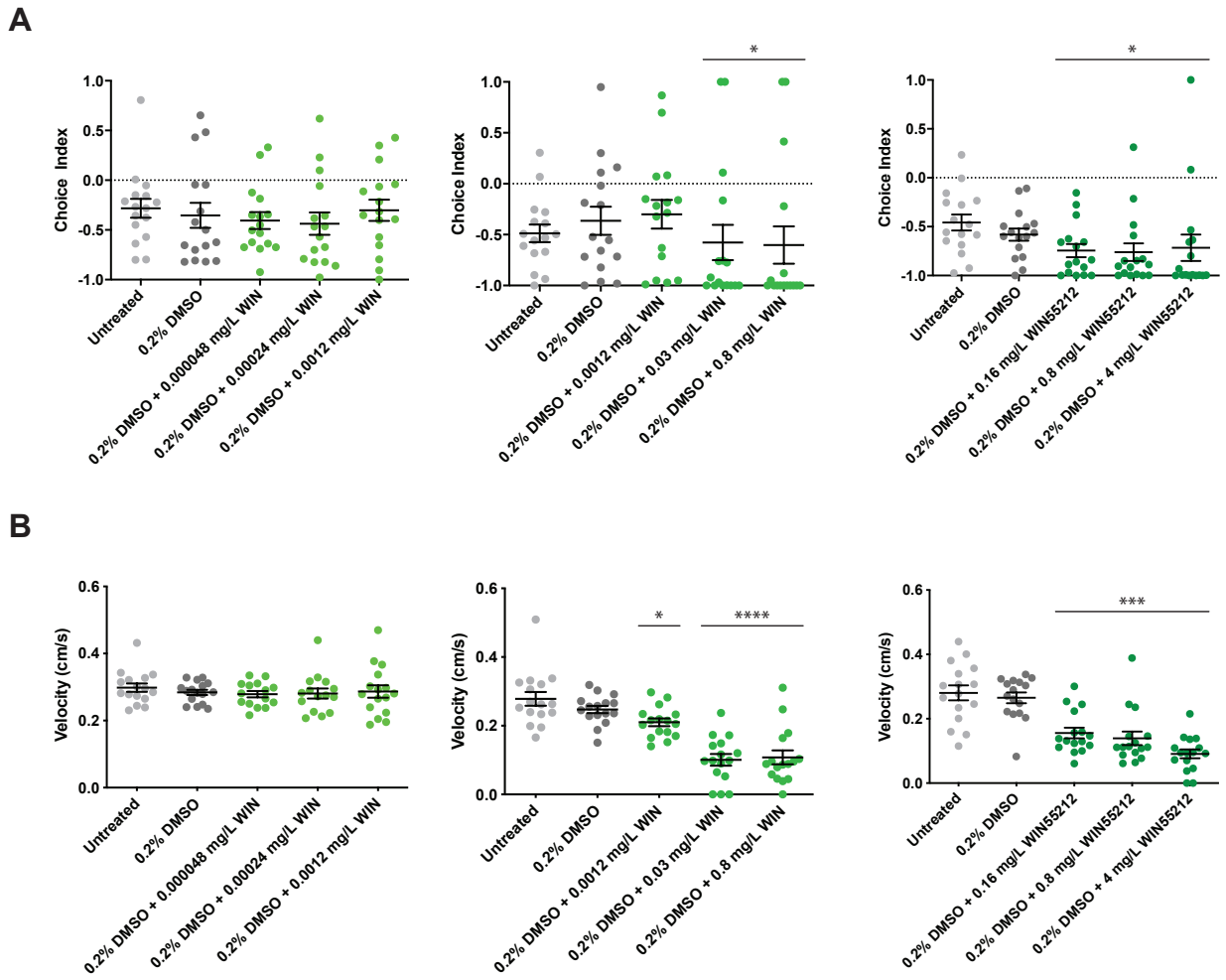

Figure 4.1 High concentrations of CB1 agonist WIN22515-2 increase dark avoidance behavior and reduce locomotor activity.

(A) The choice index of larvae treated for 1 hour with WIN55212-2 at the following concentrations: 0.000048-, 0.00024-, 0.0012 mg/L (left), 0.0012-, 0.03-, 0.8 mg/L (middle), and 0.16-, 0.8-, and 4 mg/L (right). We observed a decrease in choice index following treatment with 0.3-, 0.16-, 0.8-, and 4 mg/L WIN55212-2. n = 16 for all groups.
(B) The velocity of larvae treated for 1 hour with WIN55212-2 at the same doses as (A). We observed a decrease in velocity following treatment with 0.0012-, 0.03-, 0.16-, 0.8-, and 4 mg/L WIN55212-2. n = 16 for all groups.
All data represented as mean +/ SEM. *p < 0.05, ***p < 0.001, ****p < 0.0001; Mann-Whitney test was performed to assess statistical significance. CB1 – cannabinoid receptor 1.

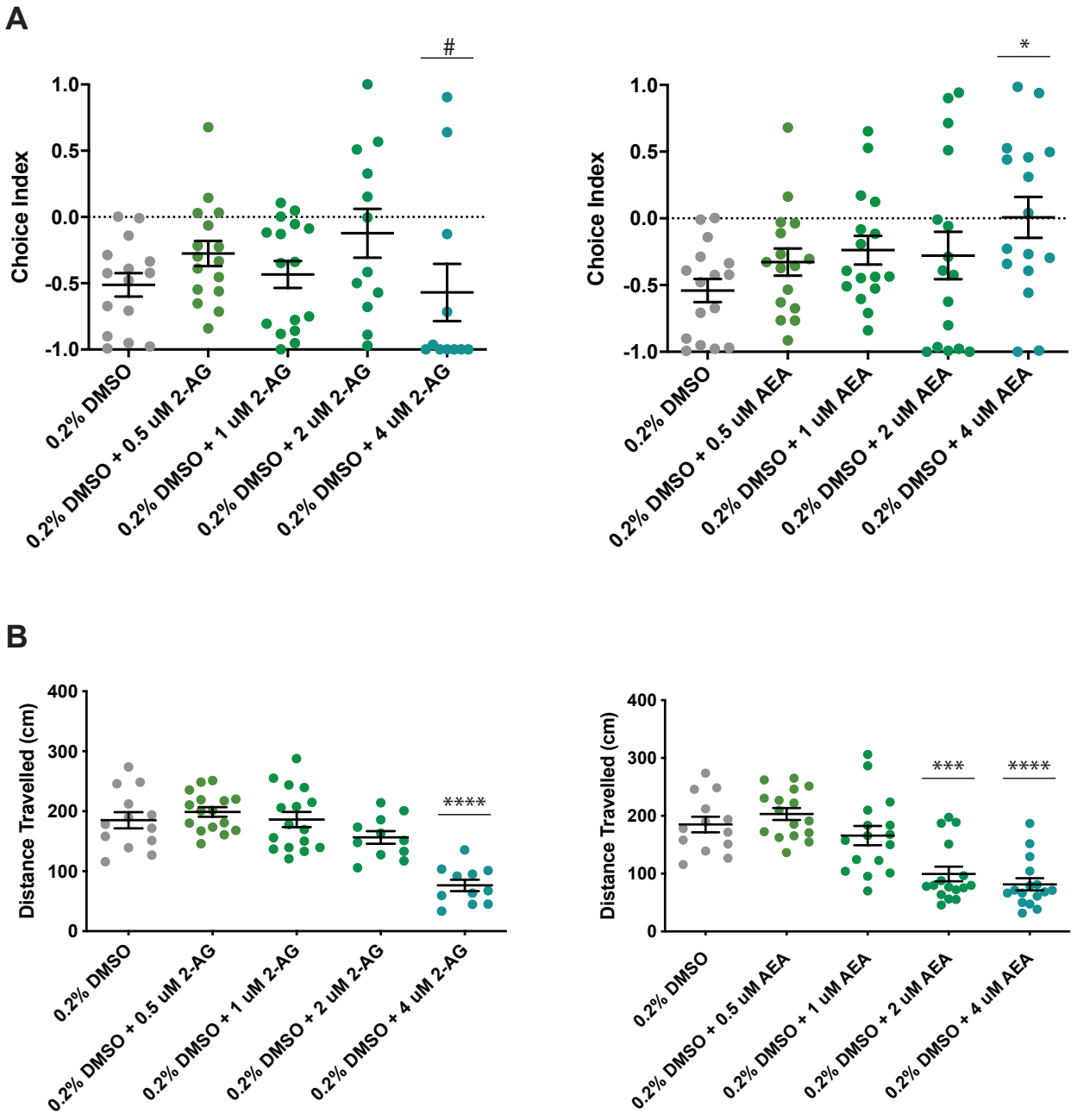

Figure 4.2 Effects of 20-minute incubation with endocannabinoids 2-AG and AEA.

(A) The choice index of larvae treated for 20 minutes with 2-AG (left) and AEA (right) at the following concentrations: 0.5-, 1-, 2-, and 4 μM. We observed a trend of decreasing choice index following treatment with 4 μM 2-AG. Conversely, we observed a significant increase in choice index following treatment with 4 μM AEA. 2-AG: 0.2% DMSO, n = 15; 0.5 μM, n = 16; 1 μM, n = 16; 2 μM, n = 13; 4 μM, n = 11. AEA: n = 16 for all groups.

(B) The distance travelled of larvae treated for 20 minutes with 2-AG (left) and AEA (right) at the same doses as (A). We observed a decrease in locomotor activity following treatment with 4 μM 2-AG and 2- and 4 μM AEA. 2-AG: 0.2% DMSO, n = 13; 0.5 μM, n = 16; 1 μM, n = 16; 2 μM, n = 11; 4 μM, n = 11. AEA: 0.2% DMSO, n = 13; n = 16 for remaining concentrations.
All data represented as mean +/ SEM. #$p < 0.01$, *$p < 0.05$, ***$p < 0.001$, ****$p < 0.0001$; Mann-Whitney test was performed to assess statistical significance. 2-AG – 2-arachadonoylglycerol; AEA – anandamide.

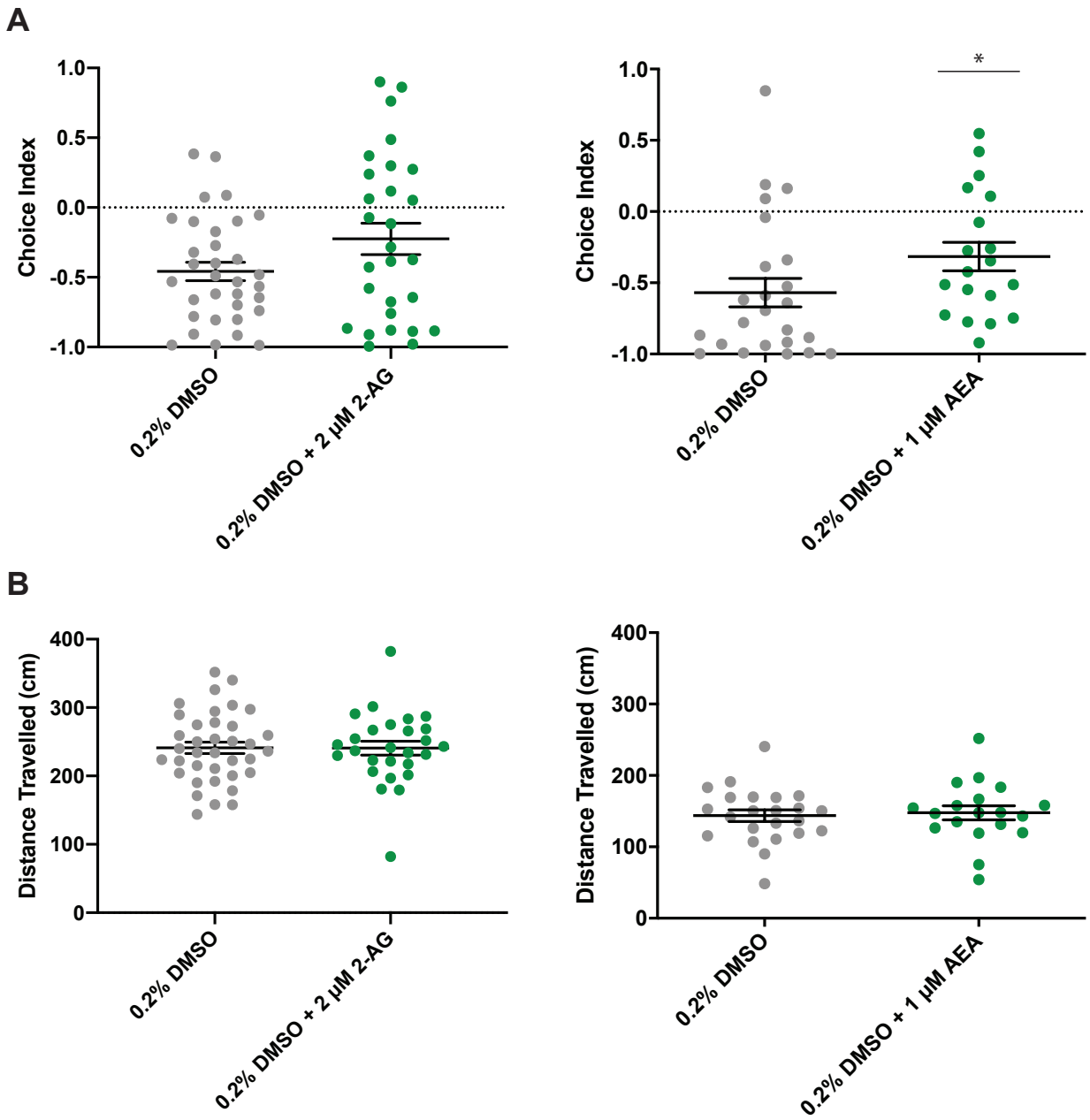

Figure 4.3 Effects of 1-hour incubation with endocannabinoids 2-AG and AEA.

(A) The choice index of larvae treated for 1 hour with 2 µM 2-AG (left) and 1 µM AEA (right). We observed no difference in choice index with 2-AG treatment, but we observed a significant increase in choice index following treatment with 1 µM AEA. 2-AG: 0.2% DMSO, n = 33; 2 µM, n = 28. AEA: 0.2% DMSO, n = 24; 2 µM, n = 19.
(B) The distance travelled of larvae treated for 1 hour with 2 µM 2-AG (left) and 1 µM AEA (right). We observed no change in locomotor activity with either treatments. 2-AG: 0.2% DMSO,

n = 37; 2 μM, n = 28. AEA: 0.2% DMSO, n = 23; 2 μM, n = 19.
All data represented as mean +/ SEM. *p < 0.05; Mann-Whitney test was performed to assess statistical significance.

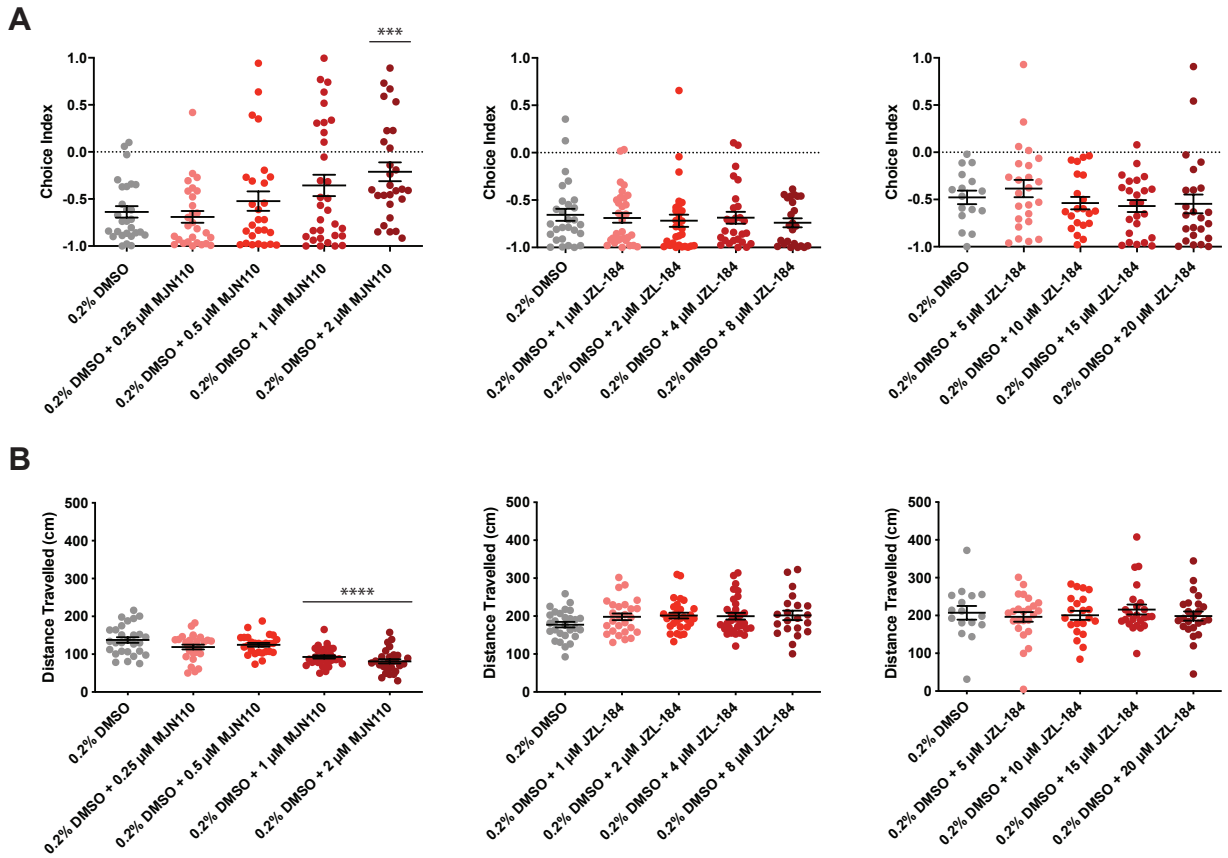

Figure 4.4 MGLL inhibitors MJN110 and JZL-184 have distinct effects on light-dark preference and locomotor activity.

(A) The choice index of larvae treated for 1 hour with MJN110 at 0.25-, 0.5-, 1-, and 2 µM (left), JZL-184 at 1-, 2-, 4-, and 8 µM (middle), and JZL-184 at 5-, 10-, 15-, and 20 µM (right). We observed an increase in choice index following treatment with 2µM MJN110. We observed no change in choice index for any concentrations of JZL-184 tested. MJN110: 0.2% DMSO, n = 28; 0.25 µM, n = 28; 0.5 µM, n = 27; 1 µM, n = 32; 2 µM, n = 28. JZL-184 (middle): 0.2% DMSO, n = 28; 1 µM, n = 32; 2 µM, n = 30; 4 µM, n = 27; 8 µM, n = 24. JZL-184 (right): 0.2% DMSO, n = 16; 5 µM, n = 24; 10 µM, n = 21; 15 µM, n = 24; 20 µM, n = 24.
(B) The distance travelled of larvae treated for 1 hour with MJN110 and JZL-184 at the same doses as (A). We observed a decrease in locomotor activity following treatment with 1- and 2 µM MJN110. We observed no change in choice index for any concentrations of JZL-184 tested. MJN110: 0.2% DMSO, n = 28; 0.25 µM, n = 28; 0.5 µM, n = 27; 1 µM, n = 32; 2 µM, n = 28. JZL-184 (middle): 0.2% DMSO, n = 28; 1 µM, n = 27; 2 µM, n = 30; 4 µM, n = 32; 8 µM, n = 21. JZL-184 (right): 0.2% DMSO, n = 16; 5 µM, n = 24; 10 µM, n = 21; 15 µM, n = 24; 20 µM, n = 24.
All data represented as mean +/ SEM. ***p < 0.001, ****p < 0.0001; Mann-Whitney test was performed to assess statistical significance. MGLL – monoglyceride lipase.

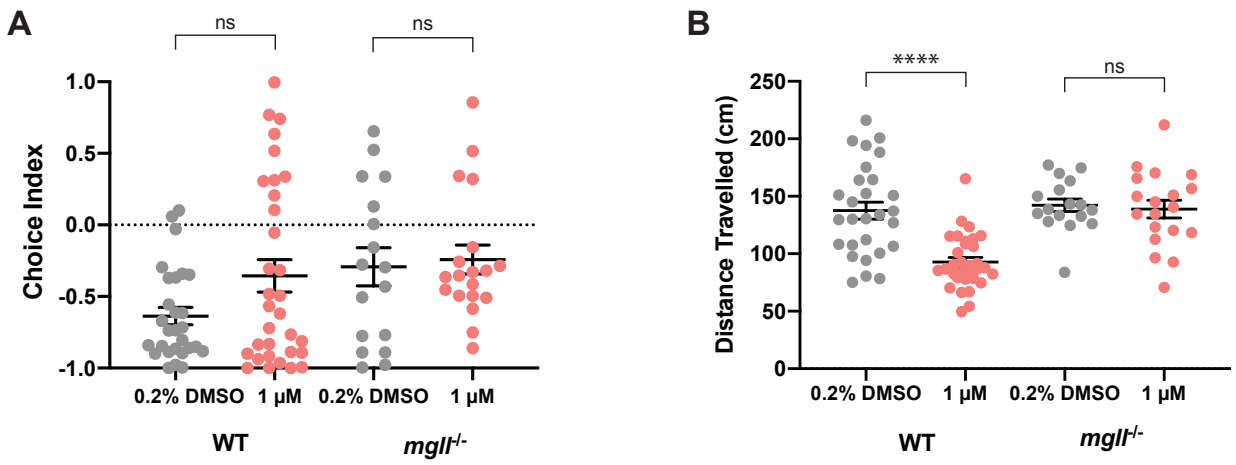

Figure 4.5 MJN110 effects on locomotor activity are lost in the *mgll* knockout.

(A) The choice index of wild type and *mgll*$^{-/-}$ larvae treated for 1 hour with 1 μM MJN110. We observed no change in drug treated wild-type nor *mgll* knockout larvae compared to controls. WT: 0.2% DMSO, n = 28; 1 μM, n = 32. *mgll*$^{-/-}$: 0.2% DMSO, n = 17; 1 μM, n = 19.
(B) The distance travelled of wild type and *mgll*$^{-/-}$ larvae treated for 1 hour with 1 μM MJN110. We observed an increase in locomotor activity in drug treated wild-type larvae ($p < 0.0001$), but no change in drug treated *faah* knockout larvae compared to controls. WT: 0.2% DMSO, n = 28; 1 μM, n = 32. *mgll*$^{-/-}$: 0.2% DMSO, n = 17; 1 μM, n = 19.
All data represented as mean +/ SEM. ns – no significance, ****$p < 0.0001$; Mann-Whitney test was performed to assess statistical significance.

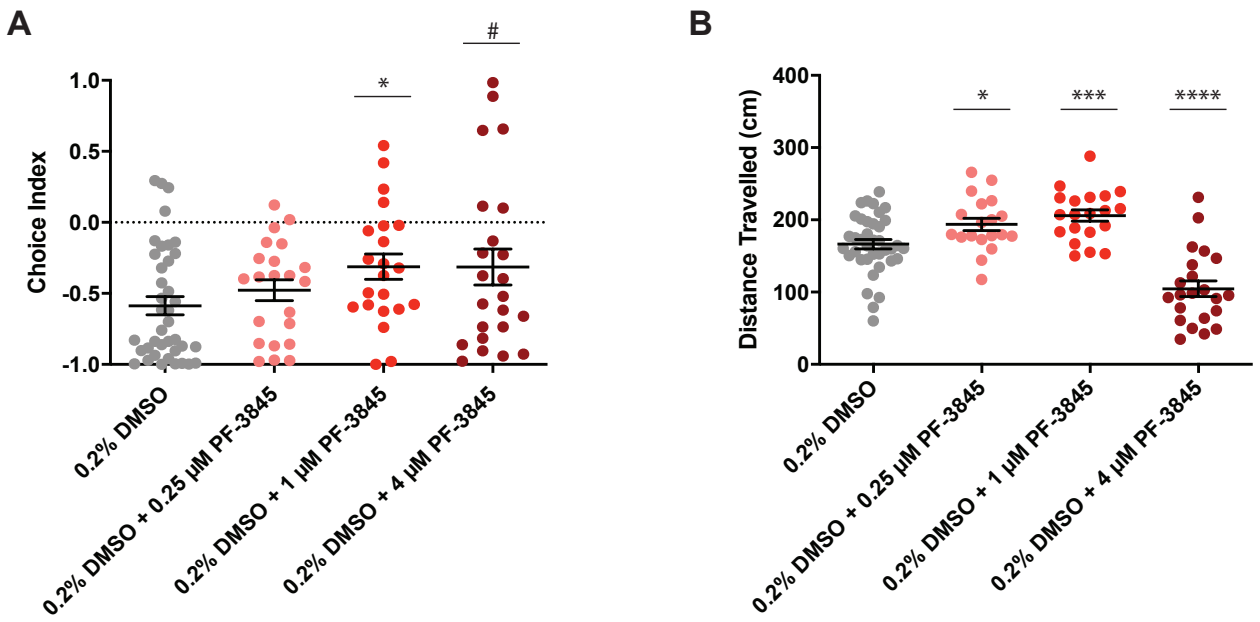

Figure 4.6 FAAH inhibitor PF-3845 increases choice index and has biphasic effect on locomotor activity.

(A) The choice index of larvae treated for 1 hour with 0.25-, 1-, and 4 µM PF-3845. We observed an increase in choice index following administration of 1 µM PF-3845 and a trend of increasing choice index with 4 µM PF-3845. 0.2% DMSO, n = 39; 0.25 µM, n = 22; 1 µM, n = 22; 4 µM, n = 23.
(B) The distance travelled of larvae treated for 1 hour with PF-3845 at the same doses as (A). We observed an increase in locomotor activity following treatment with 0.25- and 1 µM PF-3845, and a decrease in locomotor activity with 4 µM PF-3845. 0.2% DMSO, n = 39; 0.25 µM, n = 22; 1 µM, n = 22; 4 µM, n = 23.
All data represented as mean +/ SEM. #$p < 0.01$, *$p < 0.05$, ***$p < 0.001$, ****$p < 0.0001$; Mann-Whitney test was performed to assess statistical significance. FAAH – fatty acid amide hydrolase.

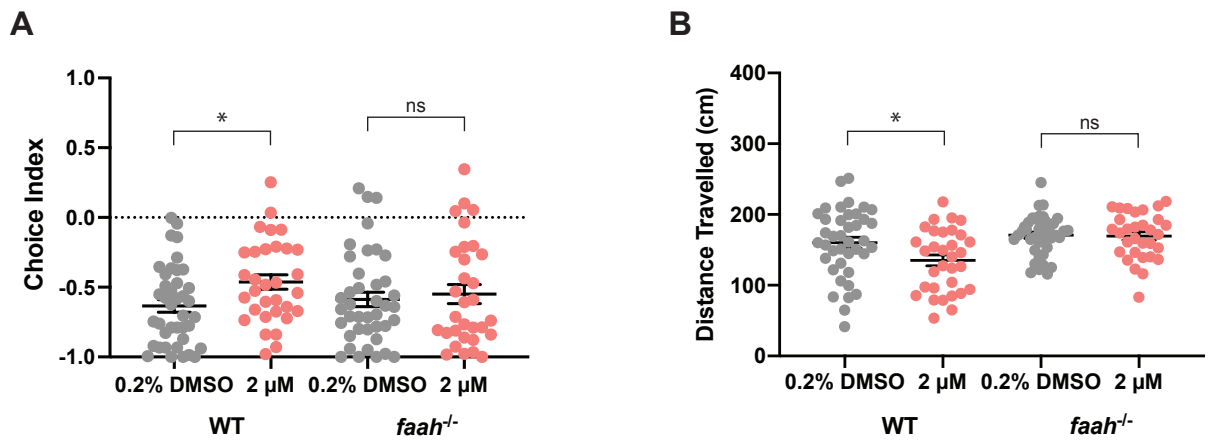

Figure 4.7 PF-3845 effects on choice index and locomotion are lost in the *faah* knockout.

(A) The choice index of wild type and *faah*$^{-/-}$ larvae treated for 1 hour with 2 µM PF-3845. We observed an increase in choice index in drug treated wild-type larvae (p = 0.0163), but no change in drug treated *faah* knockout larvae compared to controls. WT: 0.2% DMSO, n = 40; 2 µM, n = 32. *faah*$^{-/-}$: 0.2% DMSO, n = 40; 2 µM, n = 31.
(B) The distance travelled of wild type and *faah*$^{-/-}$ larvae treated for 1 hour with 2 µM PF-3845. We observed an increase in locomotor activity in drug treated wild-type larvae (0.0277), but no change in drug treated *faah* knockout larvae compared to controls. WT: 0.2% DMSO, n = 40; 2 µM, n = 32. *faah*$^{-/-}$: 0.2% DMSO, n = 40; 2 µM, n = 31.
All data represented as mean +/ SEM. ns – no significance, *p < 0.05; Mann-Whitney test was performed to assess statistical significance.

4.8 TABLES

Table 4.1 eCB-targeting pharmacological agents.

A list of all pharmacological agents used in this study along with their targets and properties.

DRUG/LIPID	TARGET	PROPERTIES
WIN55212-2	CB1	Agonist, synthetic cannabinoid
2-AG	CB1	Agonist, endocannabinoid
AEA	CB1	Agonist (partial), endocannabinoid
MJN110	MGLL	Inhibitor
JLZ-184	MGLL	Inhibitor (irreversible)
PF-3845	FAAH	Inhibitor

Table 4.2 Summary of eCB pharmacology experiment results.

Table summarizing the significant effects of each pharmacological agent on choice index and locomotor activity.

eCB PROTEIN	DRUG	EFFECT ON CHOICE INDEX	EFFECT ON LOCOMOTION
CB1	WIN55212-2	Decrease	Decrease
	2-AG	Decrease (trend)	Decrease
	AEA	Increase	Decrease
MGLL	MJN110	Increase	Decrease
	JZL-184	None	None
FAAH	PF-3845	Increase	Increase and Decrease

4.9 SUPPLEMENTAL FIGURES

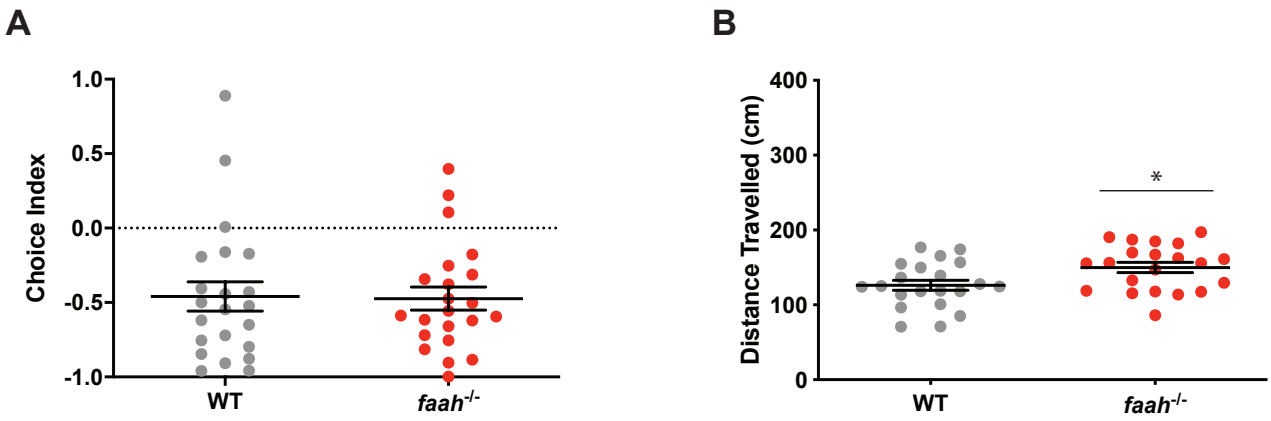

Figure 4.S1 FAAH knockout does not affect light-dark preference behavior.

(A) The choice index of wild type and *faah*$^{-/-}$ larvae. We observed no change between genotypes. WT, n = 22; *faah*$^{-/-}$, n = 22.
(B) The distance travelled of wild type and *faah*$^{-/-}$ larvae. We observed a significant increase in locomotor activity in *faah* knockout larvae. WT, n = 21; *faah*$^{-/-}$, n = 21.
All data represented as mean +/ SEM. *p < 0.05; Mann-Whitney test was performed to assess statistical significance.

4.10 REFERENCES

Amin, M.R. and Ali, D.W. (2019). Pharmacology of medical cannabis. Adv Exp Med Biol. *1162*, 151-165.

Bai, Y., Huang, B., Wagle, M., and Guo, S. (2016). Identification of environmental stressors and validation of light preference as a measure of anxiety in larval zebrafish. BMC Neuroscience. *17*, 63.

Busquets-Garcia, A., Puighermanal, E., Pastor, A., de la Torre, R., Maldonado, R., and Ozaita, A. (2011). Differential role of anandamide and 2-arachidonoylglycerol in memory and anxiety-like responses. Biol Psychiatry, *70*, 479–486.

Chaudhari, R., Fong, L.W., Tan, Z., Huang, B., and Zhang, S. (2020). An up-to-date overview of computational polypharmacology in modern drug discovery. Expert Opin Drug Discov. *15*, 1025-1044.

Chen., F., Chen, S., Liu, S., Zhang, C., and Peng, G. (2015). Effects of lorazepam and WAY-200070 in larval zebrafish light/dark choice test. Neuropharmacology. *95*, 226-233.

Chen, J.W., Borgelt, L.M., and Blackmer, A.B. (2019). Cannabidiol: A new hope for patients with Dravet or lennox-gastaut syndromes. Ann Pharmacother. *53*, 603-611.

Cooray, R., Gupta, V., and Suphioglu, C. (2020). Current aspects of the endocannabinoid system and targeted THC and CBD phytocannabinoids as potential therapeutics for Parkinson's

and Plzheimer's diseases: a review. Mol Neurobiol. *57*, 4878-4890.

Cristino, L., Bisogno, T., and Di Marzo V. (2020). Cannabinoids and the expanded endocannabinoid system in neurological disorders. Nat Rev Neurol. *16*, 9-29.

Devinsky, O., Cilio, M.R., Cross, H., Fernandez-Ruiz, J., French, J., Hill, C., Katz, R., Di Marzo, V., Jutras-Aswad, D., Notcutt, W.G., Martinez-Orgado, J., Robson, P.J., Rohrback, B.G., Thiele, E., Whalley, B., & Friedman, D. (2014). Cannabidiol: pharmacology and potential therapeutic role in epilepsy and other neuropsychiatric disorders. Epilepsia. *55*, 791–802.

Han, Q.W., Y, Y.H., and Chen N.H. (2020). The therapeutic role of cannabinoid receptors and its agonists or antagonists in Parkinson's disease. Pro Neuropsychopharmacol Biol Psychiatry. *96*, 109745.

Ignatowska-Jankowska, B., Wilkerson, J.L., Mustafa, M., Abdullah, R., Niphakis, M., Wiley, J.L., Cravatt, B.F., and Lichtman, A.H. (2015). Selective monoacylglycerol lipase inhibitors: antinociceptive versus cannabimimetic effects in mice. J Pharmacol Exp Ther. *353*, 424–432.

Kathuria, S., Gaetani, S., Fegley, D., Valiño, F., Duranti, A., Tontini, A., Mor, M., Tarzia, G., La Rana, G., Calignano, A., Giustino, A., Tattoli, M., Palmery, M., Cuomo, V., and Piomelli, D. (2003). Modulation of anxiety through blockade of anandamide hydrolysis. Nat Med. *9*, 76–81.

Kaur, R., Ambwani, S.R., and Singh, S. (2016). Endocannabinoid system: A multi-facet therapeutic target. Curr Clin Pharmacol. *11*, 110-117.

Kinsey, S.G., O'Neal, S.T., Long, J.Z., Cravatt, B.F., and Lichtman, A.H. (2011). Inhibition of endocannabinoid catabolic enzymes elicits anxiolytic-like effects in the marble burying assay. Pharmacol Biochem Behav. *98*, 21–27.

Lara, R.A. and Vasconcelos, R.O. (2021). Impact of noise on development, physiological stress and behavioral patterns in larval zebrafish. Sci Rep. *11*, 6615.

Lisboa, S.F., Gomes, F.V., Terzian, A.L.B., Aguiar, D.C., Moreira, F.A., Resstel, L.B.M., and Guimarães, F.S. (2017). The endocannabinoid system and anxiety. Vitam Horm. *103*, 193-279.

Lomazzo, E., Bindila, L., Remmers, F., Lerner, R., Schwitter, C., Hoheisel, U., and Lutz, B. (2015). Therapeutic potential of inhibitors of endocannabinoid degradation for the treatment of stress-related hyperalgesia in an animal model of chronic pain. Neuropsychopharmacology. *40*, 488–501.

Moreira, F.A., Kaiser, N., Monory, K., and Lutz, B. (2008). Reduced anxiety-like behavior induced by genetic and pharmacological inhibition of the endocannabinoid-degrading enzyme fatty acid amide hydrolase (FAAH) is mediated by CB1 receptors. Neuropharmacology. *54*, 141-150.

Moreira, F.A., Grieb, M., and Lutz, B. (2009). Central side-effects of therapies based on CB1 cannabinoid receptor agonists and antagonists: focus on anxiety and depression. Best Pract Res Clin Endocrinol Metab. *23*, 133-144.

Müller-Vahl, K.R. (2013). Treatment of Tourette syndrome with cannabinoids. Behav Neurol. *27*,

119-124.

Niphakis, M.J., Cognetta, A.B., 3rd, Chang, J.W., Buczynski, M.W., Parsons, L.H., Byrne, F., Burston, J.J., Chapman, V., and Cravatt, B.F. (2013). Evaluation of NHS carbamates as a potent and selective class of endocannabinoid hydrolase inhibitors. ACS Chem Neurosci. *4*, 1322-1332.

Pacher, P., Bátkai, S., and Kunos, G. (2006). The endocannabinoid system as an emerging target of pharmacotherapy. Pharmacol Rev. *58*, 389-462.

Patel, S. and Hillard, C.J. (2006). Pharmacological evaluation of cannabinoid receptor ligands in a mouse model of anxiety: further evidence for anxiolytic role for endogenous cannabinoid signaling. J Pharmacol Exp Ther. *318*, 304-311.

Rey, A.A., Purrio, M., Viveros, M.P., and Lutz, B. (2012). Biphasic effects of cannabinoids in anxiety responses: CB1 and GABAB receptors in the balance of GABAergic and glutamatergic neurotransmission. Neuropsychopharmacology. *37*, 2624-2634.

Rossi, A., Kontarakis, Z., Gerri, C., Nolte, H., Hölper, S., Krüger, M., and Stainier, D. Y. (2015). Genetic compensation induced by deleterious mutations but not gene knockdowns. Nature. *524*, 230–233.

Rubino, T., Guidali, C., Vigano, D., Realini, N., Valenti, M., Massi, P., and Parolaro, D. (2008). CB1 receptor stimulation in specific brain areas differently modulate anxiety-related behaviour. Neuropharmacology. *54*, 151–160.

Shonesy, B.C., Bluett, R.J., Ramikie, T.S., Báldi, R., Hermanson, D.J., Kingsley, P.J., Marnett, L.J., Winder, D.G., Colbran, R.J., and Patel, S. (2014). Genetic disruption of 2-arachidonoylglycerol synthesis reveals a key role for endocannabinoid signaling in anxiety modulation. Cell Rep. *9*, 1644–1653.

Silvestro, S., Mammana, S., Cavalli, E., Bramanti, P., and Mazzon, E. (2019). Use of cannabidiol in the treatment of epilepsy: efficacy and security in clinical trials. Molecules. *24*

Steenbergen, P.J., Richardson, M.K., and Champagne, D.L. (2011). Patterns of avoidance behaviours in the light/dark preference test in young juvenile zebrafish: a pharmacological study. Behav Brain Res. *222*, 15-25.

Viveros, M.P., Marco, E.M., and File, S.E. (2005). Endocannabinoid system and stress and anxiety responses. Pharmacol Biochem Behav. *81*, 331-342.

Wagle, M., Nguyen, J., Shinwoo, L., Zaitlen, N., and Guo, S. (2017). Heritable natural variation of an anxiety-like behavior in larval zebrafish. J Neurogenet. *31*, 138-148.

CHAPTER 5: Investigating the Neuronal Populations Underlying CB1-mediated Anxiety-Like Behavior in Larval Zebrafish

5.1 ABSTRACT

The endocannabinoid (eCB) system is a pathway in the brain that modulates anxiety states. Though inhibition of cannabinoid receptor 1 (CB1), the key protein of the eCB system, has been shown to increase anxiety, understanding of the circuitry involved is largely fragmented. Here we use zebrafish to gain insight on the neuronal populations involved in producing CB1-mediated anxiety-like behavior. We found that pharmacological and genetic inhibition of CB1 increases dark avoidance behavior in larval zebrafish, a known anxiety-like behavior. We discovered brain region-specific colocalization of *cb1* mRNA with pallial and hypothalamic glutamatergic and subpallial GABAergic neuronal markers. We gained access to CB1-expressing cells through production of a CB1 knockin fish line, and uncovered broad anatomical connectivity of CB1-expressing neurons. These results provide insight on the neural circuitry that bridges CB1 signaling and the resulting anxiety behavior.

5.2 INTRODUCTION

The endocannabinoid (eCB) system is a complex signaling pathway that modulates various brain functions. Cannabinoid receptor 1 (CB1) is a G protein-coupled receptor and the primary protein in the eCB system responsible for both short-term and long-term changes in synaptic activity and plasticity (Araque et al., 2017; Castillo et al., 2012; Heifets and Castillo, 2009; Kano et al., 2009; Matsuda et al., 1990). When activated, either by exogenous compounds such as Δ^9-Tetrahydrocannabinol (THC) found in the *Cannabis* plant (better known as marijuana) or by endogenously produced eCBs, CB1 initiates G protein-mediated signaling cascades that ultimately inhibit neurotransmitter release of the cell it is expressed on (Chan et al., 1998; Kano et al., 2009; Maneuf et al., 1996; Shen et al., 1996; Szabo et al., 1998). Depolarization-induced

suppression of inhibition (DSI) or depolarization-induced suppression of excitation (DSE) occur when CB1 is activated on GABAergic or glutamatergic neurons, respectively. (Kreitzer and Regehr, 2001; Ohno-Shosaku et al., 2001; Wilson and Nicoll, 2001). These eCB system-mediated changes in synaptic activity modulate many neurobiological processes, affecting cognition, appetite, motor control, and anxiety, to name a few (Adams et al., 1996; Berry et al., 2002; El Manira and Kyriakatos, 2010; Lafenêtre, et al., 2007, Mechoulam and Parker, 2013).

Fear and anxiety are defensive states in which an organism undergoes physiological and behavioral changes in order to avoid danger. These changes involve neuronal, hormonal, and behavioral responses that can be detrimental if the state of anxiety is excessively prolonged or disproportionately higher than the potential threat itself – ultimately resulting in neuropsychiatric disorders (Graham et al., 2011; Sylvers et al., 2011, Tovote et al., 2015). In humans, anxiety states can be attenuated or exacerbated by neuroactive drugs such as marijuana via the CB1 receptor. When activated by an agonist, CB1 generally has a biphasic effect on anxiety, producing anxiolytic responses following administration of low doses, but anxiogenic responses following high doses (Lafenêtre, et al., 2007). Unlike the biphasic effect of CB1 agonists, CB1 inhibitors have only been shown to increase anxiety (Christensen et al., 2007; Mechoulam et al., 2013).

One of the most prominent objectives of the neuroscience field is delineating neural circuits in order to deepen our understanding of brain function in health and disease. Previous studies in mice have made vast contributions to our understanding of the neural circuitry that links CB1-mediated changes in synaptic activity and the resulting change in anxiety-like states (Lutz et al., 2015; Maldonado et al., 2020). Activation of CB1 on glutamatergic neurons in the dorsal telencephalon are involved in attenuating anxiety-like behaviors (Ruehle et al. 2013). On the other hand, genetic perturbation of CB1 expressed on cortical GABAergic neurons result in an increase of exploratory behaviors. This suggests that normal-functioning CB1 on cortical

GABAergic cells facilitates neophobia, which can be interpreted as an anxiety-like behavior (Häring et al., 2011). More recent studies have honed in on specific circuits that are involved in CB1-mediated changes in anxiety-like states, with the amygdala being a key player. Deletion of CB1 in rodent basolateral amygdala inputs into the prelimbic prefrontal cortex (homologous to human amygdala-dorsomedial prefrontal cortex) reveal an increase in stress-induced anxiety behavior (Marcus et al. 2020). Another study highlights the role of CB1 on amygdala inputs to the bed nucleus of stria terminalis (BNST) in sustained fear response (Lange et al. 2017). CB1 signaling has also been shown to modulate physiological stress response through regulation of the hypothalamic-pituitary-adrenocortical (HPA) axis (Micale and Drago, 2018; Morena et al., 2016; Riebe and Wotjak, 2011). Although these studies have started to narrow in on key neuronal populations, the entire picture of cells involved in CB1-mediated anxiety circuitry remains fragmented.

Zebrafish are a powerful model organism for examining behavior and discovering circuit mechanisms (Leung et al., 2013; Li et al., 2016; Portugues et al., 2013; Stewart et al., 2014; Vanwalleghem et al., 2018). Not only have subdivisions of CNS anatomy and fundamental circuits such as those involved in anxiety been shown to be conserved between zebrafish and humans (Melgoza and Guo, 2018; Jesuthasan, 2012), but also several attributes unique to zebrafish allow for circuitry studies that are difficult, if not impossible to achieve in mice. For example, due to the minute size of the larval zebrafish brain, it is possible to record neuron activity throughout the entire brain in real time through brain-wide Ca^{2+} imaging. Because of their rapid development, 6-day-old larval zebrafish have already developed all primary neurotransmitter systems (Guo, 2009). Breeding can occur on a weekly basis and produces a large amount of progeny, allowing for quick generation progression and large sample sizes for experiments. The zebrafish genome has considerable homology with the human genome (Barbazuk et al., 2000; Howe et al., 2013), and in the context of the eCB system, proteins

involved in eCB signaling are conserved between zebrafish and humans (Elphick 2012; Oltrabella et al., 2017). These attributes make zebrafish an excellent model for studying neural circuitry, and more specifically, in the context of CB1 signaling. Here, we utilize the zebrafish model organism to expand our knowledge on the neuronal populations that make up the circuitry underlying CB1-mediated changes in anxiety.

5.3 METHODS

5.3.1 Zebrafish husbandry

Zebrafish were handled as described in Chapter 3 (section 3.3.1, p.79). Strains include the following: ABWT (light/dark preference assay, cortisol measurement assay), Tg(*cb1*$^{-/-}$) (light/dark preference assay, cortisol measurement assay), Tg(HuC-H2B-GCaMP) (HCR *in situ,* calcium imaging), Tg(*cb1*^{KalTA4}; UAS::Dendra) (projection analysis), Tg(*cb1*^{KalTA4}; UAS::Channelrhodopsin-mCherry; HuC-H2B-GCaMP) (projection analysis), and Tg(*cb1*$^{-/-}$; HuC-H2B-GCaMP) (calcium imaging).

*Note, Tg(*cb1*$^{-/-}$) is the -8 base pair mutant as described in **Figure 3.2,** p.90.

5.3.2 Generation of transgenic fish lines

sgRNA and Cas9 RNA synthesis

sgRNAs targeting the *cb1* locus were designed using CRISPRscan

(https://www.crisprscan.org), CCtop (https://cctop.cos.uni-heidelberg.de), and CHOPCHOP (https://chopchop.cbu.uib.no) web tools (sgRNA sequences are found in **Table 5.S1**). Phusion Flash High-Fidelity PCR Master Mix (ThermoFisher, #F548L) was added to 10 μM forward primer containing T7 promotor with sgRNA sequence and 10 μM reverse primer containing standard stem loop backbone (Jinek et al., 2012; Varshney, et al. 2015) and PCR was run. PCR product was purified with MinElute PCR Purification kit (Qiagen, #28006) and used for *in vitro* transcription with T7 RNA polymerase (Jiang et al. 2019). Transcription product was incubated in DNaseI (ThermoFisher, #EN0521), extracted with phenol/chloroform, and precipitated with ethanol. Ethanol was left to evaporate for 10 min, and precipitate was resuspended in nuclease free water. To produce Cas9 RNA, the template DNA pT3Ts-nls-zCas9-nls (from Wenbiao Chen, Addgene plasmid #46757) was linearized by XbaI digestion and purified with QIAprep column (Qiagen, #27115). Cas9 RNA was synthesized using mMESSAGE mMACHINE T3 Transcription kit (Invitrogen, #AM148) and purified using MEGAclear Transcription Cleanup kit (Invitrogen, #AM1908).

Microinjections

To produce Tg(*cb1*$^{-/-}$), a solution of 200 ng/μL *cb1* sgRNA and 100 ng/μL Cas9 RNA was injected into a clutch of ABWT zebrafish embryos at the 1-cell stage using a microinjector (NARISHIGE IM 300). To produce Tg(*cb1*^{KalTA4}), a solution of 100 ng/μL *cb1* sgRNA, 100 ng/μL *eGFP* sgRNA, 5 μM Cas9 protein, 25 ng/μL *eGFP*bait-E2A-KalTA4 donor plasmid, and ~0.05% phenol red dye was injected into a clutch of Tg(UAS::Dendra) embryos at the 1-cell stage. Roughly half of the embryos were set aside as uninjected controls.

Screening and genotyping

Injected F0 fish were raised to adulthood and bred with ABWT fish to produce the F1 generation. For Tg(*cb1*$^{-/-}$), primers were designed flanking the sgRNA cut site (sequences found in **Table 5.S2**). Genomic DNA was extracted from fins clipped from the F1 generation. PCR was run on a solution of 0.4 μM primers, genomic DNA, and GoTaq Green Master Mix (Promega, #M7123). PCR product was purified using Monarch DNA Gel Extraction Kit (New England BioLabs, #T1020L), and sequenced by QuintaraBio. Sequencing results were deconvoluted using the TIDE web tool (https://tide.nki.nl) to determine the number of base pairs that were inserted or deleted. F1 fish heterozygous for the same allele were bred together, and their progeny were sequenced as described above. Sequencing results for the CB1$^{-/-}$ allowed for determination of the precise mutation sequence. For the Tg(CB1^{KalTA4}), F1 larvae were screened for Dendra fluorescence and raised to adulthood. F1 adults were fin clipped and genotyped with primers shown in **Figure 5.4B** (sequences found in **Table 5.S3**).

5.3.3 Light-dark preference assay

The baseline light-dark preference assay was performed on 6 dpf zebrafish larvae as described in Chapter 3 (section 3.3.6, p.82) with the following modifications: one recording was collected for each larvae, and larvae were incubated in pharmacological agent for 1 hour prior to testing (if applicable). All behavior tests were performed between the hours of 8:00am and 1:00pm.

Videos collected from the light/dark preference assay were analyzed using Noldus Ethovision XT 13 video tracking software. Larvae were tracked and the following output parameters were collected: duration in the light zone, duration in the dark zone, latency to the light zone, latency to the dark zone, swim velocity, number of zone transitions from light to dark

(entry number to dark) and the number of zone transitions from dark to light (entry number to light). Any larvae that were frozen for the duration of the experiment were excluded. Choice index was calculated by subtracting the duration in the light from the duration in the dark then dividing by the total time. Average entry duration was calculated by dividing the duration in a zone by the number of entries into that zone. To determine decision at the border, videos were reanalyzed with an added zone in the center of the chamber as the border region. Output parameters were the transition from light to border to dark (pass-through event), and transition from light to border to light (turn back event). Percent of pass-through events was calculated by dividing the number of pass-through events divided by the total number of border events (number of pass-through events plus number of turn back events).

5.3.4 Cortisol measurement assay

6dpf larvae were separated into 100mm petri dishes with 30mL of blue egg water, n = 10 per dish. For pharmacological groups, ABWT larvae were used. For genetic groups, Tg($CB1^{-/-}$) were used as the experimental groups and a mixture of Tg($CB1^{+/+}$) and Tg($CB1^{+/-}$) were used as controls. If pharmacological agent was administered, larvae were incubated in drug (or vehicle) for 1 hour. To administer mechanical stress, a mini stir-bar was put into the dish and water was stirred on a stirrer (VWR-Hotplate/Stirrer) at 200 rpm for 5 minutes. Following larval separation, drug administration, and/or stress condition (depending on the group), larvae were poured into a Falcon Cell Strainer (Corning, #352360). A squirt bottle with blue egg water was used to gather larvae near the bottom of the cell strainer, and also squirt larvae with ice-cold 1x phosphate-buffered saline (PBS). The cell strainer containing larvae was then quickly transferred to another 100mm dish containing ice-cold PBS. A glass transfer pipette was used to transfer larvae from the cell strainer to a 1.5 mL eppendorf tube, leaving 50 µL. The collection tube was stored at -

70°C and the process was repeated until all groups and replicates were collected. Frozen samples were thawed on ice, and 150 µL PBS was added. Samples were homogenized with a hand held homogenizer (VWR Pellet Mixer #47747-370) for 1 min. 20 µL of homogenate was used to estimate total protein concentration with PIERCE BCA kit (#23225). 1400 µL of ethyl acetate was added to remaining homogenate. Samples were vortexed and centrifuged for 7000G at 4°C for 15 min. The organic layer was transferred to a fresh collection tube and left to evaporate in a fume hood overnight. Cortisol concentration was estimated using the Cayman Cortisol ELISA Kit (#500360).

5.3.5 Hybridization chain reaction (HCR) in situ

Protocol is deviated from Choi et al. 2018 and the Deisseroth lab (https://web.stanford.edu/group/dlab/). 6 dpf larvae were fixed with 4% paraformaldehyde (PFA) at 4°C for approximately 24 hours. The samples were washed with PBS, then dehydrated with a 100% Methanol (MeOH) at -20°C for 10 minutes. Larvae were rehydrated with a series of 5-min graded MeOH/PBST (1x PBS, 0.1% Tween 20 Detergent) washes (75% MeOH / 25% PBST; 50% MeOH / 50% PBST; 25% MeOH / 75% PBST), then 5 washes using 100% PBST. Samples were incubated in probe hybridization buffer (Molecular Instruments, https://www.molecularinstruments.com) at 37°C for 30 min, then in probe hybridization buffer with 2µM v3.0 HCR probes (Molecular Instruments) at 37°C for approximately 18 hours. Larvae were washed 4 times with probe wash buffer (Molecular Instruments) at 37°C, then 3 times with 5x SSCT (5x sodium chloride sodium citrate, 0.1% Tween 20). HCR hairpins were heated at 95°C for 90 seconds and cooled at room temperature for 30 minutes. Larvae were incubated in amplification buffer (Molecular Instruments) for 30 minutes, then in amplification buffer with 240nM of each hairpin for approximately 18 hours. Amplification buffer and hairpins were

washed off 5 times with 5x SSCT. Then the samples were had a series of graded glycerol washes (25% glycerol, 50% glycerol, 80% glycerol).

5.3.6 Confocal microscopy

After HCR *in situ* (**Figure 5.3**), larvae were whole-mounted on slides using 80% glycerol. For live imaging (**Figures 5.4** and **5.5**), larvae were embedded in 35 mm glass bottom dishes (MatTek, #P35G-1.5-10-C) with 2% (wt/vol) low melting agarose (Fisher Scientific, #BP165-25) in blue egg water and covered with 2 mL of blue egg water. Mounted or embedded larvae were imaged dorsal-side up using a Zeiss LSM 780-FLIM confocal microscope equipped with a W Plan-Apochromat 20x/1.0 DIC (UV) VIS-IR M27 75mm objective lens. For HCR, Alexa488, Alexa546, or Alexa647 fluorophores were excited with the 488nm, 555nm, or 647nm lines from an argon laser, respectively. For live imaging, GCaMP, Dendra, or mCherry fluorophores were excited with the 488nm, 488nm, or 555nm lines of an argon laser, respectively. Images were acquired using Zen 2012 imaging software. To acquire the entire larval brain, Z-stacks were collected for each sample starting from the ventral-most plane of the brain and ending with the dorsal-most plane at a voxel size of 0.49 x 0.49 x 2 µm (*x*, *y*, *z*), using 2 horizontal tiles with 10% overlap.

5.3.7 Image processing

Following confocal imaging, Fiji imaging software (https://imagej.net/Fiji) was used to stitch horizontal tiles via Pairwise Stitching plugin. Image stacks were reversed to make the order ventral to dorsal, rotated 180° to orient the brain anterior to posterior from left to right, and

cropped to match the reference brain image from the Z-brain atlas (Randlett et al. 2015, https://zebrafishatlas.zib.de). Images were saved in .nnrd format for registration.

5.3.8 Image registration

Computational Morphometry Toolkit (CMTK 3.3.1, https://www.nitrc.org/projects/cmtk/) was used for nonrigid image registration. Registration was performed on the University of California, San Francisco Wynton high-performance compute (HPC) cluster. All samples to be registered had Tg(HuC-H2B-GCaMP) background, which was used as the sample image stack. Each sample stack was registered to the Elavl3-H2BRFP reference stack from the Z-brain atlas. CMTK was run with the following command string: -a -w -r 010203 -X 104 -C 8 -G 160 -R 2 -J 0.050 -A '--dofs 6,9 --mi --accuracy 8' -W '--mi –accuracy 8’.

5.3.9 Image analysis

To access 6 dpf zebrafish brain anatomical masks, registered data was put through the z-brain viewer (https://github.com/owenrandlett/Z-Brain) in Matlab (MathWorks), allowing for determination of *in situ* and *cb1*-cell projection localization.

5.3.10 Quantification and statistical analysis

Graphpad Prism 8 was used to produce graphs and run student’s t-test and one-way ANOVA. Permutation analysis independence test was performed on R programming software. Statistical details of each experiment can be found in figure legends.

5.4 RESULTS

5.4.1 CB1 inhibition increases dark avoidance behavior in larval zebrafish

Though there is a wide breadth of literature that demonstrates how inhibition of CB1 elicits anxiety-like behavior responses in humans and rodents (Blasio et al., 2013; Christensen et al., 2007; Mechoulam et al., 2013, Thiemann et al., 2009), to date, no study has been done to examine anxiety-like behavior in zebrafish following CB1 inhibition – a critical foundation to establish before using this model to examine the underlying circuitry involved. The light-dark preference assay is a well-established paradigm used to examine anxiety-like behaviors in model organisms including larval zebrafish (Bai et al., 2016; Chen et al., 2015; Lara and Vasconcelos, 2021; Steenbergen et al., 2011; Wagle et al., 2017). To examine the effects of CB1 inhibition on anxiety-like behavior in zebrafish, we performed the light-dark preference assay.

In short, following pre-adaptation to a well-controlled luminance background, a zebrafish larva is placed in the center of a chamber that is half illuminated and half dark (**Figure 5.1A**). Immediately after the fish is placed, recording starts and the larva is able to swim freely throughout the chamber for the duration of the 8-minute experiment. While untreated wild-type zebrafish larvae show a baseline preference for spending their time in the light zone of the chamber, anxiogenic drugs, mutations, and experiences have been shown to further increase dark avoidance behavior (Bai et al., 2016; Lara and Vasconcelos, 2021; Steenbergen et al., 2011; Wagle et al., 2017). **Figure 5.1B** (left) demonstrates heatmap representations of larval position over time, showing a decrease in the time spent in the dark zone of the behavioral chamber upon administration of an anxiogenic drug. While control fish do have a preference for staying in the light zone, they also venture out into the dark zone, in contrast to 4 mg/L AM251-

treated fish which spend most, if not all, of their time solely in the light zone. This dark avoidance behavior can be quantified by calculating the choice index (CI) (**Figure 5.1B**, right).

After administration of the CB1 inverse agonist AM251, 6 day post fertilization (dpf) zebrafish larvae exhibited a significant increase in dark avoidance at all tested concentrations compared to controls (**Figure 5.1C**, left; 0.2% DMSO: CI = -0.69 ± 0.08, n = 16; 1 mg/L AM251: CI = -0.98 ± 0.01, p = 0.0014, n = 15; 2 mg/L AM251: CI = -0.95 ± 0.03, p = 0.0081, n = 14; 4 mg/L AM251: CI = -0.95 ± 0.03, p = 0.0058, n = 15; mean ± SEM), indicative of an anxiety-like response. Similar results were seen after administration of the CB1 antagonist SLV-319 at 5- 10- and 20 mg/L, which also showed significant increases in dark avoidance at all concentrations compared to controls (**Figure 5.1C**, middle; 0.2% DMSO: CI = -0.53 ± 0.07, n = 16; 5 mg/L SLV-319: CI = -0.79 ± 0.07, p = 0.0167, n = 16; 10 mg/L SLV-319: CI = -0.79 ± 0.06, p = 0.0121, n = 16; 20 mg/L SLV-319: CI = -0.79 ± 0.06, p = 0.0084, n = 16).

Although both CB1 inhibitors induced dark aversion phenotypes, it is possible that off-target effects distinct from CB1 may be contributing to these changes in behavior. To combat this caveat of using pharmacological agents, a CB1 knock-out line was created (**Figure 5.S1**). Corroborating pharmacological inhibition, homozygous CB1 knock-out fish showed a significant increase in dark aversion compared to wild-type siblings (**Figure 5.1C**, right; Wild-type: mean CI = -0.69, n = 20; Heterozygotes: mean CI = -0.71, n = 29; Knock-outs: mean CI = -0.91, p = 0.03365, n = 11).

To gain a more detailed understanding of how light-dark preference behavior is affected by CB1 inhibition, kinematic analysis was performed. The following parameters were examined: entry number (the number of entries made into the dark or light zone for the duration of the assay), average entry duration (the average length of time spent in dark or light before transitioning to the opposite zone), and latency (the duration of time before the larvae first enters the dark or light zone). Neither pharmacological nor genetic inhibition of CB1 significantly

altered the entry number (**Figure 5.1D**). Conversely, the average entry duration in the light zone was significantly increased after administration of 1 mg/L AM251 ($p = 0.0297$) and 20 mg/L SLV-319 ($p = 0.0398$), as well as in the CB1 knock-out ($p < 0.0001$) compared to respective controls (**Figure 5.1E**). These data suggest that CB1-inhibited larvae transition between the light and dark zones a similar number of times as controls, but each time they enter the light zone, they wait a longer duration before transitioning to the dark zone. Furthermore, though there was no significant change in latency to the dark or light zone after administration of AM251 or genetic CB1 inhibition, latency to enter the dark zone significantly increased after treatment with 10- and 20 mg/L SLV-319 (**Figure 5.1F**; 10 mg/L SLV-319: $p = 0.0085$; 20 mg/L SLV-319: $p = 0.0253$). This corroborates the phenomenon that CB1-inhibition results in increased dark avoidance behavior as fish treated with higher concentrations of SLV-319 spend more time light zone before their first transition into the dark zone. Taken together, both pharmacological and genetic inhibition of CB1 increases dark avoidance behavior.

Dark avoidance behavior can arise due to possible alterations in sensory, motor, or motivational (i.e. anxiety-like) states. In terms of sensory input, CB1-inhibited larvae do not have impaired vision as they display a stronger light preference; if vision was impaired, we would expect a loss of preference for either zone. In terms of locomotor activity, some of the CB1-inhibited groups displayed a decrease in velocity. Administration of AM251 significantly decreased the velocity of larvae at all concentrations tested (**Figure 5.S2A**; 1 mg/L AM251: $p = 0.0001$; 2 mg/L AM251: $p < 0.0001$; 4 mg/L AM251: $p = 0.0001$). In contrast, administration of 5- and 20- mg/L SLV-319 had no significant effect on velocity, though there was a decrease with 10 mg/L SLV-319 (Figure S2B; 10 mg/L SLV-319: $p = 0.0355$). There was no significant change in velocity in heterozygotes nor homozygotes for the mutant *cb1* allele compared to wild-type siblings (**Figure 5.S2C**). Though administration of 1- 2- and 4 mg/L AM251 and 10 mg/L of SLV-319 resulted in a decrease in locomotor activity, this did not prevent larvae from being able to

traverse across zones, as seen by the lack of significant change in entry number for each of these groups (**Figure 5.1D**). Therefore, larvae that spent more time in the light zone did not do so because they were incapable of traveling to dark zone.

Another measurable parameter of the light-dark preference assay is the decision that each larvae makes when approaching the border of the light and dark zones. Once the larvae reaches the border from the light zone, it has the option of either passing through into the dark zone (pass-through event), or turning back into the light zone again (turn back event). Analysis of border decision reveals that larvae treated with 4 mg/L AM251 have a significant reduction in pass-through events compared to controls (**Figure 5.S2B**, left, $p = 0.0122$). Rather than passing through to the dark zone, 4 mg/L AM251-treated larvae turn back into the light every time they approached the border. We did not see a significant difference in pass-through events with SLV-319 treated larvae compared to controls (**Figure 5.S2B**, right).

Ruling out sensory and locomotor effects – in combination with increased turn away events in AM251 treated larvae, and previous studies that have demonstrated the anxiogenic effects of CB1 inhibitors in humans and rodents – provides evidence that the increase in dark avoidance behavior seen by pharmacological and genetic inhibition of CB1 was due to an increase in anxiety-like state.

5.4.2 AM251 administration increases cortisol levels in unstressed conditions in zebrafish larvae

To further verify the notion that CB1 inhibition may increase overall stress and anxiety levels, we looked at a key physiological stress indicator – cortisol. Larvae were split into groups to examine the effects of pharmacological and genetic CB1 inhibition on cortisol under unstressed and stressed conditions (**Figure 5.2A-i**). To compare cortisol levels among groups, larvae were gathered and homogenized. A fraction of homogenate was used to estimate total protein

concentration, and the rest was used to determine cortisol concentration. Concentration of cortisol was divided by total protein concentration for each larvae, then compared (**Figure 5.2A-ii**).

Under unstressed conditions, SLV-319-treated larvae showed no change in cortisol, but AM251 administration demonstrated a significant increase in cortisol ($p = 0.0286$) (**Figure 5.2B**, left). Under stressed conditions, neither pharmacological treatment was significantly different compared to controls (**Figure 5.2B**, right). The more severe effect on cortisol levels by AM251 compared to SLV-319 in unstressed conditions is in line with the stronger effect of AM251 on increasing baseline dark avoidance behavior (**Figure 5.1C**). These results could be a consequence of AM251's stronger effects on opposing CB1 activity through its nature as an inverse agonist, as opposed to SLV-319's nature as a CB1 antagonist. For the genetic groups, the *cb1* knockout did not exhibit significant changes in cortisol compared to control in neither unstressed nor unstressed conditions (**Figure 5.2C**).

5.4.3 HCR in situ *reveals region-specific* cb1 *expression and co-expression with neuronal markers*

Determining *cb1* mRNA localization throughout the brain would provide valuable insight on brain regions and neuronal populations that may be involved in CB1-mediated behavioral changes. Previous studies have examined brain-wide *cb1* mRNA expression in larval zebrafish (Lam et al., 2006; Liu et al., 2016; Oltrabella et al., 2017; Watson et al. 2008), but as they were done using traditional chromogenic *in situ* methods, this data is limited to 2D images with low cellular resolution. Additionally, it would be most relevant to determine expression at the developmental stage we observed CB1-mediated dark avoidance behavior (6 dpf), for which there is currently no expression data. Lastly, we determine co-expression of *cb1* mRNA with markers for

glutamatergic and GABAergic neurons, two principal neurotransmitter systems which have been shown to co-express with CB1 in other animal models (Busquets-Garcia et al. 2017; Lutz, 2020).

To visualize high-resolution brain-wide expression of *cb1* mRNA and its co-expression with neuronal subtype markers in 6 dpf zebrafish larvae, we performed hybridization chain reaction (HCR) *in situ* (**Figure 5.3A**). Larvae expressing HuC-H2B-GCaMP6s were collected at 6dpf. HCR *in situ* was then performed with probes that targeted *cb1* mRNA and a neuronal marker of interest (*vglut2, gad1b,* or *crhb*). After *in situ*, larvae were imaged with a confocal microscope to collect volumetric data of GCaMP6s, the probe targeting *cb1* mRNA, and the probe targeting a neuronal marker's mRNA for each sample. The GCaMP6s data was used to register each sample to a Z-brain atlas reference brain (Randlett et al. 2015). Following registration, anatomical masks were applied and colocalization of CB1 to neuronal markers was determined.

Registered volumetric data of *cb1* HCR *in situ* reveal a region specific expression of *cb1* mRNA at 6dpf. Dorsal and lateral maximum intensity projections allow for visualization of brain regions containing the strongest *cb1* mRNA expression, which include the pallium, subpallium, rostral hypothalamus, and torus longitudinalis (**Figure 5.3B**). Other areas with high *cb1* expression are olfactory bulb dopaminergic areas, Vglut2 rind, Vmat2 cluster, and otpb cluster 3. All brain regions containing high, moderate, and weak expression of *cb1* can be found in **Table 5.1**.

Following colocalization analysis, it was revealed that *cb1* mRNA colocalizes with *vglut2.2* and *gad1b* mRNA in distinct regions in the 6dpf zebrafish brain. In the pallium, *cb1* strongly colocalizes with *vglut2.2* in the medial and anterior regions (**Figure 5.3Ci-iii**, yellow arrow heads). However, only a few *gad1b*-expressing cells colocalize with *cb1* (Figure 3Civ-vi, yellow arrow heads). In the subpallium, no co-expression of *cb1* and *vglut2.2* was observed

(**Figure 5.3Di-iii**). In contrast, *cb1* and *gad1b* mRNA strongly colocalized in the anterior portion of the subpallium (Figure 3Div-vi, yellow arrow heads). Lastly, *cb1* and *vglut2.2* was found to co-express in the medial region of the rostral hypothalamus (**Figure 5.3Ei-iii**, yellow arrowheads). No co-expression was detected between cb1 and gad1b in the rostral hypothalamus (**Figure 5.3Eiv-vi**). These results suggest that at the 6dpf zebrafish larval developmental stage, CB1 modulates glutamatergic signaling (DSE) in the pallium and hypothalamus, but also modulates GABAergic signaling (DSI) in the subpallium and several cells of the pallium. These results are in line with previous data that demonstrate CB1's ability to perform either DSE or DSI depending on where in the brain it is expressed (Diana and Marty, 2004).

We also examined *cb1* mRNA expression in relation to corticotropin-releasing factor (CRF) neurons. CRF neurons play a key role in anxiety and stress response, and increase anxiety-like behaviors in animals when stimulated (Dedic et al., 2018; Hauger et al., 2009; Pomrenze et al. 2019). In particular, our lab has observed that activation of hypothalamic CRF neurons is sufficient to induce dark aversion behavior in the light/dark preference assay (data not shown). While there was no significant co-localization of *cb1* and the CRF neuronal marker *crhb*, they are in close proximity in two brain regions of strong *cb1* expression: otpb cluster 3 (**Figure 5.3Fi-vi**, yellow arrow heads) and the rostral hypothalamus (**Figure 5.3Gi-vi**, yellow arrow heads). If connected, the CB1 containing neurons may be modulating the signal sent to nearby CRF neurons.

5.4.4 CRISPR-mediated knockin enables genetic access to CB1-expressing neurons

To date, no CB1 transgenic zebrafish line has been established. This would be an exceptionally advantageous tool, as it would open the door to specific manipulation of CB1-expressing cells. Crossing a CB1 transgenic line to a reporter line would allow for a detailed analysis of neuronal

projections, gaining insight on physical connectivity of CB1-expressing cells. On the other hand, crossing it with optogenetic fish lines would allow for on-demand activation or deactivation of this cell population. Coupling the CB1 transgenic line with an nitroreductase (NTR) line would allow for specific ablation of CB1-expressing cells, while coupling with a genetically encoded calcium indicator (GECI), such as GCaMP, would make tracking neuronal activity over time possible. Overall, a transgenic CB1 zebrafish line would be a valuable tool to enhance our knowledge of CB1-expressing cells.

To produce this transgenic line, a targeted knockin approach using CRISPR/Cas9 technology was used, as described in Auer et al. (2014). **Figure 5.4A** illustrates the steps taken to introduce the transcription factor KalTA4 into the *cb1* locus (this knockin allele will be denoted as Tg(*cb1*^{KalTA4})). In short, sgRNA was designed to target CB1 at the beginning of Exon 1 (**Figure 5.4B**). A sgRNA designed by Auer et al. was used to target the eGFPbait-E2A-KalTA4 plasmid. The sgRNAs, donor plasmid, and Cas9 protein were injected into a Tg(UAS::Dendra) fish line at the 1-cell stage. Mosaic F_0 founders were selected, raised to breeding age, then outcrossed. Their progeny, the F1 generation, were screened for Dendra fluorescence then genotyped via PCR. Two F1 fish produced PCR products for the WT sequence, as well as sequences that span the 5' and 3' ends of the knock-in allele, indicative of a successful heterozygote knock-in (**Figure 5.4C**). Sequencing of the 5' junction reveals an in-frame knockin for KalTA4 expression (**Figure 5.4D**). Confocal imaging of these heterozygous larvae at 6dpf reveal similar expression patterns as the *cb1* HCR in situ (**Figure 5.4Ei-ix**), such as strong expression in the pallium, subpallium, hypothalamus, and torus longitudinalis. Interestingly, the CB1 transgenic line exhibited stronger expression in the habenula compared to HCR *in situ* (**Figure 5.4Ex-xi**). Sequences for sgRNAs and primers are shown in **Tables 5.S1** and **5.S3**.

5.4.5 Projection analysis of CB1-expressing cells

A key difference between *cb1 in situ* and the Tg(*cb1*^{KalTA4}) line is the ability to visualize CB1-expressing cell axonal projections in the knockin. This provides the advantage of allowing for analysis of neuronal projections at the 6dpf developmental stage. To examine projections of CB1-expressing cells, 6dpf larvae expressing *cb1*^{KalTA4}, UAS::ChR-mCh, and HuC-H2B-GCaMP6s were collected and imaged. 3D whole-brain data was registered and analyzed to determine sites of neuronal connectivity (local projections, inter-regional projections, and varicosities) throughout the fore-, mid-, and hindbrain. (**Figure 5.5A**).

In the forebrain, we observed three regions with strong CB1-driven fluorescence – the pallium, subpallium, and habenula – which all show local projections within each respective region (**Figure 5.5Bi-iii**). We also observed CB1-expressing inter-regional projections in the caudal hypothalamus, which contained fluorescent cells projecting to the rostral hypothalamus (**Figure 5.5Biv-vi**). Cells in the posterior side of the caudal hypothalamus had local connections with cells in the anterior side of the caudal hypothalamus (**Figure 5.5Biv**), and the anterior group of cells project out in a bundle of fibers to the rostral hypothalamus (**Figure 5.5Bv-vi**). In the midbrain, CB1-expressing neurons in both the torus longitudinalis and tectum striatum were observed to project to the tectum neuropil (**Figure 5.5Ci-ii**). Interestingly, not all cells in the tectum striatum of Tg(*cb1*^{KalTA4}) larvae contained fluorescent signal, but rather a subset of cells dispersed throughout the brain region (**Figure 5.5Cii**). In the hindbrain, varicosities of CB1-expressing cells were found in the olig2 and gad1b enriched areas of the cerebellum (**Figure 5.5D**, left). We also observed CB1-expressing cells and axon bundles in ventral (**Figure 5.5D**, middle) and dorsal (**Figure 5.5D**, right) regions of rhombomere 7.

5.5 DISCUSSION

Animal brain states and behaviors are driven by neural circuits, which are composed of intricately connected neurons that send signals throughout the brain and body. One brain state of great interest is anxiety, due to the high prevalence, debilitating nature, and difficulty in treatment of anxiety disorders (Maron and Nutt, 2017; Tovote et al., 2015). It has been well established that modulation of CB1 results in changes in anxiety state (Blasio et al., 2013; Christensen et al., 2007; Lafenêtre, et al., 2007; Mechoulam et al., 2013; Thiemann et al., 2009). Because most studies examining the neural circuitry involved in CB1-mediated changes in anxiety were done by examining changes following perturbation of CB1 in a small brain region (Gomes-de-Souza et al. 2021; Lange et al. 2017; Marcus et al. 2020), our understanding of the neural circuitry involved remains fragmented. Here we take a global approach, examining behavior and various aspects of the whole brain of zebrafish larvae in the context of CB1 signaling, providing an outstanding opportunity to elucidate the underlying cellular mechanisms of CB1's role in modulating anxiety-like behavior.

Our understanding of CB1's devastating effects on anxiety and mental health developed with the release of the drug rimonabant. Rimonabant is a CB1 inverse agonist that was indicated as an anti-obesity drug. Though it was efficacious in promoting weight loss for patients, rimonabant was ultimately pulled off the market due to incidences of anxiety, depression, and suicide (Mitchell and Morris, 2007; Soyka 2008). Our first aim for this study was to determine if zebrafish also exhibited an increase in anxiety-like behavior following global inhibition of CB1. Indeed, we found that inhibiting CB1 pharmacologically (with AM251, a CB1 inverse agonist with structural similarity to rimonabant, and SLV-319, a CB1 antagonist) and genetically in 6 dpf zebrafish larvae resulted in an increase in dark avoidance, an anxiety-like behavior (**Figure 5.1**). Furthermore, CB1 inhibition with AM251 also resulted in an increase in

cortisol, the stress hormone (**Figure 5.2**). Though both CB1 inhibitors increased dark avoidance behavior, AM251 induced a stronger effect in both the light-dark preference and cortisol assays. This may be due to AM251's nature as a CB1 inverse agonist, compared to SLV-319's mechanism of action as a CB1 antagonist.

We next determined the distribution of *cb1* mRNA throughout the 6 dpf zebrafish larvae to gain a deeper understanding of the brain regions and neuronal subtypes that may be modulated by CB1 at this developmental stage. We found highest *cb1* expression in the pallium (homologous to the human cortex, hippocampus, and amygdala), subpallium (homologous to the human amygdala), rostral hypothalamus, and torus longitudinalis (**Figure 5.3B, Table 1**). HCR *in situ* also allowed us to examine co-expression of *cb1* with neuronal markers, and we found that *cb1* colocalizes with *vglut2.2* and *gad1b* in distinct regions in 6 dpf larvae. It was revealed that *cb1* strongly co-expresses with *vglut2.2* in the pallium and hypothalamus, while strong co-expression of *cb1* with *gad1b* is seen in the subpallium (**Figure 5.3C-E**). We also found that *cb1* in the otpb3 cluster and rostral hypothalamus regions are in proximity to *crhb*, the marker for CRF neurons (**Figure 5.3F-G**). These findings lay the foundation in providing insight on potential circuit mechanisms; it is likely that DSE occurs in the pallium and hypothalamus, while DSI occurs in the subpallium. Furthermore, proximity of *cb1* to *crhb* may suggest interaction between CB1 and CRF neurons in regions of proximity.

Using a CRISPR-Cas9 knockin technique, we were able to successfully create the first reported transgenic CB1 zebrafish line (**Figure 5.4**). We coupled this line with a reporter line, which allowed for visualization of neuronal projections of CB1-expressing cells (**Figure 5.5**). We also observed local projections within areas of strong CB1 expression, namely the pallium, subpallium, and lateral habenula (**Figure 5.5B**), as well as interregional projections between CB1-expresing cells in the torus longitudinalis and tectum neuropil, the tectum striatum and tectum neuropil, and the caudal hypothalamus and rostral hypothalamus (**Figure 5.5B-C**). We

also observed varicosities of CB1-expressing cells in olig2- and gad1b- rich regions of the cerebellum (**Figure 5.5D**, left) and CB1-expressing cell bodies and axon fibers in rhombomere 7 (**Figure 5.5D**, middle and right). These data on physical connectivity provide insight on the neural circuitry that CB1-expressing cells are involved in.

Our study utilized the power of the zebrafish model to examine the effects of global CB1 inhibition on behavior, and cortisol levels, as well as brain-wide *cb1* expression and projections of CB1-expressing cells. Now that the transgenic CB1 zebrafish line has been created, further studies can be done to gain more insight on CB1 circuitry. The Tg(*cb1*^{KalTA4}) line coupled with a reporter line could be further utilized for examination of neuronal projections across different developmental stages up to adulthood. Combining Tg(*cb1*^{KalTA4}) with a genetically encoded calcium indicator, such as GCaMP, would allow for examination of CB1-expressing cell neuron activity. Neuron activity could be examined following inhibition of CB1, providing a means to find candidate cells; if neuron activity in particular cell populations is affected by CB1 inhibition, it is possible that they are involved in the neural circuit that connects CB1 activity to anxiety. Additionally, coupling Tg(*cb1*^{KalTA4}) with optogenetic fish lines such as Tg(UAS::Channelrhodopsin) or Tg(UAS::Halorhodopsin) would allow for optogenetic control of CB1-expressing cells. Spatiotemporal optogenetic activation or inhibition could be used to test candidate cells and regions to confirm their participation in the CB1-mediated anxiety circuit. Overall, the CB1 transgenic line is a tool that can allow for a more complete picture of this circuit, which will provide insight not only on the origin of CB1-mediated changes in anxiety state, but also fundamental organization of brain connectivity.

5.6 ACKNOWLEDGMENTS

We would like to thank all Guo lab members for fruitful discussions and Michael Munchua,

Hongbin Yuan, and Xingnu Zhai for excellent fish care. These studies were supported by the National Science Foundation Graduate Research Fellowship Program (NSF GRFP) and the Kavli Institute for Fundamental Neuroscience Fellowship fund.

5.7 FIGURES

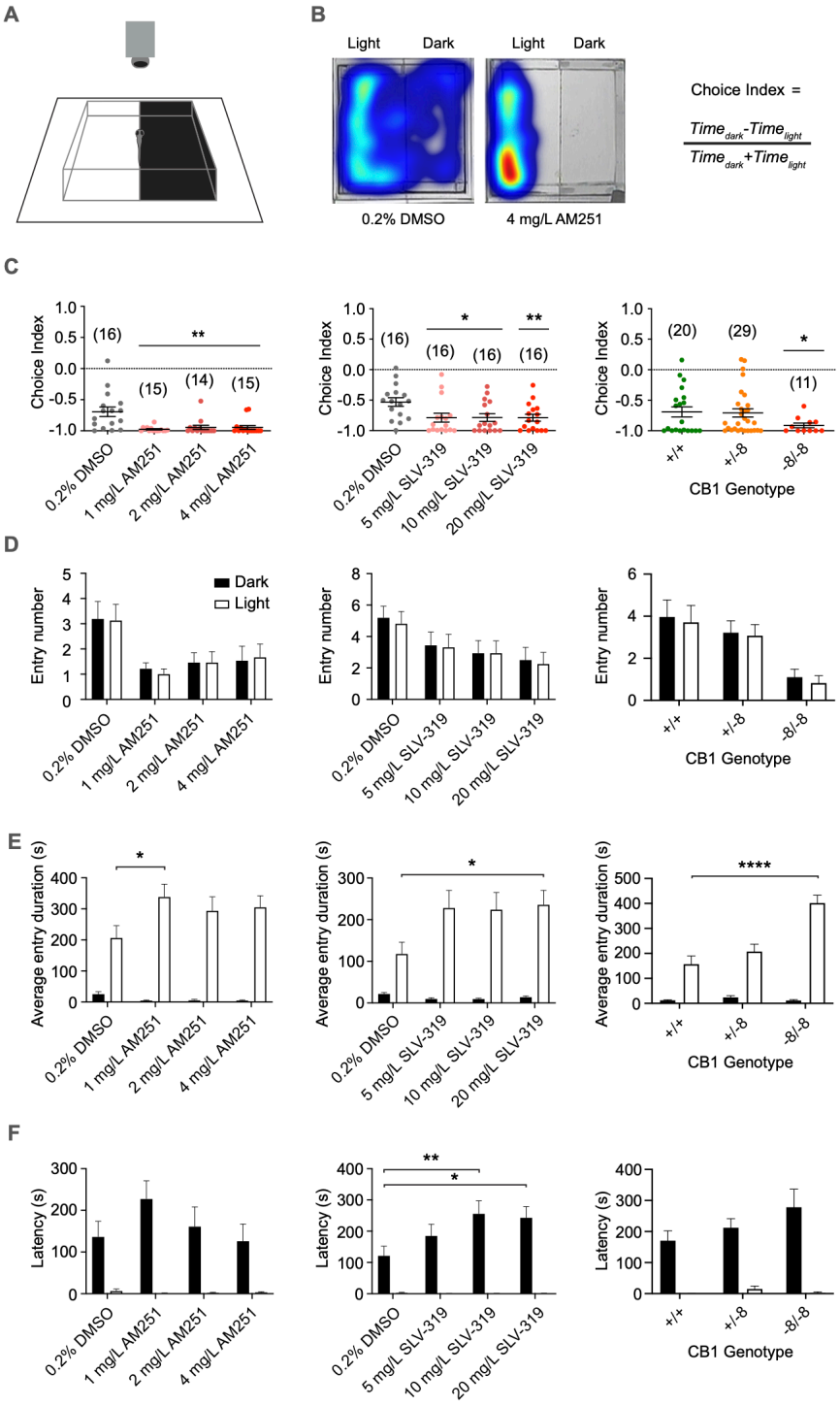

Figure 5.1 CB1 inhibition increases dark aversion behavior in zebrafish larvae.

(A) Schematic representation of the Light/Dark preference assay.

(B) Left: A heatmap representation of the locomotor pattern of a control fish vs. 4 mg/L AM251-treated fish. Right: Calculation to determine the choice index.
(C) Left: Larvae treated with CB1 inverse agonist AM251 at 1, 2, and 4 mg/L have a significantly lower choice index compared to 0.2% DMSO-treated controls. Middle: Larvae treated with CB1 antagonist SLV-319 at 5, 10, and 20 mg/L have a significantly lower choice index compared to 0.2% DMSO-treated controls. Right: CB1 knock-out fish with the -8 allele exhibit a significant reduction in choice index compared to WT siblings.
(D, E, and F) Entry number (D), average entry duration (E), and latency (F) for AM251 (Left), SLV-319 (Middle), and CB1 Knockout (Right) experiments done in Figure 1C. Filled bars represent kinematic parameter measured in the dark, empty bars represent kinematic parameter measured in the light.
All quantitative data represented as mean +/ SEM. *$p < 0.05$, **$p < 0.01$, ****$p < 0.0001$ (student's t-test for C Left and Middle, permutation analysis independence test for C Right, one-way ANOVA for D-F). See also figures S1 and S2.

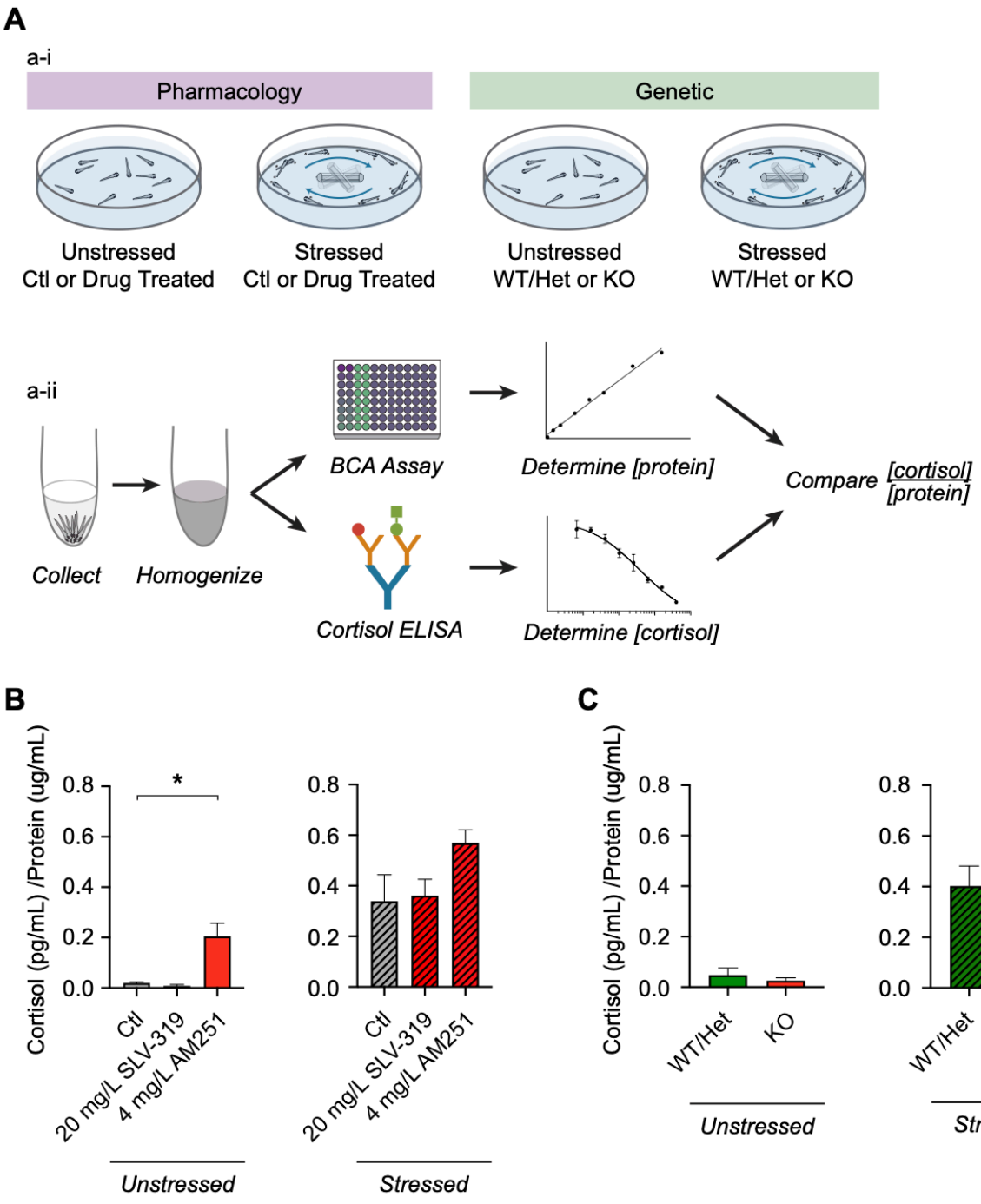

Figure 5.2 AM251 administration increases cortisol levels in larval zebrafish.

(A) Schematic representation of the cortisol assay. Zebrafish larvae were split into groups to examine pharmacological inhibition and genetic inhibition of CB1 on cortisol levels during unstressed and stressed conditions (a-i). After treatment and/or stressor administration, larvae were collected and homogenized, and assays were performed to determine cortisol concentration divided by total protein concentration (a-ii).

(B) Left: In unstressed conditions, larvae treated with 20 mg/L SLV-319 have no change in cortisol levels compared to controls, but treatment with 4 mg/L AM251 reveals a significant increase in cortisol. Right: In stressed conditions, neither treatment with 20 mg/L SLV-319 nor 4 mg/L AM251 causes a significant change in cortisol.
(C) In both unstressed (left) and stressed (right) conditions, *cb1* knockout larvae have no significant change in cortisol levels compared to controls.
All quantitative data represented as mean +/ SEM. *$p < 0.05$ (Mann-Whitney test was performed to assess statistical significance).

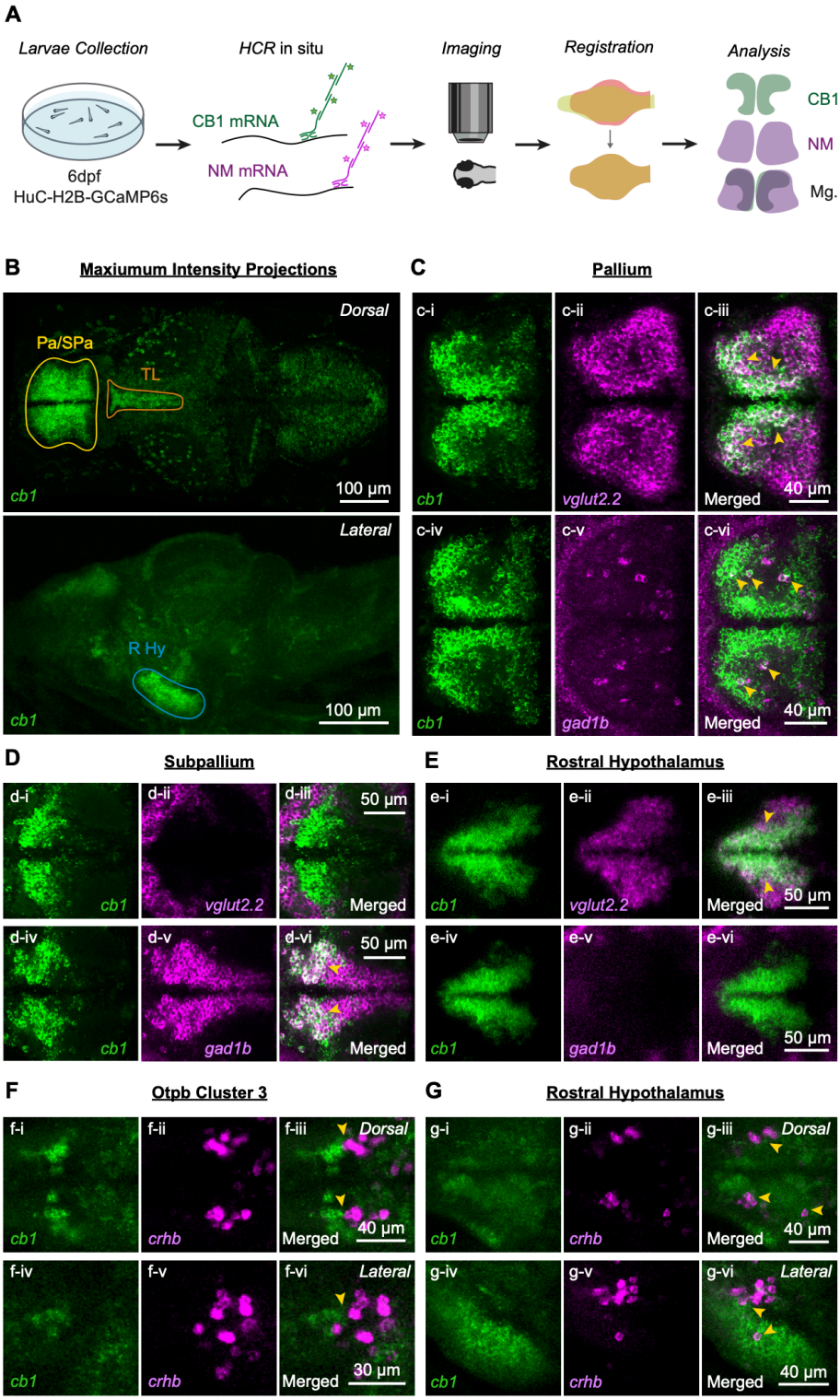

Figure 5.3 Comprehensive analysis of brain-wide CB1 expression.

(A) Schematic demonstrating the workflow of data collection and analysis of HCR *in situ* data.

(B) Maximum intensity projections of confocal data showing *cb1* mRNA throughout an entire 6 dpf zebrafish brain (b-i and b-ii are dorsal & lateral, respectively). The pallium (Pa) and subpallium (SPa) are highlighted in yellow, torus longitudinalis (TL) in orange, and rostral hypothalamus (R Hy) in blue.
(C, D, E) Colocalization analysis of *cb1* with *vglut2.2* (i-iii) and *cb1* with *gad1b* (iv-vi) is shown in the pallium (B), hypothalamus (C), and subpallium (D).
(F, G) *cb1* is shown to be in close proximity to *crhb* in the hypothalamus (Ei-iii dorsal, Eiv-vi lateral) and otpb cluster 3 (Fi-iii dorsal, Fiv-vi lateral).
With the exception of the maximum intensity projections, each image depicts a single z-plane. CB1 – cannabinoid receptor 1; NM – neuronal marker; Mg. – merged; Vglut2 – vesicular glutamate transporter 2; Gad1b – glutamate decarboxylase 1b; crhb – corticotropin releasing hormone b. See also Table 1. A-ii was collected with 10x objective and the rest with 20x.

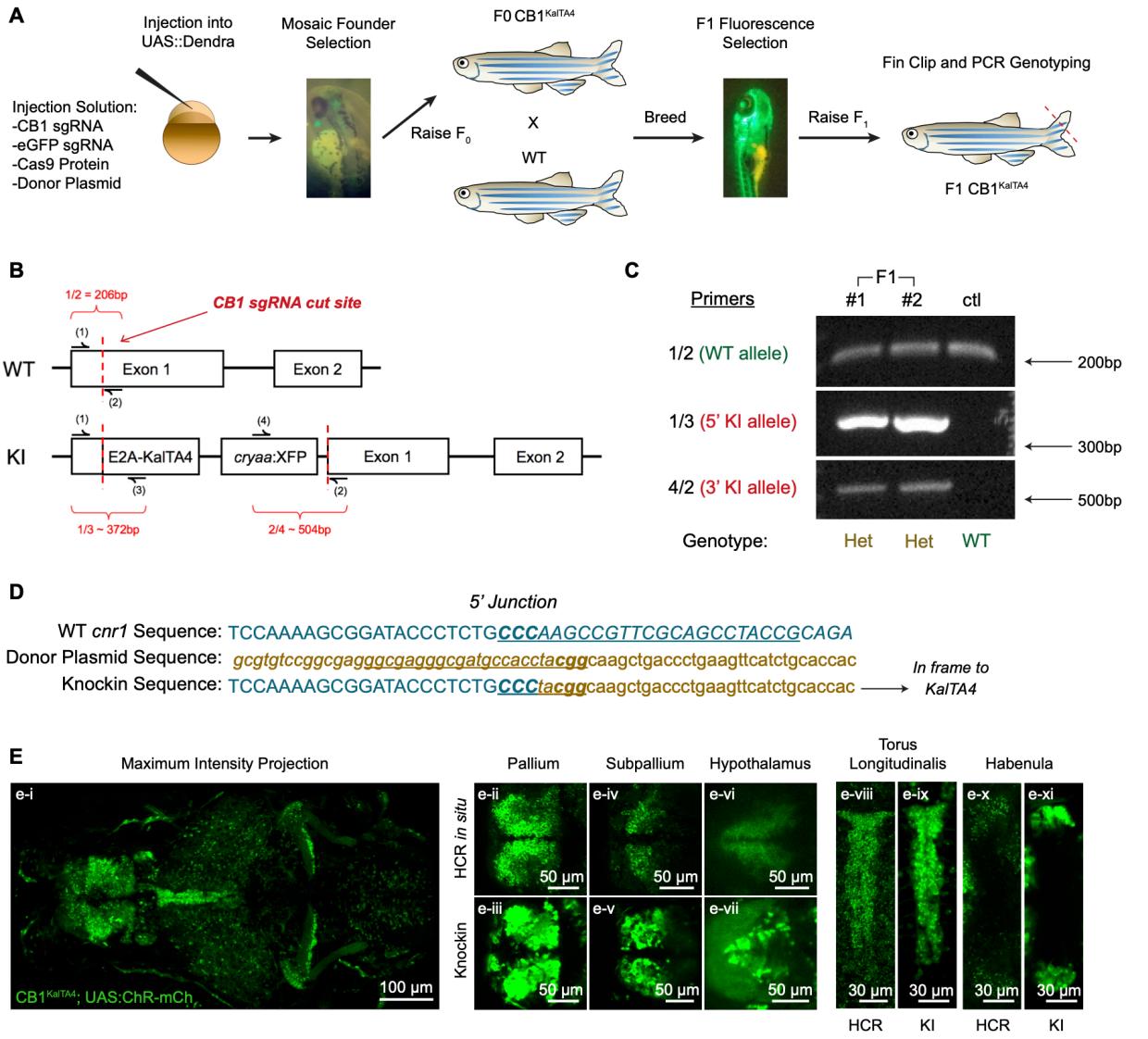

Figure 5.4 CRISPR-mediated knockin enables genetic access to CB1-expressing neurons.

(A) Schematic showing the process of using CRISPR-Cas9 technology to knock in KalTA4 at the *cb1* locus.
(B) Diagram depicting the wild-type *cb1* allele (WT) and the knockin allele (KI). The sgRNA cut site is in exon 1 of the *cb1* locus and represented by a dashed red line. Half arrows with numbers represent genotyping primers. Primers 1 and 2 detect the presence of the wild-type allele, primers 1 and 3 detect the 5' end of the knockin allele, and primers 2 and 4 detect the 3' end of the knockin allele with PCR product sizes of 206, approximately 372, and approximately 504 base pairs, respectively.
I Genotyping results of two F1 adult knockin fish and one wild-type control. Bands that detect the wild-type allele (primers 1 and 2) are present for all 3 fish. Bands that detect the 5' (primers 1 and 3) and 3' (primers 2 and 4) ends of the knockin allele are only present in the F1 fish, confirming their heterozygous status for the knockin allele.

(D) Sequence alignment of the wild-type *cb1* sequence, donor plasmid sequence, and sequencing results for the F1 knockin fish line at the 5' junction. The sgRNA targeting the *cb1* locus is underlined in blue, and the sgRNA targeting the donor plasmid is underlined in gold. Sequencing results reveal the location of donor plasmid integration and confirm that the plasmid integrated in frame to KalTA4.
(E) Maximum intensity projection of Cb1 knockin from confocal imaging (e-i) and single z-slice images of the Cb1 knockin and comparison to *cb1* HCR *in situ* in the pallium (e-ii and e-iii), subpallium (e-iv and e-v), hypothalamus (e-vi and e-vii), torus longitudinalis (e-viii and e-ix), and habenula (e-x and e-xi). All images were captured with 20x objective.

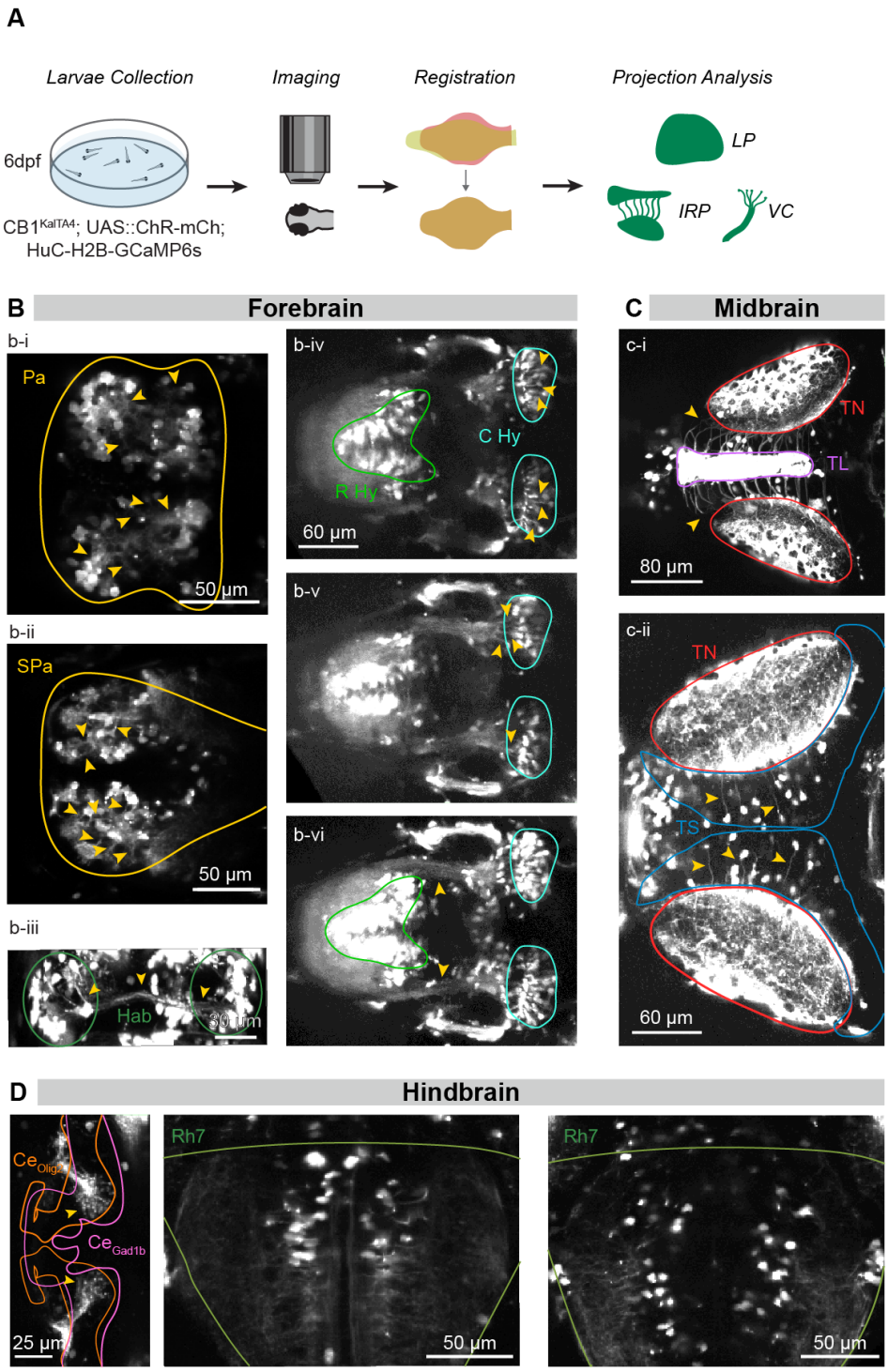

Figure 5.5 Projection analysis of CB1-expressing cells.

(A) Schematic demonstrating the workflow of neuronal projection data collection and analysis. (B, C, D) Analysis of neuronal projections in various regions of the fore- (B), mid- (C), and hindbrain (D).

Yellow arrows point to neuronal projections (B & C) or varicosities (D). LP – local projections; IRP – interregional projections; VC – varicosities; Pa – pallium; SPa – subpallium; Hab – habenula; R Hy – rostral hypothalamus; C Hy – caudal hypothalamus; TN – tectum neuropil; TL – torus longitudinalis; TS – tectum striatum; Ce_{olig2} – olig2-enriched regions of the cerebellum; Ce_{Gad1b} – gad1b-enriched regions of the cerebellum; Rh7 – rhombomere 7.

5.8 TABLES

Table 5.1 Brain regions expressing *cb1* mRNA in 6dpf zebrafish.

Based on the *cb1* HCR in-situ data and registration, *cb1* expression is divided by strong, moderate, and weak expression in brain regions.

HIGH EXPRESSION	MODERATE EXPRESSION	WEAK EXPRESSION
Telencephalon		
Olfactory bulb dopaminergic areas	Subpallial DA cluster	S1181t cluster
Pallium		
Subpallial gad1b cluster		
Vglut2 rind		
Vmat2 cluster		
Diencephalon		
Rostral Hypothalamus	Pretectal Gad1b & DA cluster	Hypothalamus Vglut2 cluster 2,3
Otpb cluster 3		
Mesensephalon		
Torus Longitudinalis	Vglu2 cluster 1	NucMLF
		Tegmentum
Rhombencephalon		
-	Area Postrema	-
	Lobus caudalis cerebelli	
	Qrfp neuron cluster sparse	
	Rhombomere 6 & 7	
	Vglu2 stripe 1	

5.9 SUPPLEMENTAL FIGURES AND TABLES

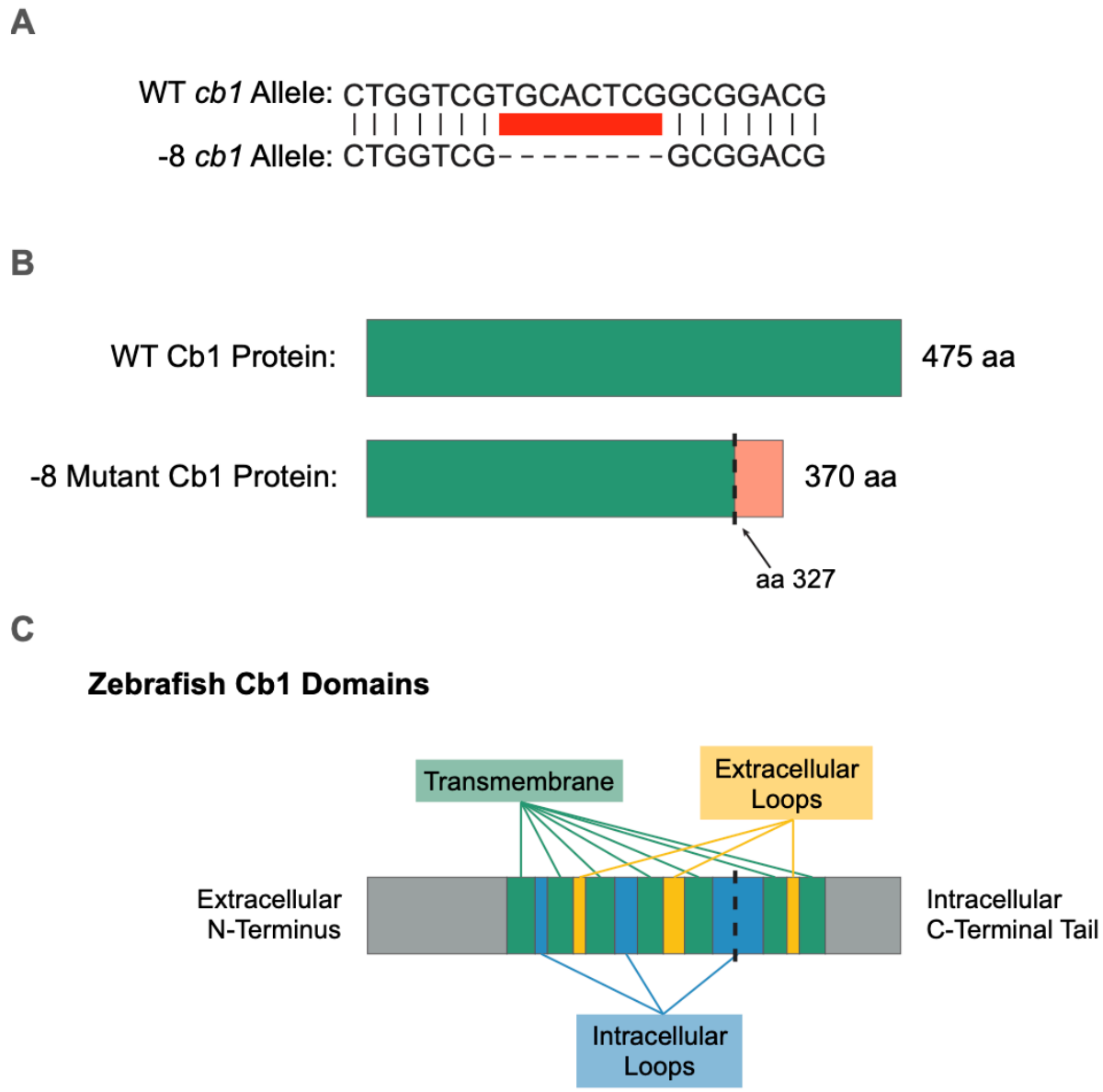

Figure 5.S1 CB1 knockout fish line genetics.

(A) Depiction of wild-type and mutant genome sequences at the sgRNA target site in the *cb1* gene.
(B) The -8 base pair deletion at the guide site (dashed line) is located in amino acid 327. This results in a scrambled amino acid sequence from amino acid 327-370, then a premature stop codon at amino acid 475.
I A schematic of zebrafish Cb1 domains. The scrambled sequence and subsequent premature

stop codon (starting from the dashed line) results in loss of the second half of the 3rd intracellular loop, and every subsequent domain, including the C terminal tail, which are necessary for Cb1 function (Nie et al., 2001; Howlett and Shim, 2013). Domain information from Uniprot Database.

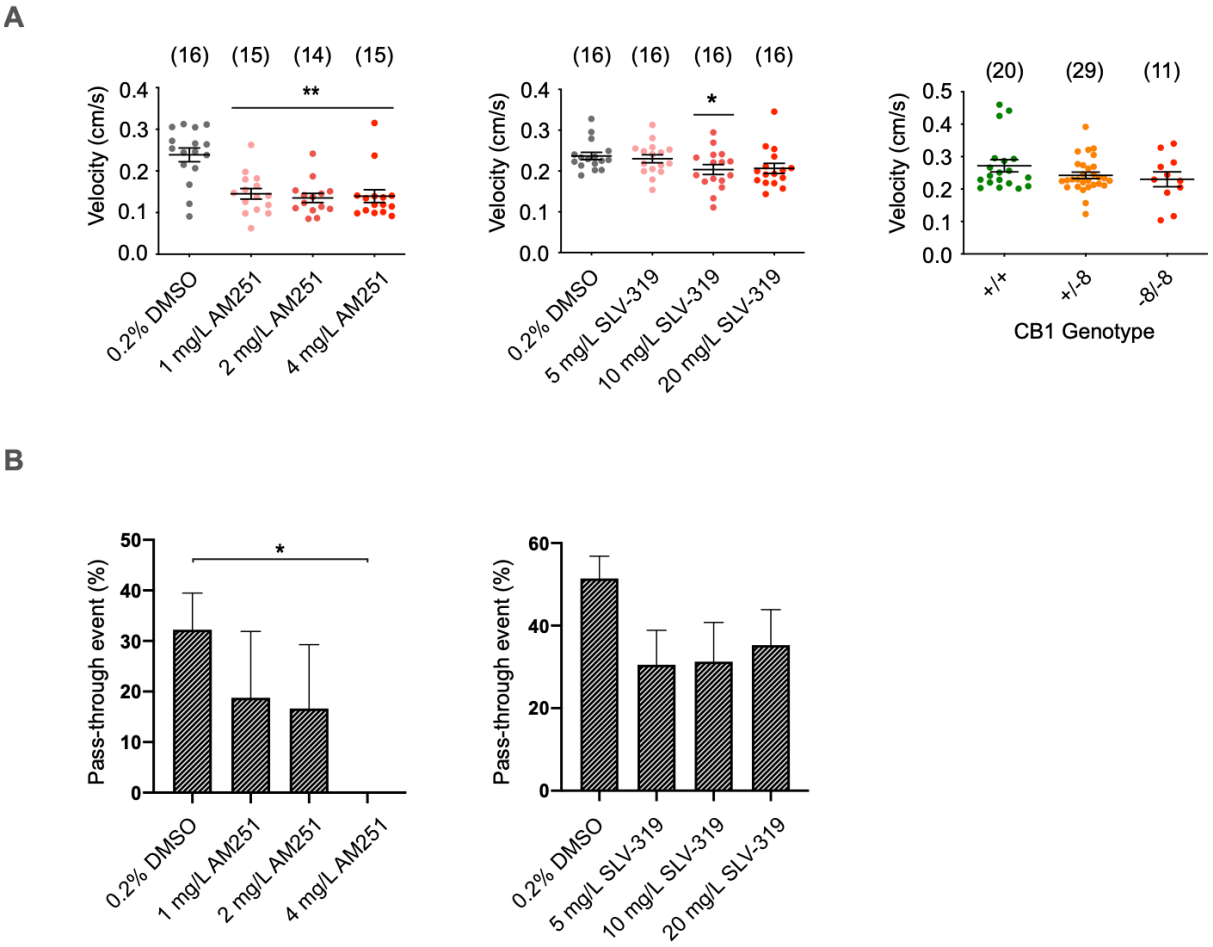

Figure 5.S2 CB1 inhibition effects on locomotor activity and border decision.

(A and B) Average velocity (A) and pass-through percentage for each border event (B) for AM251 (Left), SLV-319 (Middle), and CB1 KO (Right) experiments done in Figure 1C.
All quantitative data represented as mean +/- SEM. *p < 0.05, **p < 0.01 (student's t-test for A, Kruskal-Wallis test for B).

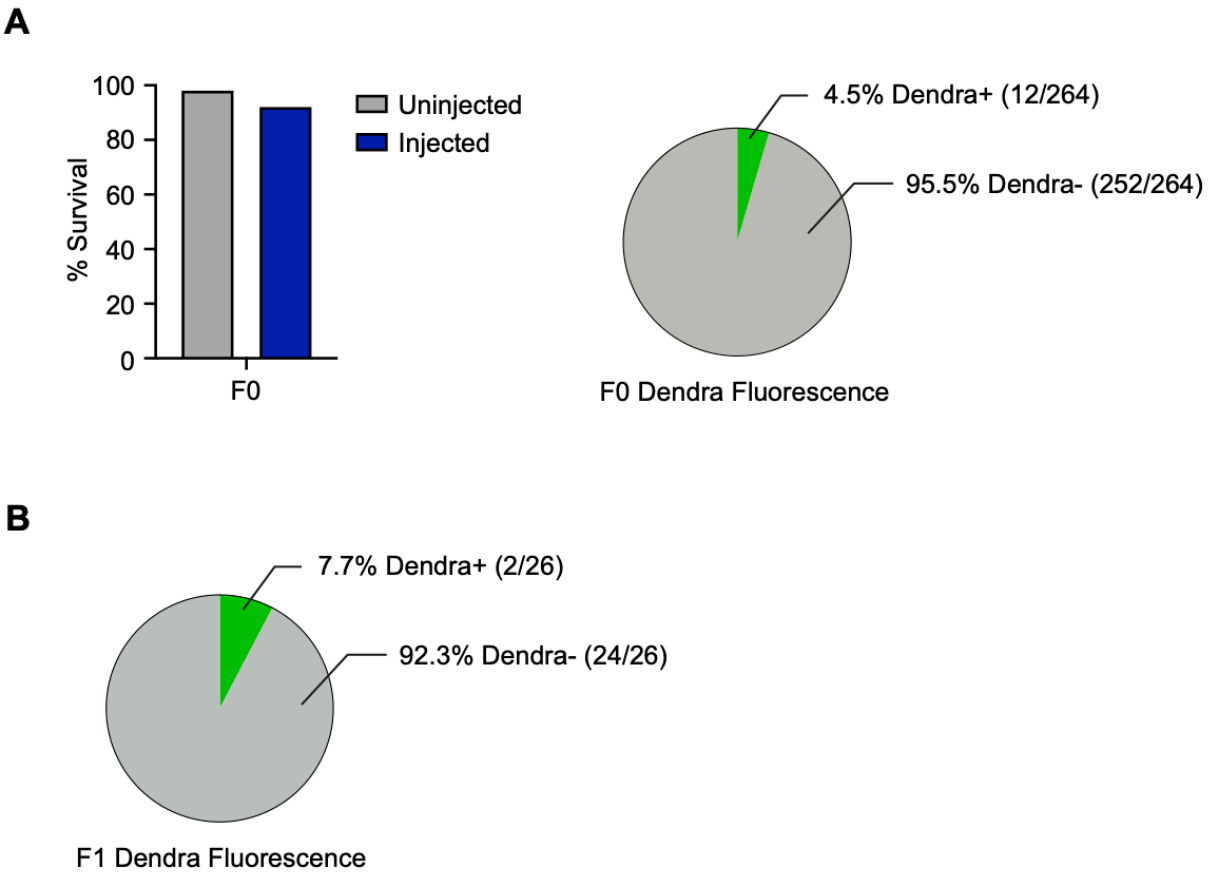

Figure 5.S3 Survival and screening results of knockin F0 and F1 generations.

(A) Percent survival of uninjected vs injected (left) and mosaic Dendra screening results (right) for knockin F0 generation.
(B) Dendra screening results for knockin F1 generation.

Table 5.S1 sgRNA sequences for *cb1* knockout and knockin generation.

Sequences for the sgRNAs used to generate the Tg(*cb1*$^{-/-}$) and Tg(cb1^{KalTA4}) fish lines. For Tg(*cb1*$^{-/-}$), sgRNA0 was used to introduce a deleterious mutation at the *cb1* locus. For Tg(*cb1*^{KalTA4}), sgRNA1 was used for linearization of the eGFPbait-E2A-KalTA4 plasmid, and sgRNA2 targeted exon 1 of the *cb1* locus. PAM sequences are in parentheses.

NAME	TARGET	SEQUENCE
Tg(CB1$^{-/-}$)		
sgRNA0	*cb1* locus, exon 1	GAGCCTGGTCGTGCACTCGG(CGG)
Tg(CB1^{KalTA4})		
sgRNA1	eGFP bait sequence on plasmid	GGCGAGGGCGATGCCACCTA(CGG)
sgRNA2	*cb1* locus, exon 1	CGGTAGGCTGCGAACGGCTT(GGG)

Table 5.S2 Genotyping primer sequences for *cb1* knockout.

Sequences for the primers flanking the sgRNA site for the Tg(*cb1*$^{-/-}$) fish line. Primers produced a PCR product with a total length of 608 bp.

NAME	SEQUENCE
TIDE Primer F	GATCTCCTCGGCAGTGTTAT
TIDE Primer R	CAATAGTGATATATCGTGCTAACG

Table 5.S3 Genotyping primer sequences for *cb1* knockin.

Sequences for the primers used to genotype the Tg(cb1^{KalTA4}) fish line as shown in Figure 4B.

NAME	SEQUENCE	BP FROM SGRNA SITE
Primer 1	CTGTTCCCGGCCTCAAAGTC	175
Primer 2	TTATCCGCGAAGGAGCTTCTG	31
Primer 3	GCTCTCAACATCTCCAGCCAATTTC	197
Primer 4	TCTAGCACTGAATGGCTCAGAC	473

5.10 REFERENCES

Adams I.B., and Martin B.R. (1996). Cannabis: pharmacology and toxicology in animals and humans. Addiction. *91*, 1585-1614.

Araque, A., Castillo, P.E., Manzoni O.J., and Tonini R. (2017). Synaptic functions of endocannabinoid signaling in health and disease. Neuropharmacology. *15*, 13-24.

Auer, T.O., Duroure, K., De Cian, A., Concordet, J.P., and Del Bene, F. (2014). Highly efficient CRISPR/Cas9-mediated knock-in in zebrafish by homology-independent DNA repair. Genome Res. *24*, 142-153.

Bai, Y., Huang, B., Wagle, M., and Guo, S. (2016). Identification of environmental stressors and validation of light preference as a measure of anxiety in larval zebrafish. BMC Neuroscience. *17*, 63.

Barbazuk, W.B., Korf, I., Kadavi, C., Heyen, J., Tate, S., Wun E., Bedell J.A., McPherson J.D., and Johnson, S.L. (2000). The syntenic relationship of the zebrafish and human genomes. Genome Res. *10*, 1351-1358.

Berry, E.M., and Mechoulam, R. (2002). Tetrahydrocannabinol and the endocannabinoids in feeding and appetite. Pharmacol. Ther. *95*, 185-90.

Blasio A., Iemolo, A., Sabino, V., Petrosino, S., Steardo, L., Rice, K.C., Orlando, P., Iannotti, F.A., Di Marzo, V., Zorilla, E.P., and Cottone, P. (2013). Rimonabant precipitates anxiety in rats

withdrawn from palatable food: role of the central amygdala. Neuropsychopharmacology. *38*, 2498-2507.

Busquets-Garcia, A., Bains, J., & Marsicano, G. (2018). CB1 Receptor Signaling in the Brain: Extracting Specificity from Ubiquity. Neuropsychopharmacology. *43*, 4-20.

Castillo, P.E., Younts, T.J., Chavez, A.E., and Hashimotodani, Y. (2012). Endocannabinoid signaling and synaptic function. Neuron. *76*, 70-81.

Chan P.K., Chan S.C., and Yung W.H. (1998). Presynaptic inhibition of GABAergic inputs to rat substantia nigra pars reticulata 178andomi by a cannabinoid agonist. Neuroreport. *9*, 671-675.

Chen., F., Chen, S., Liu, S., Zhang, C., and Peng, G. (2015). Effects of lorazepam and WAY-200070 in larval zebrafish light/dark choice test. Neuropharmacology. *95*, 226-233.

Choi, H.M.T., Schwarzkopf, M., Fornace, M.E., Acharya, A., Artavanis, G., Stegmaier, J., Cunha, A., and Pierce, N.A. (2018). Third-generation *in situ* hybridization chain reaction: multiplexed, quantitative, sensitive, versatile, robust. Development. *145*, dev165753.

Christensen R., Kristensen, P.K., Bartels, E.M., Bliddal, H., and Astrup, A. (2007). Efficacy and safety of the weight-loss drug rimonabant: a meta-analysis of 178andomized trials. Lancet. *370*, 1706-1713.

Dedic N., Chen, A. and Deussing, J.M. (2018). The CRF family of neuropeptides and their receptors – mediators of the central stress response. Curr Mol Pharmacol. *11*, 4-31.

Diana, M.A. and Marty A. (2004). Endocannabinoid-mediated short-term synaptic plasticity: depolarization-induced suppression of inhibition (DSI) and depolarization-induced suppression of excitation (DSE)

El Manira A., and Kyriakatos A. (2010). The role of endocannabinoid signaling in motor control. Physiology (Bethesda). *25*, 230-238.

Elphick, M.R. (2012). The evolution and comparative neurobiology of endocannabinoid signalling. Philos Trans R Soc Lond B Biol Sci. *367*, 3201-3215.

Fuguo, J., Liu, J.J., Osuna, B.A., Xu, M., Berry, J.D., Rauch, B.J., Nogales, E., Bondy-Denomy, J., and Doudna, J.A. (2019). Temperature-responsive competitive inhibition of CRISPR-Cas9. Mol Cell. *73*, 601-610.

Gomes-de-Souza, L., Bianchi, P.C., Costa-Ferreira, W., Tomeo, R.A., Cruz, F.C., and Crestani, C.C. (2012). CB_1 and CB_2 receptors in the bed nucleus of the stria terminalis differently modulate anxiety-like behaviors in rats. Prog Neuropsychopharmacol Biol Psychiatry. *110*, 110284.

Graham, B.M., Langton, J.M., and Richardson, R. (2011). Pharmacological enhancement of fear reduction: preclinical models. Br. J. Pharmacol. *164*, 1230-1247.

Guo, S. (2009). Using zebrafish to assess the impact of drugs on neural development and function. Expert Opin Drug Discov. *4*, 715-726.

Häring, M., Kaiser, N., Monory, K., and Lutz, B. (2011). Circuit specific functions of cannabinoid CB1 receptor in the balance of investigatory drive and exploration. PloS ONE. *6*, e26617.

Hauger, R.L., Risbrough, V., Oakley, R.H., Olivares-Reyes, J.A., and Dautzenberg, F.M. (2009). Role of CRF receptor signaling in stress vulnerability, anxiety, and depression. Ann N Y Acad Sci. *1179*, 120-143.

Heifets, B.D., and Castillo, P.E. (2009). Endocannabinoid signaling and long-term synaptic plasticity. Annu. Rev. Physiol. *71*, 283-306.

Howe, K., Clark, M.D., Torroja, C.F., Torrance, J., Berthelot, C., Muffato, M., Collins, J.E., Humphray, S., McLaren, L., Matthews, L., et al. (2013). The zebrafish genome sequence and its relationship to the human genome. Nature. *496*, 498-503.

Howlett AC, Shim JY. Cannabinoid Receptors and Signal Transduction. In: Madame Curie Bioscience Database [Internet]. Austin (TX): Landes Bioscience; 2000-2013. Available from: https://www.ncbi.nlm.nih.gov/books/NBK6154/

Jesuthasan, S. (2012). Fear, anxiety, and control in the zebrafish. Dev Neurobiol. *72*, 395-403.

Jinek M., Chylinksi, K., Fonfara, I., Hauer, M., Doudna, J.A., and Charpentier, E. (2012). A programmable dual-RNA-guided DNA endonuclease in adaptive bacterial immunity. Science. *337*, 816-821.

Kano, M., Ohno-Shosaku, T., Hashimotodani, Y., Uchigashima, M., and Watanabe, M. (2009).

Endocannabinoid-mediated control of synaptic transmission. Physiol. Rev. *89*, 309-380.

Kreitzer, A.C., and Regehr, W.G. (2001). Retrograde inhibition of presynaptic calcium influx by endogenous cannabinoids at excitatory synapses onto Purkinje cells. Neuron. *29*, 717-727.

Lafenêtre, P., Chaouloff, F., and Marsicano, G. (2007). The endocannabinoid system in the processing of fear and how CB1 receptors may modulate fear extinction. Pharmacol. Res. *56*, 367-381.

Lam, C.S., Rastegar, S., and Strähle, U. (2006). Distribution of cannabinoid receptor 1 in the CNS of zebrafish. Neuroscience. *138*, 83-95.

Lange, M.D., Daldrup, T., Remmers, F., Szkudlarek, H.J., Lesting, J., Guggenhuber, S., Ruehle, S., Jüngling, K., Seidenbecher, T., Lutz, B., and Pape, H.C. (2017). Cannabinoid CB1 receptors in distinct circuits of the extended amygdala determine fear responsiveness to unpredictable threat. Mol Psychiatry. *22*, 1422-1430.

Lara, R.A. and Vasconcelos, R.O. (2021). Impact of noise on development, physiological stress and behavioral patterns in larval zebrafish. Sci Rep. *11*, 6615.

Leung, L.C., Wang, G.X., and Mourrain, P. (2013). Imaging zebrafish neural circuitry from whole brain to synapse. Front Neural Circuits. *7*, 76.

Li, M., Zhao, L., Page-McCaw, P.S., and Chen, W. (2016). Zebrafish genome engineering using the CRISPR-Cas9 system. Tends. Genet. *32*, 815-827.

Liu, L.Y., Alexa, K., Cortes, M., Schatzman-Bone, S., Kim, A.J., Mukhopadhyay, B., Cinar, R., Kunos, G., North, T.E., and Goessling, W. (2016). Cannabinoid receptor signaling regulates liver development and metabolism. Development. *143*, 609-622.

Lutz, B., Marsicano, G., Maldonado, R., and Hillard, C.J. (2015). The endocannabinoid system in guarding against fear, anxiety and stress. Nat Rev Neurosci. *16*, 705-18.

Lutz, B. (2020). Neurobiology of cannabinoid receptor signaling. Dialogues Clin Neurosci. *22*, 207-222.

Maldonado, R., Cabañero, D., and Martín-Garcia, E. (2020). The endocannabinoid system in modulating fear, anxiety, and stress. Dialogues Clin Neurosci. *22*, 229-239.

Maneuf, Y.P., Crossman, A.R., and Brotchie, J.M. (1996). Modulation of GABAergic transmission in the globus pallidus by the synthetic cannabinoid WIN 55,212-2. Synapse. *22*, 382-385.

Marcus, D.J., Bedse, G., Gaulden, A.D., Ryan, J.D., Kondev, V., Winters, N.D., Rosas-Vidal, L.E., Altemus, M., Mackie, K., Lee, F.S., Delpire, E., and Patel, S. (2020). Endocannabinoid signaling collapse mediates stress-induced amygdalo-cortical strengthening. Neuron. *105*, 1062-1076.

Maron, E. and Nutt, D. (2017). Biological markers of generalized anxiety disorder. Dialogues Clin Neurosci. *19*, 147-158.

Matsuda, L.A., Lolait, S.J., Brownstein M.J., Young, A.C., and Bonner T.I. (1990). Structure of a cannabinoid receptor and functional expression of the cloned cDNA. Nature. *346*, 561-564.

Mechoulam, R., and Parker, L.A. (2013). The endocannabinoid system and the brain. Annu. Rev. Psychol. *64*, 21-47.

Melgoza, A. and Guo, S. (2018). Systematic screens in zebrafish shed light on cellular and molecular mechanisms of complex brain phenotypes. In: R.T., Gerlai, ed., Molecular-Genetic and Statistical Techniques for Behavioral and Neural Research, 1st ed. Academic Press: Elsevier, 385-400.

Micale, V. and Drago, F. (2018). Endocannabinoid system, stress and HPA axis. Eur J Pharmacol. *834*, 230-239.

Mitchell, P.B. and Morris, M.J. (2007). Depression and anxiety with rimonabant. Lancet. *370*, 1671-2.

Morena, M., Patel, S., Bains, J.S., and Hill, M.N. (2016). Neurobiological interactions between stress and the endocannabinoid system. Neuropsychopharmacology. *41*, 80-102.

Nie, J., and Lewis, D.L. (2001). Structural domains of the CB1 cannabinoid receptor that contribute to constitutive activity and G-protein sequestration. J Neurosci. *21*, 8758-8764.

Ohno-Shosaku, T., Maejima, T., and Kano, M. (2001). Endogenous cannabinoids mediate

retrograde signals from depolarized postsynaptic neurons to presynaptic terminals. Neuron. *29*, 729-738.

Oltrabella, F., Melgoza, A., Nguyen, B., and Guo, S. (2017). Role of the endocannabinoid system in vertebrates: Emphasis on the zebrafish model. Develop. Growth Differ. *59*, 194-210.

Pomrenze, M.B., Giovanetti, S.M., Maiya, R., Gordon, A.G., Kreeger, L.J. and Messing, R.O. (2019). Dissecting the roles of GABA and neuropeptides from rat central amygdala CRF neurons in anxiety and fear learning. Cell Rep. *29*, 13-21.

Portugues, R., Severi, K.E., Wyart, C., and Ahrens, M.B. (2013). Optogenetics in a transparent animal: circuit function in the larval zebrafish. Curr. Opin. Neurobiol. *23*, 119-126.

Randlett, O., Wee, C.L., Naumann, E.A., Nnaemeka, O., Schoppik D., Fitzgerald, J.E., Portugues, R., Lacoste, A.M.B., Riegler, C., Engert, F., and Schier, A.F. (2015). Whole-brain activity mapping onto a zebrafish brain atlas. Nat Methods. *12*, 1039-1046.

Riebe, C.J. and Wotjak, C.T. (2011). Endocannabinoids and stress. Stress. *14*, 384-397.

Ruehle, S. *et al.* (2013). Cannabinoid CB1 receptor in dorsal telencephalic glutamatergic neurons: distinctive sufficiency for hippocampus-dependent and amygdala-dependent synaptic and behavioral functions. J. Neurosci. *33*, 10264-10277.

Shen M., Piser T.M., Seybold V.S., and Thayer S.A. Cannabinoid receptor agonists inhibit glutamatergic synaptic transmission in rat hippocampal cultures. J. Neurosci. *16*, 4322-4334.

Soyka, M. (2008). Rimonabant and depression. Pharmacopsychiatry. *41*, 204-205.

Steenbergen, P.J., Richardson, M.K., and Champagne, D.L. (2011). Patterns of avoidance behaviours in the light/dark preference test in young juvenile zebrafish: a pharmacological study. Behav Brain Res. *222*, 15-25.

Stewart A.M., Braubach, O., Spitsbergen, J., Gerlai, R., and Kalueff, A.V. (2014). Zebrafish models for translational neuroscience research: from tank to bedside. Trends. Neurosci. *37*, 264-278.

Sylvers, P., Lilienfeld, S.O., and LaPrairie, J.L. (2011). Differences between trait fear and trait anxiety: implications for psychopathology. Clin. Psychol. Rev. *31*, 122-137.

Szabo B., Dorner L., Pfreundtner C., Norenberg W., and Starke K. (1998). Inhibition of GABAergic inhibitory postsynaptic currents by cannabinoids in rat corpus striatum. Neuroscience. *85*, 395-403.

Thiemann, G., Watt, C.A., Ledent, C., Molleman, A., and Hasenöhrl, R.U. (2009). Modulation of anxiety by acute blockade and genetic deletion of the CB(1) cannabinoid receptor in mice together with biogenic amine changes in the forebrain. Behav Brain Res. *200*, 60-67.

Tovote, P., Fadok, J.P., and Lüithi A. (2015). Neuronal circuits for fear and anxiety. Nat Rev Neurosci. *16*, 317-331.

Vanwalleghem, G.C., Ahrens, M.B., and Scott, E.K. (2018). Integrative whole-brain neuroscience in larval zebrafish. Curr. Opin. Neurobiol. *50*, 136-145.

Varshney, G.K., Pei, W., LaFave, M.C., Idol, J., Xu, L., Gallardo, V., Carrington, B., Bishop, K., Jones, M., Li, M., Harper, U., Huang, S.C., Prakash, A., Chen, W., Sood, R., Ledin, J., and Burgess, S.M. (2015). High-throughput gene targeting and phenotyping in zebrafish using CRISPR/Cas9. Genome Res. *25*, 1030-42.

Wagle, M., Nguyen, J., Shinwoo, L., Zaitlen, N., and Guo, S. (2017). Heritable natural variation of an anxiety-like behavior in larval zebrafish. J Neurogenet. *31*, 138-148.

Wilson, R.I., and Nicoll, R.A. (2001). Endogenous cannabinoids mediate retrograde signalling at hippocampal synapses. Nature. *410*, 588-592.

Watson, S., Chambers, D., Hobbs, C., Doherty, P., and Graham, A. (2008). The endocannabinoid receptor, CB1, is required for normal axonal growth and fasciculation. Mol Cell Neurosci. *38*, 89-97.

Wilson, R.I. and Nicoll, R.A. (2001). Endogenous cannabinoids mediate retrograde signalling at hippocampal synapses. Nature. *410*, 588-592.

CHAPTER 6: Conclusions and Future Directions

6.1 CONCLUSIONS, PERSPECTIVES, AND FUTURE DIRECTIONS

In this dissertation, we examined various aspects of the endocannabinoid (eCB) system to gain a more thorough understanding of the roles of eCB genes in behavior and neural signaling. Chapters 1 and 2 provided foundational information on how we can utilize the strength of the zebrafish model to gain insight on neurobiological mechanisms, as well as the current status of known roles for eCB genes. In Chapters 3, 4, and 5, we used this foundational knowledge to systematically determine how perturbation of various eCB proteins alters behavior, as well as investigate the connection between CB1 signaling and changes in anxiety-like behavior in zebrafish.

In Chapter 3, we utilized CRISPR/Cas9-induced mutagenesis to produce and present six new eCB knockout fish lines: *cb1*, *dagla*, *daglb*, *abhd4*, *mgll*, and *faah*. We phenotyped *dagla* knockout fish and observed an increase in locomotor activity, as well as changes in *gpr55a*, *dagla*, and *fas* mRNA transcripts between wild-type and knockout cousins. These exciting findings open the door for discovering new mechanisms by which eCB genes such as *dagla* are involved in, such as its involvement with locomotion or eCB signaling. Though genetic knockouts are an excellent way to disrupt a gene of interest with high specificity, it is worth noting that a common challenge when producing germline knockouts is the possibility of phenotypes being masked by phenomena such as maternal contribution of the knockout gene or genetic compensation of alternate genes. Indeed, our observation of no change in locomotor activity when examining *dagla* wild-type and knockout siblings could be explained by possible *dagla* contribution from the heterozygous mother. A follow up experiment to address this could be quantifying *dagla* mRNA and protein levels in *dagla* knockouts produced from a heterozygous in-cross compared to *dagla* knockouts produced from knockout parents. Both types of phenotype masking – maternal contribution and genetic compensation – should be

considered when continuing to phenotype the remaining eCB mutant fish lines. To address possible cases of genetic compensation of alternate genes, RNA-seq could be performed to determine any genes that have altered transcript levels in the genetic knockout.

In Chapter 4, we addressed the same question of how eCB protein perturbation affects behavior, but instead of using genetic mutations, we administered pharmacological agents targeting eCB proteins. It was here that we observed a wide range of effects on dark avoidance behavior: CB1 agonists demonstrated opposing effects on dark avoidance, while MGLL and FAAH inhibitors demonstrated a decrease in dark avoidance (or no effect, as in the case of JZL-184). As dark avoidance is an anxiety-like behavior, this data has implications for CB1, MGLL, and FAAH on anxiety state. All tested drugs demonstrated a decrease in locomotor activity at higher tested doses, except for MGLL inhibitor JZL-184, which did not show any affect at any dose. Though the use of pharmacology to produce perturbations has the advantage of being faster and easier to use than producing genetic knockout lines (which take around 6 months to produce an adult F1 generation), pharmacological agents have the caveat of off-target effects. It is here that genetic knockouts can synergize with pharmacological experiments to address specificity. As in the case of the FAAH inhibitor PF-3845, effects on choice index and locomotion were lost when administered to the *faah* knockout line. Future pharmacological experiments can make use of the eCB knockout fish lines to address specificity and produce clearer results.

In Chapter 5, we narrowed in on the primary eCB signaling gene, *cb1*, and investigated the neuronal populations that may be involved with its connection to anxiety-like behavior. Our study revealed that, as observed in humans and mice, inhibiting CB1 in zebrafish via both pharmacological and genetic perturbations increases anxiety-like behavior. We also observed an increase in cortisol – a physiological stress hormone – in larvae treated with the drug AM251. As AM251 has structural similarity to Rimonabant, the drug that caused incidences of anxiety

and suicide in humans, these findings strengthen the case for using zebrafish to investigate the role of eCB signaling in anxiety-like behavior. We next aimed to gain insight on the neural circuit, or the cell populations, that drive *cb1*-mediated changes in anxiety. After using *HCR* in-situ, we determined that in 6 dpf zebrafish, *cb1* mRNA is highly expressed in the telencephalon (olfactory bulb dopaminergic areas, pallium, subpallial gad1b cluster, Vglu2 rind, Vmat2 cluster), diencephalon (rostral hypothalamus, Otpb cluster 3), and mesencephalon (torus longitudinalis). We also observed strong co-expression between *cb1* and *vglut2.2* in the pallium and rostral hypothalamus, as well as co-expression between *cb1* and *gad1b* in the subpallium. Our study is the first to thoroughly examine *cb1* expression and colocalization in 6 dpf zebrafish – the developmental stage that demonstrates anxiety-like behavior following *cb1* inhibition, as well as an ideal developmental stage for future calcium imaging experiments that examine neuron behavior. Based off our co-expression data and the eCB system's nature as a retrograde inhibiting signaling pathway, we hypothesize that *cb1* performs DSE in the pallium and rostral hypothalamus, and DSI in the subpallium. Following this logic, if CB1 is inhibited, then DSE and DSI are disturbed in these locations. This may be a factor that can contribute *cb1*-mediated changes in anxiety. Future experiments include brain-wide calcium imaging to find cells that have altered activity following CB1 perturbation. Lastly, we used a CRISPR/Cas9-mediated knockin technique produce the first recorded CB1 transgenic fish line. We coupled this line to a reporter line and determined sites of neuronal projections. Of note, we observed local connections in the pallium, subpallium, and habenula. We determined interregional projections between the caudal and rostral hypothalamus, as well as the torus longitudinalis and tectum neuropil, and the tectum striatum and tectum neuropil. We also observed varicosities in the cerebellum, and cell bodies and axon fibers in rhombomere 7. These sites of connectivity between CB1-expressing cells aid in producing a more complete picture of the regions that are participating in the CB1-anxiety circuit, and highlight the utility of the CB1 transgenic line. Now

that the line is produced, further projection analysis can be done at various developmental stages addressing the connectivity of CB1 expression cells across development into adulthood. Additionally, the CB1 transgenic line can be crossed with Tg(UAS::GCaMP6s) to perform calcium imaging of CB1-expressing cells, or Tg(UAS::Channelrhodopsin)/ Tg(UAS::Halorhodopsin) to activate or inhibit these cells, allowing for testing of a cell's participation in the CB1-anxiety circuit.

In conclusion, this dissertation aims to shed light on the endocannabinoid system, neural signaling, and behavior. As we have shown, experiments in zebrafish are an excellent strategy for addressing this, and from our work comes seven new fish lines that can be utilized for exploring the roles of eCB genes in not only neurobiological mechanisms, but any of the diverse biological processes that the eCB system is known to modulate. We encourage the use of these lines in order to bridge our knowledge gaps of the eCB system, bringing us closer to a full understanding of the fundamental neuroscience of eCB signaling, and therapeutic/toxicological considerations for eCB protein-targeting drugs.

Publishing Agreement

It is the policy of the University to encourage open access and broad distribution of all theses, dissertations, and manuscripts. The Graduate Division will facilitate the distribution of UCSF theses, dissertations, and manuscripts to the UCSF Library for open access and distribution. UCSF will make such theses, dissertations, and manuscripts accessible to the public and will take reasonable steps to preserve these works in perpetuity.

I hereby grant the non-exclusive, perpetual right to The Regents of the University of California to reproduce, publicly display, distribute, preserve, and publish copies of my thesis, dissertation, or manuscript in any form or media, now existing or later derived, including access online for teaching, research, and public service purposes.

DocuSigned by:

826733A167144F0...

Author Signature

8/9/2021

Date